

AD A108351

LEVEL III

Form Approved
Budget Bureau No. 22-R0293

DEPARTMENT OF GEOLOGICAL SCIENCES
210 KIMBALL HALL
CORNEILL UNIVERSITY
ITHACA, NEW YORK 14853

SEMI-ANNUAL TECHNICAL REPORT
FOR PERIOD 1 APRIL 1975 - 31 SEPTEMBER 1975

to

AIR FORCE OFFICE OF SCIENTIFIC RESEARCH

from


CORNELL UNIVERSITY
DEPARTMENT OF GEOLOGICAL SCIENCES


DTIC
EXTRACTED

DEC 10 1981

H

Title of Proposal:	Integrated Geophysical and Geological Study of Earthquakes in Normally Aseismic Areas	
Sponsored by:	Advanced Research Projects Agency ARPA Order No. 1827	
Program Code:	4F10	
Effective Date of Contract:	1 March 1973	
Contract Expiration Date:	31 December 1975	
Amount of Contract Dollars:	\$210,218	
Contract Number:	AFOSR 73-2494	
Principal Investigators:	Jack E. Oliver (607) 256-2377	Bryan L. Isacks (607) 256-2307


Jack E. Oliver, Principal
Investigator


Bryan L. Isacks, Principal
Investigator

DISTRIBUTION STATEMENT A
Approved for public release;
Distribution Unlimited

DTIC FILE COPY

81 12 08 09

402984

TECHNICAL REPORT SUMMARY

Accession For	NTIS GRA&I	DTIC TAB	Unannounced	Justification
By	Director	Aviation	Codes	Index
				Special
				A

Technical Problem

Although a consistent and relatively successful theoretical and empirical framework has been developed for understanding seismicity near lithospheric plate boundaries, earthquakes occurring within these boundaries remain a little understood phenomenon. Intraplate earthquakes are less common than seismic events in active tectonic regions, but they are known to reach large magnitudes. The fact that propagation of seismic energy is more efficient in at least some intraplate regions coupled with the general lack of engineering precautions against the occurrence of nearby earthquakes in these regions dramatically increases the potential destructiveness of a large intraplate event. In addition to the implications for seismic hazard evaluation, the general lack of knowledge concerning intraplate seismicity makes discrimination of such events from nuclear explosions very difficult. The problem which this study addresses is therefore to correlate what is known about intraplate seismicity, and to apply old and new research techniques to this study in order to develop a better understanding of the characteristics of the events.

General Method

In order to circumvent the limitations placed on studies of intraplate seismicity by the infrequent occurrence of such earthquakes, data from sources outside of seismology must be incorporated and evaluated in a study such as this one. Collection and synthesis of information from precise leveling, theoretical geomechanics, sea level observations, geomorphology, photogeology, the sedimentary record, igneous activity and faulting

have been undertaken and are continuing. Several literature reviews on related subjects have been completed and others are being compiled. A complete data set of elevation change measurements for the eastern United States has been prepared in cooperation with the National Geodetic Survey. This leveling data is being used to provide valuable information on vertical crustal movements in the eastern United States. Theoretical computations are being used to derive physical models of the forces which may be responsible for these leveling derived movements. The study group in photogeology is continuing to obtain and analyze ERTS and SKYLAB photographs of Eurasia and the United States. Special U-2 missions have been scheduled to provide detailed coverage of regions of particular interest in the United States. Mapping of photo features is being integrated with available seismic fault plane solutions, seismicity patterns, and in situ stress measurements. Field excursions are being undertaken to verify and identify features indicated in aerial photographs of the eastern United States, as well as to investigate areas of particular interest as suggested by leveling and seismic studies.

In addition to the detailed research concerning the eastern United States, considerable effort is being directed at another intraplate region, China. In attempting to study the seismicity of intraplate regions one finds that mainland China is ideally suited for this type of investigation because of its relatively high seismic activity and large number of destructive earthquakes. In addition, the recorded history of Chinese earthquakes goes back much farther than any other area in the world, thus making China the best location for the study of earthquakes with time. The use of the ERTS imagery and geomorphology permit one to determine recent crustal movements and to better define the tectonic

structure of China. Study of individual earthquake series and their aftershocks is being carried out in order to define fault trends and to investigate the space, time, and magnitude variations along these zones of weakness. It is hoped that such studies will be able to determine the cause of the larger earthquakes such as the 1966 series near Hsing-t'ai in an area that was previously thought to be seismically inactive.

In order to evaluate the generality of the conclusions reached in the detailed research concerning the eastern United States and China, results of similar studies in other regions, particularly in Japan, Europe, and the Soviet Union, are being examined so that any fundamental relationships common to all areas can be discerned and contrasts understood.

Technical Results

Our efforts toward understanding normally aseismic regions with an integrated, interdisciplinary approach have most recently been progressing on two major fronts, with specific programs under each:

- (1) Seismotectonics of China and surrounding region
 - (a) Investigation of patterns of historical and instrumental seismicity.
 - (b) Preparation of a photo-mosaic of China from LANDSAT-1 satellite imagery.
 - (c) Comparison and correlation of geologic and tectonic features from mosaic with seismicity.
 - (d) Examination and compilation of work published by the Chinese.
 - (e) Quaternary faulting in nearby Taiwan.

(2) Recent vertical crustal movements

- (a) Correlation of regional surface deformation as measured by releveled with geologic structure in the eastern United States.
- (b) Comparison of tide gauge data with leveling data along the eastern seaboard of the United States.
- (c) Evaluation of the refraction error in precise leveling.
- (d) Indication of fault movement from leveling data.
- (e) Field study of earthquakes in the eastern United States.

Following are summaries of research results not previously reported in detail. Comprehensive technical discussions of each summary are appended.

China Research: Summary

China is one of the most seismically active continental regions in the world. In order to study the large and destructive earthquakes that occur there, detailed earthquake maps were produced from both the historical record and from instrumental epicenters. The results of this study demonstrate how dramatically the seismicity pattern has changed with time in China. Eastern China was far more active in historical times than it is today. The Shansi graben has been nearly aseismic for the past 70 years and yet from the historical record it is known that some of China's most destructive earthquakes occurred there in the past.

In order to compare observable geologic features in China with earthquake patterns, a mosaic of LANDSAT-1 imagery was prepared at the same scale as the seismicity maps. This comparison reveals different zones of earthquake activity that correlate with geological and tectonic regions. Activity is mainly concentrated in faulted mountain belts and

nearly absent from the large undeformed basins. A continuing study reveals that most of the large earthquakes occur on or near major fault zones.

See Appendix A for a detailed discussion of these results.

Quaternary Faulting in Eastern Taiwan: Summary

Several recent hypotheses suggest that the intraplate seismicity within China is related to the tectonic activity along nearby plate boundaries. One poorly understood nearby plate boundary lies in Taiwan. There has been conflicting evidence on what type of boundary this is. Whether two plates converge here or slide by one another might change the predicted stress pattern within China. Therefore, geologic field work, partially supported by the AFOSR, was undertaken in Taiwan to help resolve this problem. A detailed report is attached as Appendix B. The main conclusion is that there has been a complicated combination of convergent and strike-slip motion in Taiwan over at least the past few million years.

Recent Vertical Crustal Movements: Summary

Study of recent vertical crustal movements via leveling data has focused on the eastern seaboard of the United States. A comparison has been made of the elevation changes indicated by leveling and those indicated by sea level measurements. It has been found that a significant disagreement exists between the two data sets. Profiles of vertical crustal movement from Maine to Florida have been constructed from these data sets using various models for distributing the discrepancies between them. Inspection of these profiles indicates that, in spite of the apparent contradictions within the data, several persistent crustal movement features along the profile correlate with geologic and tectonic features, indicating that real crustal movements are being measured.

Leveling and tide gauge data have also been examined for evidence of short period (about 100 years) tectonic movements. There is evidence for such movements, although the uncertainties in both leveling and tide gauge methods as well as the limited amount of relevant measurements preclude the unequivocal acceptance of their existence. Analysis is also being made of leveling profiles to determine if the Atlantic coastal plain is tilting down to the coast, as indicated in earlier studies. Preliminary results confirm this model, although a large number of exceptions have been found. The relationship, if any, between seismicity and these crustal movements remains ambiguous, although a number of interesting correlations have been noted. It is clear that more field leveling must be done in order to begin to define this relationship.

See Appendix C for a detailed discussion of these results.

Fault Movement and Leveling Data: Summary

When near surface faults suffer displacement with a significant vertical component (due either to earthquakes or gradual slip), one would expect to see relatively steep tilts in the surface deformation pattern derived from repeated levelings across active faults.

One of the most striking examples in the leveling data of the eastern United States which resembles fault displacement was noted in western Kentucky, just inside the Mississippi Embayment. After a detailed study of the data and the region, it was concluded that a fault here is indeed a plausible explanation of the anomalous movement seen in the leveling data. See Appendix D for a detailed discussion of these results.

Other examples of features in the leveling data possibly indicative of fault movement need to be investigated, especially in the western United States.

The Refraction Error in Precise Leveling: Summary

Changes in the index of refraction of light, caused mainly by changes in air temperature, may cause systematic errors in leveling. Comparisons of two levelings with different errors will result in apparent, but unreal, vertical movements. Because our work is in part concerned with leveling data, the possible effect of such an error was investigated theoretically. Preliminary results with simple temperature gradients suggest that this error is not significant, but all possible temperature gradients have not yet been investigated thoroughly. This investigation is continuing. See Appendix E for a detailed discussion of these results.

Field Study of Earthquakes in Eastern United States

Evidence of surface faulting during an earthquake in an intraplate area would increase our understanding of such events by demonstrating that the earthquake was associated with faulting instead of another mechanism, possibly by showing that the earthquake occurred along a pre-existing fault, and by partially determining the direction of the stresses which caused the earthquake. Therefore our interest in field study of earthquakes in the eastern United States has continued. Unfortunately, no such evidence has yet been found.

A search for surface faulting was made during a two-day field trip to Plattsburgh, New York, immediately following an earthquake there on 9 June 1975. The earthquake was small, magnitude 3.7. The local geology consisted mainly of undeformed Cambrian sandstone. This area was glaciated during the Pleistocene. We searched for both fresh fault scarps and faults which offset glacial striations. No convincing evidence for either was found. Although surface faulting is rarely seen for earthquakes this small, the importance of such faulting warranted this investigation.

China Research

by Richard Cardwell

Asia is one of the most seismically active continental regions in the world. The study of earthquakes in intraplate regions has received less attention than the seismicity related to subduction zones. The problem of how and why intraplate earthquakes occur is poorly understood due to the sporadic and complicated nature of their occurrence.

The study of intraplate earthquakes is necessary for understanding the tectonics of continental regions and critical in evaluating the seismic risk of a populated area. The study of Chinese seismicity is crucial for understanding intraplate tectonics. The Chinese record of seismicity is not only the longest one available, covering over 3000 years, but in addition it contains many events with magnitude greater than eight. The reasons for such large magnitude events are very poorly understood. China is not alone in possessing large and destructive earthquakes. The Charleston earthquake of 1882 is an example of such an event in North America. In recent years various authors have attempted to study the seismicity and tectonics of Asia.

The major emphasis of previous papers has been on the tectonics of China and surrounding regions by studying the large earthquake distribution ($m \geq 6$), fault plane solutions, reviews of geological literature, and temporal variations of earthquake parameters. The most complete compilation of the state of stress in Asia through the study of fault plane solutions are the papers by Shi et al. (1973), Molnar et al. (1974), and Molnar et al. (1975). These studies are important for understanding the present state of stress in Asia. These papers also briefly review the geological literature relevant to the tectonic structure.

The distribution of seismicity in Asia has been described by Li and Gorshkov (1957), Min (1957), Mei (1960), Lang and Sun (1966), and Shi et al. (1973), Molnar et al. (1975), Academia Sinica (1956, 1970), and Lee (1957). A history of early compilations of Chinese earthquake data is given by Drake (1912). The first maps of strong earthquake epicenters in China was published by Li and Gorshkev in 1957. For the most part, the previous studies investigated the large events ($m \geq 6.0$) for varying intervals of time from historical records and instrumentally recorded data. For example, Shi et al. (1973) studied the seismicity pattern for events with magnitude ≥ 6.0 from 1500 A.D. until 1971. Molnar and Tapponier (1975) included a map of historical and instrumentally located events only for magnitudes greater than 7.0 with the exception of well located events between 1961 and 1970. The most extensive historical compilation is by Academia Sinica (1956). This is a collection from various sources of varying quality. Only Mei (1960) has attempted to look at the detailed historical and instrumental seismicity for magnitude less than 6.0. Unfortunately, that study in 1960 used data from various sources and made no attempt to discuss the compatibility of the different data sets. In addition, there was little attempt to relate the overall seismicity pattern to the tectonics of Asia. It is clear that with the increasing interest in Asian tectonics it is necessary to have an accurate representation of Asian seismicity to correlate with other geological and geophysical data.

The main purpose of this report is to provide a complete and detailed description of the seismicity of China and surrounding regions from both the historical and instrumental records. Carefully chosen data sources are used to produce maps of both historical seismicity (1177 B.C. through 1903 A.D.) and up to date instrumentally located seismicity (1904 through

February 1975).

By carefully choosing the most reliable data for any period of time, one can produce accurate representation of Asian seismicity. In addition to the seismicity maps a photomosaic of LANDSAT-1 imagery was produced at the same scale. Because of the recent availability of space photography, it is possible for the first time to produce a mosaic that one can overlay with a seismicity map in order to directly observe the correlation of earthquakes and geologic features on a large scale. This is accomplished by using the computer to produce a suitable map projection that best matches the LANDSAT-1 imagery. One can then easily plot seismicity and other geophysical data on the same projection to correlate with the observable features. The LANDSAT-1 imagery has made possible new evaluation of faulting and linears in Asia. In addition, it allows direct comparison of earthquake patterns with visible ground features such as linears, faults, and volcanism.

A set of criteria that may distinguish faults active during the Quaternary from other lineations on the imagery has been developed. These lineations are being studied at a scale of 1:1,000,000 and a map of possible Quaternary faults is being constructed on a scale of 1:6,000,000. This map is to be compared with both the historical and instrumental seismicity maps, thereby providing evidence to distinguish which faults might have been active during historic time. This approach avoids the problems of trying to correlate seismicity with lineations that are not faults or that are faults that have been inactive since the Precambrian. In many cases these lineations have been correctly identified as Quaternary faults from the geologic literature. Knowledge of Quaternary faulting is of considerable importance to the understanding of the contemporary tectonics of Asia.

The purpose of this report then, is to make a detailed study of seismicity in China and surrounding regions. This study will be a valuable complement to the published fault plane solution studies and the synthesis of other geological and geophysical data. This report is composed of several sections. Section I will describe the preparation of the LANDSAT-1 imagery and the choice of map projection used for the seismicity maps. Section II will discuss the quality of the earthquake data and the spatial distribution of seismicity. The historical and instrumental seismicity maps as well as the LANDSAT-1 mosaic have been sent prior to this report. A map of Quaternary faulting determined from LANDSAT-1 imagery is being developed.

Section I: LANDSAT-1 Imagery

The use of remote sensing techniques is becoming increasingly useful in the earth sciences. The development of orbital photography using multispectral imagery has proven very valuable for geologic mapping purposes. NASA's earth resources program began in 1963 and LANDSAT-1 (formerly ERTS-A) was one of the first space satellites to produce high resolution multispectral imagery and digital data of the earth. It had the capability of producing coverage over most of the earth on an 18-day repetitive cycle. The images from a given region had sidelap from adjacent orbits and overlap in the direction of flight. This overlapping of images permits the construction of a mosaic of individual frames of a large area. Each frame covers about 100 nautical miles on a side. Because the orbit was also sun synchronous, the image for a given location was taken at the same local time for each pass of the satellite. This capability permits one to choose nearly cloud-free and well-illuminated scenes from a number of images taken. Four multi-spectral scanner wave bands are available in different wavelengths.

Each image is therefore a uniformly illuminated, roughly planimetric, vertical view covering a large portion of the earth's surface. A mosaic of these images is very close to being orthographic, and is close to being like an Albers Equal Area Projection or a Lambert Conic Conformal Projection. A mosaic of China and surrounding regions was compiled from over 1000 9-inch by 9-inch individual photos with little or no cloud cover. The photos were mostly uncontrolled Band 7 imagery (0.8 to 1.1 micrometers) at a scale of 1:1,000,000. The stated resolutions of these photos is about 70 m (ERTS Data Users Handbook, 1972). This original mosaic measured 8 m by 5 m and was composed of 24 1.3 m by 1.3 m masonite boards. Only a slight stretching of the images during mounting was needed to join

adjacent features along the edges of the images. The mosaic was controlled by matching features with the 1972 Operational Navigation Chart (O.N.C.) (1:1,000,000 scale).

The resulting mosaic covers an area from south of the Himalayas to Lake Baikal and from the Hindu Kush in the west to Taiwan in the east. From a glance at a world seismicity map one can see that the tectonics of this region appear to be unrelated to the rest of Eurasia. Because LANDSAT-1 experienced recording difficulty after March 1973, there are some gaps in the photo coverage. These gaps were filled with the O.N.C. map series at the same scale. The resulting mosaic is nearly orthographic with an accuracy of ± 10 km when compared to O.N.C. Lambert Conic Conformal Projections. All photo interpretation work was done from this 1:1,000,000 scale original. For practical purposes, the original mosaic was reduced to a 1:6,000,000 scale. This format measures 101 cm by 81 cm. In order to accurately plot large quantities of seismic, geological and geophysical data, a computer with an automated plotting routine was used to make various maps. In order to directly compare this data with the LANDSAT-1 mosaic it was necessary to find the map projection that best matches the imagery of the whole region. The projection should have minimal scale and angular distortion, i.e. it should be conformal. In addition to showing true shapes as the imagery does, the projection should have the shortest distance between two points be nearly a straight line. This compromise of shape, area, and scale is best suited to Lambert's Conic Conformal Projection with two standard parallels.

The 1:6,000,000 scale mosaic is best matched by this projection with standard parallels at 33°N and 45°N . This projection provides an excellent overall fit to the mosaic. The scale factor or scale distortion at the latitude extremes is only 1.01 and at the middle latitude it is only .99,

compared with 1.00 at the standard parallels. It is not surprising that Lambert's Conic Conformal Projection should match the entire mosaic so well, because the O.N.C. maps are nearly perfectly matched to the individual photos using the same projection. The use of this projection for seismicity data now allows a direct comparison of earthquake epicenters with observable tectonic features. In making these studies the data were plotted on clear plastic sheets and overlaid directly on the mosaic.

The physiographic features of Central Asia are easily discernable from the mosaic. In the southwest is the concave northward arc of the Great Himalaya Range and the Tibetan Plateau. North of the plateau are many east-west trending features such as the Kunlun and Altyn Tagh Mountains, the Tarim Basin, the Tien Shan, the Dzungarian Basin, and the NW-SE trending Altai Mountains. West of the Tarim Basin are the Pamir Mountains and south of them are the Hindu Kush. On the east of the Tarim Basin is the Tsaidam Basin between the Kunlun and Altyn Tagh Mountains. Between the Himalaya Range and southeastern China are the north-south trending ranges of the Kang Ting Mountains. East of the Altyn Tagh Mountains is another roughly east-west trending mountain belt of the Nan Shan. East of these ranges are the Ordos Desert, the Shansi Graben system, and the North China Plain.

North of the Ordos Desert are the Gobi Desert and the northeast-trending features of Lake Baikal and the Greater Kingan Range. To the east is the Manchurian Plain. Off the coast of southeastern China are the islands of Taiwan and Hainan. Note that the coverage on this mosaic does not include the Ryukyu Islands, the Philippines, or southwestern Japan. The political boundaries of China and Mongolia were taken from the Peoples Republic of China, Atlas (1971).

The uniform illumination of LANDSAT-1 imagery is readily suited to

lineament analysis. One can immediately recognize numerous linear features from 10 km up to 1000 km in length. The apparent large shear fault between the Tarim Basin and the Tibetan Plateau can be readily traced for hundreds of kilometers. Caution must be exercised in relating observed linears to geologic phenomena. A careful study of such linear features is currently being pursued.

Section II: Seismicity - Data

The purpose of this section is to give a complete and consistent evaluation of the seismicity of China from both the historical and instrumental records. The most important earthquake parameters for the study are the epicenter, depth, and magnitude. Only by carefully defining the data sets of earthquakes used can one make a significant correlation of seismicity with other data such as Quaternary faulting and the major observable geologic features for this intraplate area. Note that no relocations of individual hypocenters have been attempted. This study includes over 5,000 earthquakes and attempts to describe the overall patterns of seismicity in China using data from other sources. This paper attempts to select the best data available on hypocenter and magnitude for any given period of time. The five sources of data used in this paper and the years covered are listed below.

1177 B.C.-1903 A.D. Chinese Earthquake Catalog (1970),
Academia Sinica, Institute of Geophysics.

1904-1952 Seismicity of the Earth (1954), Gutenberg and
Richter.

1953-1965 The Seismicity of the Earth (1969), Rothé.

1966-1970 Bulletin of the International Seismological
Centre (I.S.C.)

1971-Feb. 1975 Preliminary Determination of Epicenters (P.D.E.)

Each of these sources will be discussed below.

One of the first seismic stations in China was established at Zeikawei in 1904, but before 1953 China had few seismic stations (Lee, 1957). Gutenberg and Richter have reliably determined instrumental epicenters for earthquakes back to 1904. In order to get an adequate description of Chinese seismicity one must include the historical events

recorded by newspapers and historical chronicles.

In 1956 the Academia Sinica published a 2 volume set entitled Chronological Tables of Earthquake Data of China. This is the most extensive compilation of earthquake data of China available. It was compiled by the Third Institute of History, Academia Sinica, from dynastic histories, local annals, memoirs, newspapers, and seismic station reports in the later years. Mei (1960) discusses the historical compilation of data from distinct records. These volumes contained over 3,000 years of earthquake data.

These data were later compiled in 1970 into the Chinese Earthquake Catalog by the Academia Sinica, Institute of Geophysics (in Chinese). The period of time covered was from 1177 B.C. to 1949 A.D. In this work intensities were assigned to all areas that reported a given earthquake. The epicenter was assigned to the region of greatest destruction. Lee (1958) determined an empirical relationship between intensity at the epicenter and the surface wave magnitude (M) based on a study of instrumentally located earthquakes with well determined magnitudes and intensities. This magnitude (corresponding to M of Gutenberg and Richter) was assigned to historical earthquakes and ranges in magnitude from 4.75 to 8.5. Lee estimated that this magnitude determination is accurate to half a scale of magnitude. This empirical formula between magnitude and intensity has been updated by Savarensky and Mei (1960), Mei (1965), and most recently by Chen et al. (1975). More modern relationships include the effect of the focal depth, but from Chen et al. (1975), it appears that the relationship determined by Lee is still good to ± 0.5 magnitude units.

Even though the first reported event is 1177 B.C., more thorough coverage begins from the Han Dynasty in 206 B.C. where several provinces

have a continuous record up to the present. The description of smaller tremors are more complete and detailed after about 1500 due to the increase in the number of local chronicles (Mei, 1960). The historical seismicity data depend crucially on the population density. Therefore, the historical seismicity data for western China and Taiwan are incomplete due to the sparse populations in these areas or lack of chronicles.

This study is primarily interested in the seismicity of China and has not incorporated any historical data for areas outside this region. Thus although there have probably been many historical earthquakes in the Himalayas, these events have not been reported in the Chinese earthquake catalog because of the low population density there. Likewise, the Chinese did not report the large Assam earthquake of 1897 in their compilation because it occurred outside of China and it is not included in this compilation. In summary, the historically reported seismicity data for eastern Mainland China is relatively complete from about 1500 A.D.

The instrumentally recorded data are composed of the four above mentioned sources. The data from Gutenberg and Richter (1954) covers the period from 1904 to 1952. The body wave magnitude m is used for the events reported. For the larger events the revised magnitudes (M) as given by Richter (1958) are used. The data from Rothe (1969) cover the period 1953 to 1965. The magnitude, M , is taken as the average of the magnitudes given by different stations after standardizing the different station magnitudes. The data from the I.S.C. and P.D.E. are used for the years 1966 to February 1975. Both data sets use the unified body wave magnitude (m_b) defined by Gutenberg and Richter (1956).

For the I.S.C. and P.D.E. earthquake data those events located with less than ten stations were rejected. Although ten is an arbitrary number, it was found upon examination that the earthquakes with less than ten

Section II: Seismicity - Discussion

Upon examining the seismicity maps of China and surrounding regions several features immediately become apparent. The most obvious feature is that China is extremely active for a continental region. By examining a map of world seismicity it readily becomes apparent that no other large continental region in the world has as much seismic activity as China does. The second interesting feature is that this region has had some extremely large earthquakes throughout both the historical and instrumental record. There have been 29 large earthquakes with magnitude of 7.8 or greater shown on the map excluding those in the oceanic subduction zones. A third interesting feature is that there are two continental regions of intermediate depth earthquakes just outside of China in the Hindu Kush and northwestern Burma. These facts will be discussed more below, but they do point out that China and the surrounding regions are not typical intraplate areas.

In discussing the seismicity distribution it is important to note the large earthquakes. The large magnitude events not only are located more accurately, but they are also more important tectonically. If there is to be any pattern in the epicenter distributions, it should be more apparent for earthquakes with magnitude greater than 6.0.

Western China is presently far more seismically active than eastern China. The map of historical epicenters shows little to no seismic activity in western China only because western China was relatively unpopulated and most earthquakes occurring there were not recorded. Taiwan does not have good historical records until after 1900 and this explains the lack of activity shown on the historical map. By comparing the instrumental and historical epicenters it becomes apparent that

eastern China was far more active in the past than it presently is.

There are two interesting differences in the historical and instrumental epicenter distributions for eastern China. Whereas south-eastern China is nearly aseismic today, it had a moderate amount of activity in the past. Another more prominent feature is the seismicity distribution in the Shansi Graben system and the North China Plain. It is especially evident that the historical epicenters occur near the graben faults and yet no large events have occurred there in the last 70 years. Many of the other large events to the east occur on or near a system of northeast-striking faults in the North China Plain. This comparison of instrumental and historical seismicity demonstrates that caution should be used in basing seismic risk maps on only a brief instrumental record. It is clear that even the instrumental seismicity for 70 years is inadequate to describe the historical seismicity of China. Both historical and instrumental maps include the complex north-south belt of seismicity between 100° and 110° .

It is obvious from the maps that all earthquakes do not occur along linear fault planes, but that they occur along broad zones of activity. At present it is difficult to determine if the strain release occurs along discrete faults or if it occurs over broad zones of intraplate deformation. Only careful geologic mapping of faults along with accurate locations of earthquakes can determine this.

A brief description of the relationship between seismic activity and geologic features is given below. Western China and surrounding regions are characterized by east-west trending features that are distinctly different from northeast-striking grabens and faults in eastern China. These features are the Himalayan Range, Tibetan Plateau, Tanglha Mountains, Kunlun Shan, Austin Tagh Mountains, Tsaidam Basin, Tarim Basin, Tien Shan,

Dzungarian Basin, and the Altai Mountains.

The nearly aseismic Tarim, Tsaidam, and Dzungarian Basins are quite distinct features as seen on the LANDSAT-1 mosaic. All three basins are roughly east-west trending features and are bounded by more seismically active mountain ranges. In the Altai Mountains to the north of the Dzungarian Basin there have been a few large shallow focus earthquakes such as the 1931 (7.9) and the 1957 (8.3) events. The faults in central Mongolia strike east-west while those in western Mongolia strike to the northwest. Two small intermediate depth earthquakes in the region from Rothe were probably more correctly located as shallow events by the I.S.C. and P.D.E.

South of the Dzungarian Basin are the Tien Shan with east-west striking faults. This range is very active with many large shallow focus earthquakes. The activity increases toward the south in the South Tien Shan. South of this lie the Pamirs and the Hindu Kush. Earthquakes occur into the intermediate depths and the activity is intensely concentrated in an east-west belt below the Hindu Kush.

The Kunlun Shan and Austin Tagh Mountains lie at the northern edge of the Tibetan Plateau and form the southern boundary of the Tarim Basin. The seismicity in these ranges as well as in the rest of the Tibetan Plateau is diffuse. The very large faults at the northern end of the plateau are easily seen in the mosaic. These major faults are similar to the Alpine and Atacama faults in that none of them are well defined seismically by large earthquakes.

To the south of the plateau the seismicity pattern clearly defines the arcuate shape of the Himalayan Mountain Range. The earthquakes are almost all shallow and their magnitudes can be very large, as seen from the large seismicity map. The earthquakes become intermediate depth foci

at the southeastern end of the Himalayas as they did at the northwestern end. There is an increase in both shallow and intermediate depth seismicity in this region of northern Burma.

The very complex north-south seismic belt lies to the east of the Tibetan Plateau. This is a region of folded and faulted north-south trending mountain ranges that lie east of the nearly aseismic area of southeastern China. At the northern end of the seismic belt are the east-west faulted Nan Shan. This range is well defined seismically and several large shallow focus earthquakes have occurred here both historically and during the instrumental periods.

East of this belt lie the northeast-striking Shansi Graben system and the faults of the North China Plain. This has been a region of large shallow focus earthquakes throughout history. Some of these events include the great earthquake near Peking in 1679 and the destructive series of earthquakes near Hsing-t'ai in 1966. Note that the 1966 series was one of several sequences of many events that occurred throughout China. Further east along the Tancheng-Lukiang fault zone was the magnitude 8.5 earthquake of 1668 and the recently predicted Liaoning Province earthquake of February 1975 (Allen et al., 1975). Except for near this fault, the Manchurian Plain appears relatively aseismic.

The northeast trend to tectonic features extends north to Lake Baikal, which is a faulted graben system similar to the Shansi Graben system. Here there are presently shallow earthquakes occurring in and near the graben. To the southeast is the subduction-related seismicity of the Ryukyus and the Philippines. Taiwan is the most active area of this entire region studied. Here the Longitudinal Valley fault is defined seismically along with the plate margin seismicity of the Philippine plate.

LARGE EARTHQUAKES OF CHINA AND SURROUNDING REGIONS

DATE	ORIGIN TIME (G.M.T.)	LATITUDE (°N)	LONGITUDE (°E)	MAGNITUDE	DEPTH (KM)
17/07/303	—	36.3	111.7	8.0	—
23/01/1536	—	34.5	109.7	8.0	—
29/12/1634	—	25.0	119.5	8.0	—
25/07/1668	—	35.3	118.6	8.5	—
02/07/1669	—	40.0	117.0	8.0	—
18/05/1695	—	36.0	115.0	8.0	—
03/01/1759	—	38.9	106.5	8.0	—
16/07/1883	—	25.2	103.0	8.0	—
22/08/1902	—	39.5	76.0	8.25	—
07/06/04	08:17:54	40.0	134.0	7.9	350
24/03/04	20:59:54	30.0	130.0	7.9	0
04/04/05	00:50:00	33.0	76.0	8.6	0
02/06/05	05:39:42	34.0	132.0	7.9	100
09/07/05	09:40:24	49.0	97.0	8.4	0
23/07/05	02:46:12	49.0	98.0	8.7	0
22/12/06	18:21:00	43.5	88.0	8.3	0
07/07/09	21:37:50	36.5	70.5	8.1	230
10/11/09	06:13:30	32.0	131.0	7.9	150
12/04/10	00:22:13	25.5	122.5	8.3	200
03/01/11	23:25:45	43.5	77.5	8.7	0
18/02/11	18:41:03	40.0	73.0	7.8	0
15/04/11	14:26:00	29.0	129.0	8.7	160
23/05/12	02:24:06	21.0	97.0	7.9	0
05/06/20	04:21:28	23.5	122.0	8.3	0
16/12/20	12:05:48	36.0	105.0	8.6	0
15/11/21	20:56:38	36.5	70.5	8.1	215
22/05/27	22:32:42	36.75	102.0	8.3	0
10/03/31	21:18:40	47.0	90.0	7.9	0
15/01/34	08:43:18	26.5	86.5	8.4	0
14/02/34	03:59:34	17.5	119.0	7.9	0
12/09/46	15:20:20	23.5	96.0	7.8	0
20/12/46	19:19:25	32.5	134.5	8.4	0
29/07/47	13:43:22	28.5	94.0	7.9	0
13/08/50	14:09:30	28.5	96.5	8.7	0
18/11/51	09:35:47	30.5	91.0	7.9	0
27/05/57	00:09:28	56.4	116.5	7.9	33
4/12/57	03:37:48	45.2	99.2	8.3	33

References

- Academia Sinica, Seismological Committee, 1956, Chronological Tables of Earthquake Data of China, Science Press, Peking, 2 vol., 1653 pp. (in Chinese).
- Academia Sinica, Institute of Geophysics, 1970, Chinese Earthquake Catalog, Academia Sinica, Peking, 361 pp. (in Chinese).
- Allen, C.R., M.G. Bonilla, W.F. Brace, M. Bullock, R.W. Clough, R.M. Hamilton, R. Hofheinz, C. Kisslinger, L. Knopoff, M. Park, F. Press, C.B. Raleigh, and L.R. Sykes, 1975, Earthquake research in China, Trans., Am. Geophys. Union, 56, p. 838-881.
- Central Intelligence Agency, 1971, Peoples Republic of China, Atlas, U.S. Government Printing Office, Washington, D.C., 82 pp.
- Chen, P., and J. Liu, 1975, A study of the relation between seismic magnitude and intensity by using the dislocation model, Acta Geophysica Sinica, 18, 183-195.
- Drake, N.F., 1912, Destructive earthquakes in China, Bull. Seism. Soc. Am., 2, 40-133.
- Earth Resources Technology Satellite Data Users Handbook, General Electric Document No. 71504249, Sept. 1971, Revised, 1972.
- Gutenberg, B., and C.B. Richter, 1954, Seismicity of the Earth and Associated Phenomena, Princeton University Press, 310 pp.
- Gutenberg, B., and C.F. Richter, 1956, Magnitude and energy of earthquakes, Annals. Geofis., 9, 1 ff.
- Lang, W.J., and R.J. Sun, 1966, Seismicity in: Atlas of Asia and Eastern Europe to Support Detection of Underground Nuclear Testing, U.S. Geol. Surv., vol. 3, Washington, D.C.
- Lee, S.P., 1957, The map of seismicity of China, Acta Geophysica Sinica, 6, 127-158 (in Chinese).

- Lee, S.P., 1958, A practical magnitude scale, Acta Geophysica Sinica, 7, 98-102 (in Chinese).
- Li, S.P., and G.P. Gorshkov, 1957, A map of the seismic regions of China, Acta Geophysica Sinica, 6.
- Mei, S.Y., 1960, The seismic activity of China, Akad. Nauk. SSR Izv. Ser. Geofiz. (English transl.), 254-264.
- Min, T.C., 1957, Study of strong earthquakes from historical records, Acta Geophysica Sinica, 6, 49-58.
- Molnar, P., T.J. Fitch, and F.T. Wu, 1973, Fault plane solutions of shallow earthquakes and contemporary tectonics in Asia, Earth Planet. Sci. Letters, 19, 101-112.
- Molnar, P., and P. Tapponnier, 1975, Cenozoic tectonics of Asia: effects of a continental collision, Science, 189, 419-426.
- Richter, C.B., 1958, Elementary Seismology, W.H. Freeman and Company, Inc., San Francisco, 768 pp.
- Rothé, 1969, The Seismicity of the Earth, UNESCO, Belgium, 336 pp.
- Savarensky, E.F., and S.Y. Mei, 1960, On the evaluation of the intensity of earthquakes in the territory of China, Akad. Nauk. SSR Izv. Ser. Geofiz. (English transl.), 86-88.
- Shi, Z.L., W.L. Huan, H.R. Wu, and X.L. Cao, 1973, On the intensive seismic activity in China and its relation to plate tectonics, Sci. Geol. Sinica, 281-293 (in Chinese).

APPENDIX B

QUATERNARY FAULTING IN EASTERN TAIWAN

James E. York

Department of Geological Sciences

Cornell University

Kimball Hall

Ithaca, New York 14853

ABSTRACT

The Longitudinal Valley of eastern Taiwan probably marks the suture of a late Cenozoic collision between an island arc and the Asian continent. At present, the Longitudinal Valley represents the main active tectonic feature of the boundary between the Eurasian and Philippine plates in Taiwan. Previously published instantaneous poles of rotation indicate that this boundary in the Taiwan region is predominantly convergent with a component of left-lateral strike-slip motion, although cases of historic surface faulting suggest that the boundary is mainly strike-slip. New geologic field work provides evidence of both convergence and strike-slip motion in the Longitudinal Valley during the Quaternary. Some convergence is apparently also occurring west of the Longitudinal Valley, resulting in uplift of the Central Range.

Key words: Taiwan, faulting, Quaternary tectonics.

The island of Taiwan, lying between the Philippine Sea and mainland China, is part of the seismically active region near the ends of the Ryukyu and Manila trenches (Figure 1). The seismicity of Taiwan is concentrated in the eastern part, although earthquakes do occur throughout the island. Known historic surface faulting in Taiwan (Figure 2) and fault plane solutions near Taiwan (Wu, 1970) indicate that the tectonics of the Taiwan region is complicated, but from the geology, one main boundary in Taiwan between the Philippine and Eurasian plates appears evident. This boundary is the Longitudinal Valley (Figure 2). One main plate boundary amid a zone of active faults of different types is typical of other seismically active areas also, such as California.

Because the Longitudinal Valley separates two geologically distinct mountain ranges, one of which has island arc affinities, it probably represents the suture of an island arc-continent collision (Biq, 1972). The age of this collision is late Cenozoic. Earthquakes extending to depths of 100 km beneath Taiwan (Katsumata and Sykes, 1969) probably result from subduction associated with the closing of the oceanic basin which probably once existed between the two mountain ranges. From studying large earthquakes elsewhere along the Philippine-Eurasian plate boundary to determine the pole and rate of rotation, Fitch (1972) concluded that this boundary in Taiwan is predominantly convergent. His conclusion is in accordance with the hypothesis that the collision is still occurring. However, surface faulting in 1951 (Hsu, 1962) showed predominantly left-lateral strike-slip faulting. To help resolve the problem of the relative importance of strike-slip versus convergent motion, new geologic field work was undertaken in 1974.

Solving this problem includes the determination of the type and B-3 age of activity of major faults in and along the Longitudinal Valley. Such a study is important for evaluating seismic risk (Allen, 1975), as well as for studying the process of an island arc-continent collision (Dewey and Bird, 1970). In addition to evidence for a strike-slip fault running through the valley, we found evidence for Quaternary thrusting in the southern part of the valley along a fault that may represent the main surface expression of a subduction zone.

GEOLOGY OF TAIWAN

The geology of Taiwan has recently been reviewed by Ho (1967), and only a brief summary will be given here. The island is separated from mainland China by the shallow (less than 100 m depth) Taiwan Straits. Taiwan consists of four main geologic provinces (Figure 2). The Coastal Range consists of Miocene andesites (Tuluanshan Formation), Miocene-Pliocene flysch (Chimei and Takangkou Formations), a Plio-Pleistocene melange (Lichi Formation) that contains exotic blocks interpreted as fragments of oceanic lithosphere, and a Plio-Pleistocene conglomerate (Pinanshan conglomerate) with clasts from the Central Range. These rock units differ considerably from most of the other rock units in Taiwan. The andesites and melange probably represent island arc volcanics and trench deposits, respectively. Eastward dipping thrust faults within the Coastal Range and the sharp boundary between the Coastal and Central Ranges together with the presence of the andesites and melange suggest that an oceanic basin once existed between the two ranges and that this basin was consumed in a subduction zone dipping eastward beneath the Coastal Range. Plate tectonic models with such an interpretation have been presented by Biq (1972), Chai (1972), and Karig (1973), although alternative interpretations have been

given by Jahn (1972) and Murphy (1973). A gravity profile across Taiwan supports the concept of an eastward dipping subduction zone (Lu and Wu, 1974). Intermediate depth earthquakes occur beneath Taiwan (Katsumata and Sykes, 1969; M.T. Hsu, 1971) but do not define a clear direction of dip, perhaps because subduction is presently occurring over a wide zone.

The Central Range contains a schist belt overlain by Paleogene slates and quartzites. The schist belt contains greenschist, marble, black schist, siliceous schist, and migmatite. Deformed fossils in the schists gives a Permo-Triassic age (Yen, 1954). Radiometric dates give ages of 33 and 86 million years (Yen and Rosenblum, 1963), but the ages may be affected by subsequent thermal events. The topography of the Central Range is rugged and steep, despite the high rainfall and abundance of weak schists and slates. The topography probably indicates rapid Plio-Pleistocene and Recent uplift.

The Foothill zone consists mainly of Miocene sandstones and shales and Plio-Pleistocene conglomerates. The conglomerates, which are made of clasts from the Central Range, probably record the rapid uplift of that range. These conglomerates are both overlain and underthrust by the Quaternary sediments of the Coastal Plain.

LONGITUDINAL VALLEY

The linearity, narrowness, and low elevation of the Longitudinal Valley make it prominent on satellite imagery (Figure 3). In addition to this peculiar morphology, the Longitudinal Valley has exceptional thicknesses of alluvium. Thicknesses of about 2 km have been measured by seismic refraction along the western side of the valley (Tsai et al., 1974). Alluvium in the center may well be thicker. Along most of the valley,

alluvium separates the Central and Coastal Ranges by a few kilometers. Spectacular bare alluvial fans are visible on the satellite imagery (Figure 3), as well as on aerial photography (Figure 5).

At a few localities, possible contacts between the two ranges have been described. Yen (1965) described a locality near Juisui (Figure 4) where rocks of the Central Range overthrust young sediments, but these sediments show no clear resemblance to rocks of the Coastal Range. Hsu (1956) reported an outcrop or possibly a large boulder of schist near Fuli (Figure 4) within a few meters of exposures of rocks of the Coastal Range, but the contact relation could not be determined. Only in the southernmost part of the valley do the alluvial deposits narrow sufficiently for geologic contacts to be exposed and traceable across the alluvium (Figure 6).

Quaternary Fault Movements

The seismicity (Figure 1) suggests that eastern Taiwan is the most tectonically active part of Taiwan. Left-lateral strike-slip faulting (Figure 2 and F1 and F2 in Figure 4) in the Longitudinal Valley occurred during two earthquakes in 1951 (Hsu, 1962). The one reported measured strike-slip displacement was 1.63 m (Hsu, 1962). In addition to strike-slip faulting, a smaller component of vertical faulting, with the east side moving up relative to the west side, was observed at some localities in 1951. The fault planes were nearly vertical. Re-triangulation showed average left-lateral movement of 3.65 m across the northern part of the Longitudinal Valley between surveys in 1971 and 1909-1942 (Chen, 1974). Hsu (1962) also described a linear scarp near Chihshang (F3 in Figure 4) with water ponded on the west side. This scarp, preserved at a drainage divide, probably represents Quaternary faulting. The high seismicity, surface

faulting, and linearity of the Longitudinal Valley are good evidence for a continuous major strike-slip fault running through the valley (Allen, 1962).

To complement the field work, aerial photographs were examined during this study. In the northern third of the Coastal Range and a few kilometers east of the Longitudinal Valley, another strike-slip fault appears on air photos (Figure 5 and F4 in Figure 4). The main river in this section of the Longitudinal Valley flows northward, yet many westward flowing tributaries are offset to the south (as viewed from upstream). Such offsets are suggestive of Quaternary left-lateral strike-slip movement. The linear trace of the fault across the varying topography indicates that the fault plane is nearly vertical. Although no historic movement on this fault has been documented, it probably is part of an active system of strike-slip faulting in eastern Taiwan.

In addition to strike-slip faulting, evidence of Quaternary thrust faulting was found during this study in the southern part of the Longitudinal Valley. There a Plio-Pleistocene unit, the Pinanshan conglomerate, is exposed between the slates of the Central Range and the melange unit, the Lichi Formation, of the Coastal Range (Figure 6). The contact between the conglomerate and the melange is a thrust fault that is well exposed in river cliffs. At one locality this thrust fault cuts across a serpentine block in the melange. At another locality, the thrust fault offsets flat-lying alluvial deposits that are probably Quaternary in age (Figure 7 and F5 in Figure 4). Because this fault separates two widely different rock units, a conglomerate with clasts derived from the Central Range and a melange probably formed in an oceanic trench, and because the fault offsets Quaternary alluvial deposits, it appears to be a major fault that has been

accommodating some of the convergent motion between the Philippine and Eurasian plates during the Quaternary.

B-7

West of the Pinanshan conglomerate is another major fault (F6 in Figure 4) was found during this study. The fault separates the conglomerate from the slates of the Central Range. A complicated fault zone is exposed at one locality, but no conclusive evidence to determine the sense of motion on the fault was found. This fault is probably a continuation of the left-lateral strike-slip fault which moved during 1951 farther north, because field work and aerial photograph investigations limit a continuous strike-slip fault to this locality. At least several kilometers of movement has probably occurred on this fault since deposition of the Plio-Pleistocene Pinanshan conglomerate, because the source for the clasts in the Pinanshan conglomerate is not the same source which is depositing gravels presently. Besides quartzites and schists, the Pinanshan conglomerate contains marble, which is absent both from terrace gravels unconformably overlying the Pinanshan conglomerate and from Central Range rocks immediately to the west. Also, the younger terrace gravels contain predominantly slate, which is virtually absent from the older conglomerate. Thus there appear to be two major faults in the southern part of the Longitudinal Valley (Figure 5).

CONCLUSIONS

The Longitudinal Valley, remarkably linear and averaging about 4 km in width, is the major tectonic feature in eastern Taiwan. Yet alluvial fill prevents unambiguous interpretations of the kind of faulting along the valley for most of its length. Fluvial activity probably has been important in determining the morphology of the Longitudinal Valley. The 1951 surface faulting occurred in the alluvium, and evidence for these breaks had been

obliterated by 1974, because of the very active erosional processes during the typhoon season. Along most of the valley the only evidence for Quaternary tectonic activity found during this study was dissected terrace gravels that have been steeply tilted at three localities (near Hualien, Juisui, and Luyeh, Figure 4) and five small hills of younger alluvium that have been tilted and dissected at the western side of the Coastal Range a few kilometers southwest of Tungli (Figure 4).

Only in the southernmost part of the valley were fault zones between major rock units seen. The thrust of the Lichi melange of the Coastal Range over the Pinanshan conglomerate, derived from the Central Range, and Quaternary alluvial deposits may represent the boundary of the island arc-continent collision. Although no historic earthquakes can definitely be attributed to this thrust, its Quaternary activity suggests that it may be a potentially active fault (Allen, 1975). The zone of collision is not simple, however, and certainly strike-slip faulting has been occurring also. The existence of a thrust fault and a probable strike-slip fault, both possibly active, spaced only a few kilometers apart (Figure 6) raises interesting questions about how they were generated, how continued activity might affect the morphology of the Longitudinal Valley, what happens at depth, and what happens farther north in the valley. At present, any answers to these questions are mainly speculative, and hence only possibilities are suggested here.

Fitch (1972) has proposed a simple model that accommodates oblique subduction by two faults, a thrust and a vertical strike-slip fault, instead of one dipping fault with oblique motion. If such a model is applicable to Taiwan, the generation of both types of faults may be explained. Whether continued thrusting will decrease the width and increase the elevation of

the Longitudinal Valley or not largely depends on the rate of erosional processes. Small incremental movements of the Coastal Range westward relative to the Central Range can easily be compensated for by erosion, thereby keeping the width of the valley nearly constant. However, in the southern part of the valley the surface trace of the thrust is in some places west of the main river running south through this part of the valley (Figure 6), and thus there the valley might be closing. Answers regarding what happens to the faults at depth and what type of rocks exist between the faults at depth must depend on further detailed geophysical work on land, some of which is in progress (C.P. Lu, personal communication, 1975), as well as further work on the nearby marine geology. Concerning the northward extension of the thrust fault, no exposures of the thrust were found north of the area in Figure 6. Because no exposures of the strike-slip fault were found in 1974 in the north either, the existence of the thrust at the surface farther north is still an open question.

Not all of the convergent motion in Taiwan between the Philippine and Eurasian plates has been taking place in the Longitudinal Valley. The geology and seismicity of the Central Range plus the fault plane solution by Wu (1970) suggest that thrusting is also occurring there. The geologic evidence supports eastward dipping thrusts there, although right-lateral strike-slip faulting, nearly conjugate to the left-lateral faulting in the Longitudinal Valley, has also occurred near the Central Range during historic earthquakes (Figure 2). Subsequent crustal thickening and isostatic uplift may be responsible for the high topography of the Central Range.

Appreciation is expressed to Biq Chingchang, T. L. Hsu, Hui-Cheng Chang, H. N. Hu, and Hsein-Ching Chang, all of the Geological Survey of Taiwan, for collaboration in doing the field work. Beneficial discussions were held with Y. B. Tsai and Chih-Ping Lu of the Chinese Earthquake Research Center. The manuscript was critically read by M. Barazangi, D. Karig and J. Oliver. This research was supported by the United States-Republic of China Cooperative Science Program of the National Science Foundation under Grant Number OIP-7419400 and by the Advanced Research Projects Agency of the Department of Defense and was monitored by the Air Force Office of Scientific Research under Contract Number AFOSR-73-2494. Cornell University Department of Geological Sciences Contribution Number 000. Reviewed by F. T. Wu.

- Allen, C.R., 1962, Circum-Pacific faulting in the Philippines-Taiwan region: J. Geophys. Res., v. 67, p. 4795-4812.
- Allen, C.R., 1975, Geological criteria for evaluating seismicity: Geol. Soc. Amer. Bull., v. 86, p. 1041-1057.
- Biq, Chingchang, 1972, Dual-trench structure in the Taiwan-Luzon region: Geol. Soc. China Proc., no. 15, p. 65-75.
- Biq, Chingchang, 1974, Taiwan, in Spencer, A.M., ed., Mesozoic-Cenozoic Orogenic Belts, Geological Society, London, p. 501-511.
- Chai, B.H.T., 1972, Structure and tectonic evolution of Taiwan: Amer. J. Sci., v. 272, p. 389-422.
- Chang, L.S., Chow, M., and Chen, P.Y., 1947, The Tainan earthquake of December 5, 1946: Taiwan Geol. Surv. Bull., no. 1, p. 11-20.
- Chen, C.Y., 1974, Verification of the north-northeastward movement of the Coastal Range, eastern Taiwan, by retriangulation: Taiwan Geol. Surv. Bull., no. 24, p. 119-123.
- Dewey, J.F., and Bird, J.M., 1970, Mountain belts and the new global tectonics: J. Geophys. Res., v. 75, p. 2625-2647.
- Fitch, T.J., 1972, Plate convergence, transcurrent faults, and internal deformation adjacent to southeast Asia and the western Pacific: J. Geophys. Res., v. 77, p. 4432-4460.
- Ho, C.S., 1967, Structural evolution of Taiwan: Tectonophysics, v. 4, p. 367-378.
- Hsu, M.T., 1971, Seismicity of Taiwan and some related problems: Internatl. Inst. of Seismology and Earthquake Eng. Bull., v. 8, p. 41-160.
- Hsu, T.L., 1956, Geology of the Coastal Range, Taiwan: Taiwan Geol. Surv. Bull., no. 8, p. 39-63.

- Hsu, T.L., 1962, Recent faulting in the Longitudinal Valley of eastern Taiwan: Geol. Soc. China Mem., no. 1, p. 95-102.
- Jahn, B.M., 1972, Re-interpretation of geologic evolution of the Coastal Range, east Taiwan: Geol. Soc. Amer. Bull., v. 83, p. 241-248.
- Karig, D.E., 1973, Plate convergence between the Philippines and the Ryukyu Islands: Marine Geology, v. 14, p. 153-168.
- Katsumata, M., and Sykes, L.R., 1969, Seismicity and tectonics of the western Pacific: Izu-Mariana-Caroline and Ryukyu-Taiwan regions: J. Geophys. Res., v. 74, p. 5923-5948.
- Lu, C.P., and Wu, F.T., 1974, Two-dimensional interpretation of a gravity profile across Taiwan: Taiwan Geol. Surv. Bull, no. 24, p. 125-132.
- Murphy, R.W., 1973, The Manila trench-west Taiwan foldbelt: a flipped subduction zone: Geol. Soc. Malaysia Bull., no. 6, p. 27-42.
- Richter, C.F., 1958, Elementary Seismology, San Francisco, W.H. Freeman, 768 pp.
- Tsai, Y.B., Teng, T.L., Ysiung, Y.M., and Lo, C.M., 1973, New seismic data of Taiwan region: Inst. of Physics, Academia Sinica, Ann. Rept., p. 223-237.
- Tsai, Y.B., Hsiung, Y.M., Liaw, H.B., Lueng, H.P., Yao, T.H., Yeh, Y.H., and Yen, Y.T., 1974, A seismic refraction study of eastern Taiwan: Petroleum Geology of Taiwan, no. 11, p. 165-182.
- Wu, F.T., 1970, Focal mechanisms and tectonics in the vicinity of Taiwan: Seism. Soc. Amer. Bull., v. 60, p. 2045-2056.
- Yen, T.P., 1954, Some problems on the Tananao schist: Taiwan Geol. Surv. Bull., no. 7, p. 47-50.
- Yen, T.P., 1965, A thrust fault near Juisui, eastern Taiwan: Geol. Soc. China Proc., no. 8, p. 97-99.
- Yen, T.P., and Rosenblum, S., 1963, Potassium-argon ages of micas from the Tanano-schist terrain of Taiwan: Geol. Soc. China Proc., no. 7, p. 80-87.

- Figure 1: Seismicity of the Taiwan region, 1961-1972. Circles represent hypocenters less than 70 km deep; squares, 70-300 km deep. Epicenters redrawn from Tsai et al. (1973). Trench depths in km.
- Figure 2: Geologic provinces of Taiwan (from Biq, 1974). Also shown are known cases of historic surface faulting (data from Chang et al., 1947; Richter, 1958; Hsu, T.L., 1962). Elevations of highest peaks in Central and Coastal Ranges in meters.
- Figure 3: Mosaic of Landsat-I imagery of Taiwan. Imagery of MSS band 5, taken 1 November 1972.
- Figure 4: Longitudinal Valley, Coastal Range, and part of Central Range. Fault localities are referenced in text. Contours at 400, 1000, 2000 and 3000 m.
- Figure 5: Vertical aerial photograph of a fault (arrows) showing left-lateral stream offsets in the northern part of the Coastal Range. A part of the Longitudinal Valley is in the western half of the photograph; some hills of the Central Range are visible along parts of the western edge of the photograph. Fenglin (Figure 4) is in the southwestern quarter of the photograph.
- Figure 6: Geologic map of the southern portion of the Longitudinal Valley. Qal - alluvium, PQp - Pinanshan Conglomerate, PQl - Lichi Formation, MPs - Chimei Formation, Ml - limestone,

Mt - Tuluanshan Formation, Eo - slate and quartzite. See text and T. L. Hsu (1956) for descriptions of rock units. The contacts between Eo and PQp and between PQp and PQl are faults, dashed where approximate and dotted where concealed. Elevations are in meters.

Figure 7: Thrust fault (arrows) separating Lichi Formation (hanging wall) from Pinanshan conglomerate and overlying alluvial deposits (footwall). Distance from top to bottom is about 5 meters.

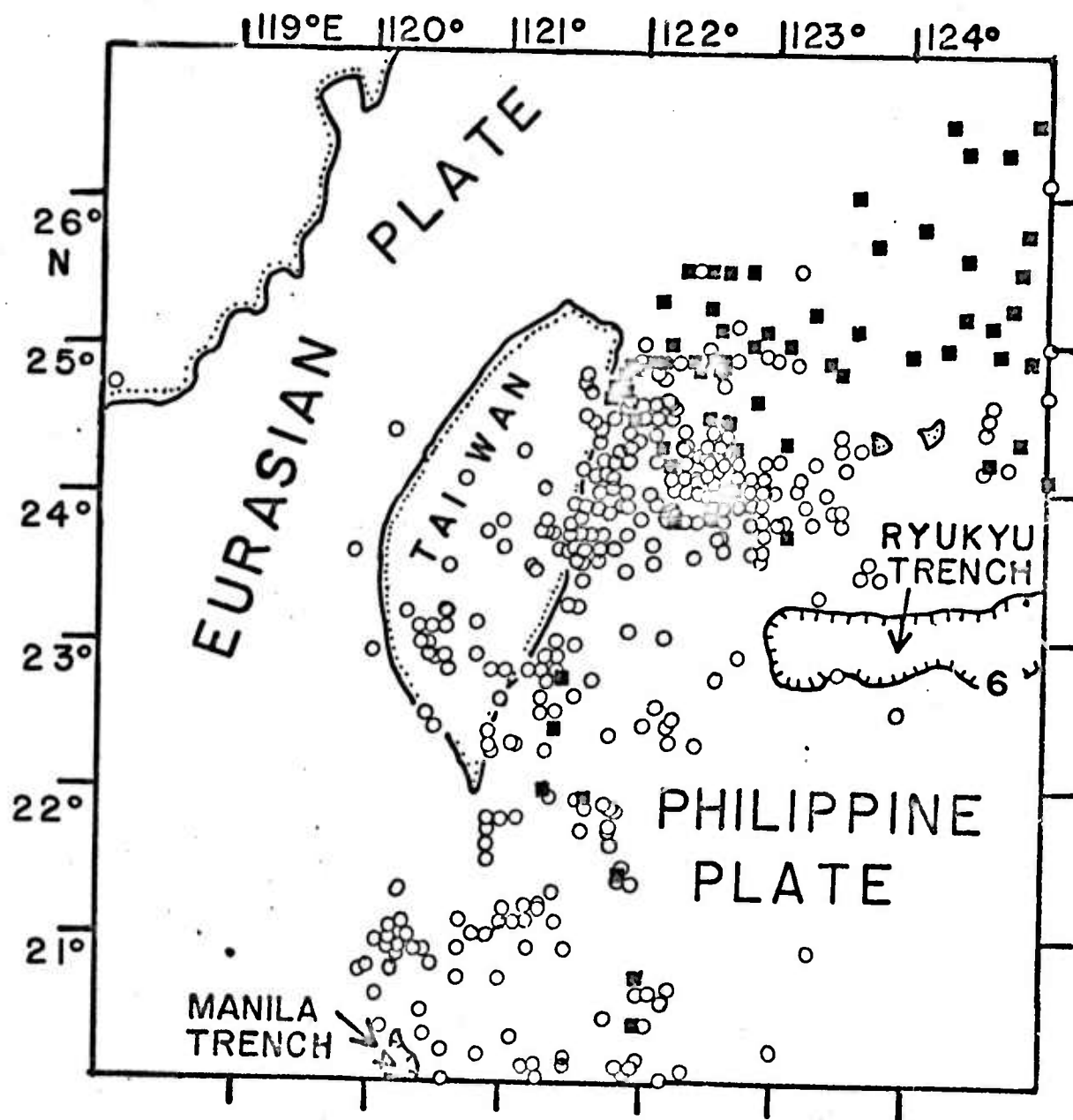


Figure 1.

1120°E

1121°

1122° B-16

25°
N

24°

23°

22°

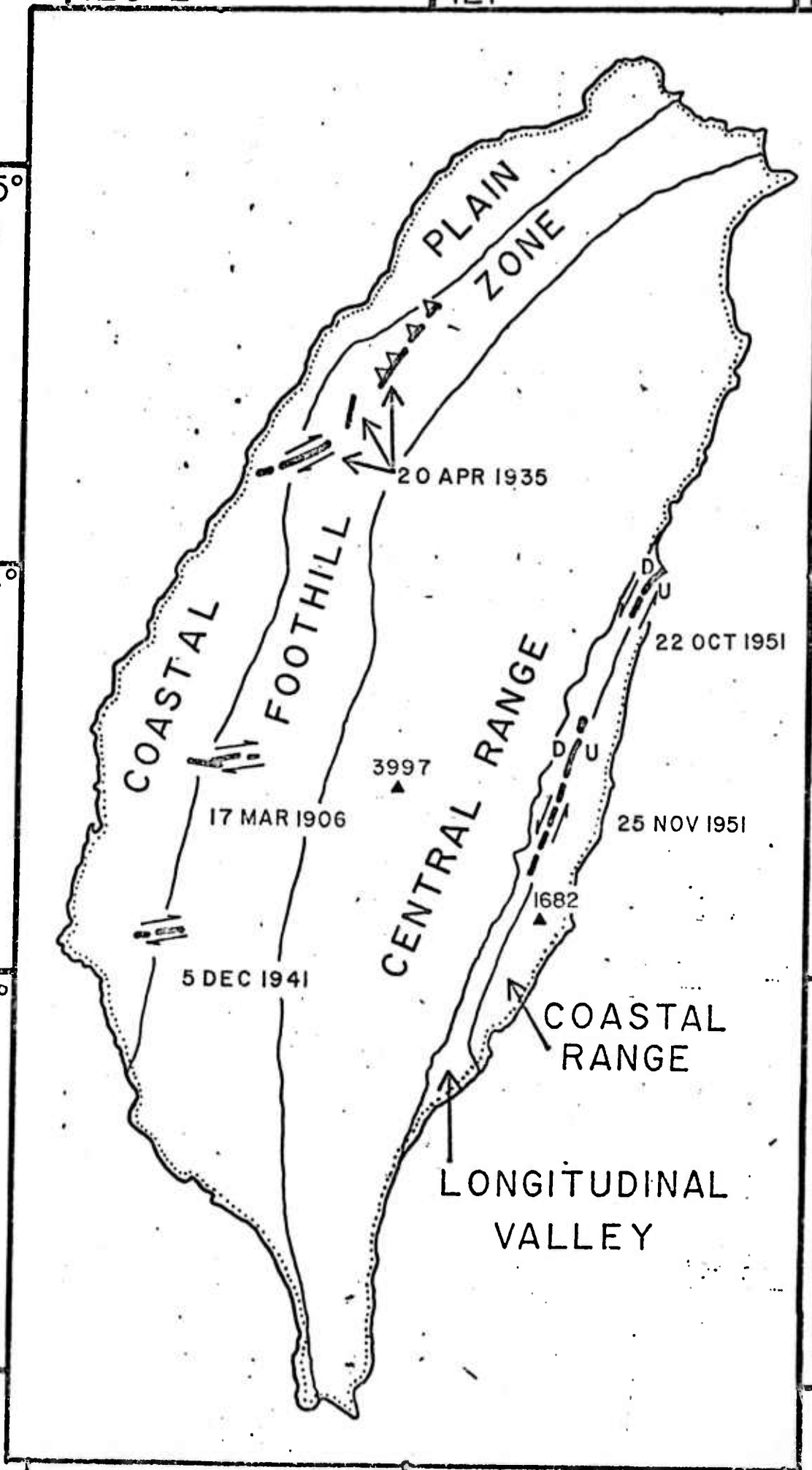


Fig.
2

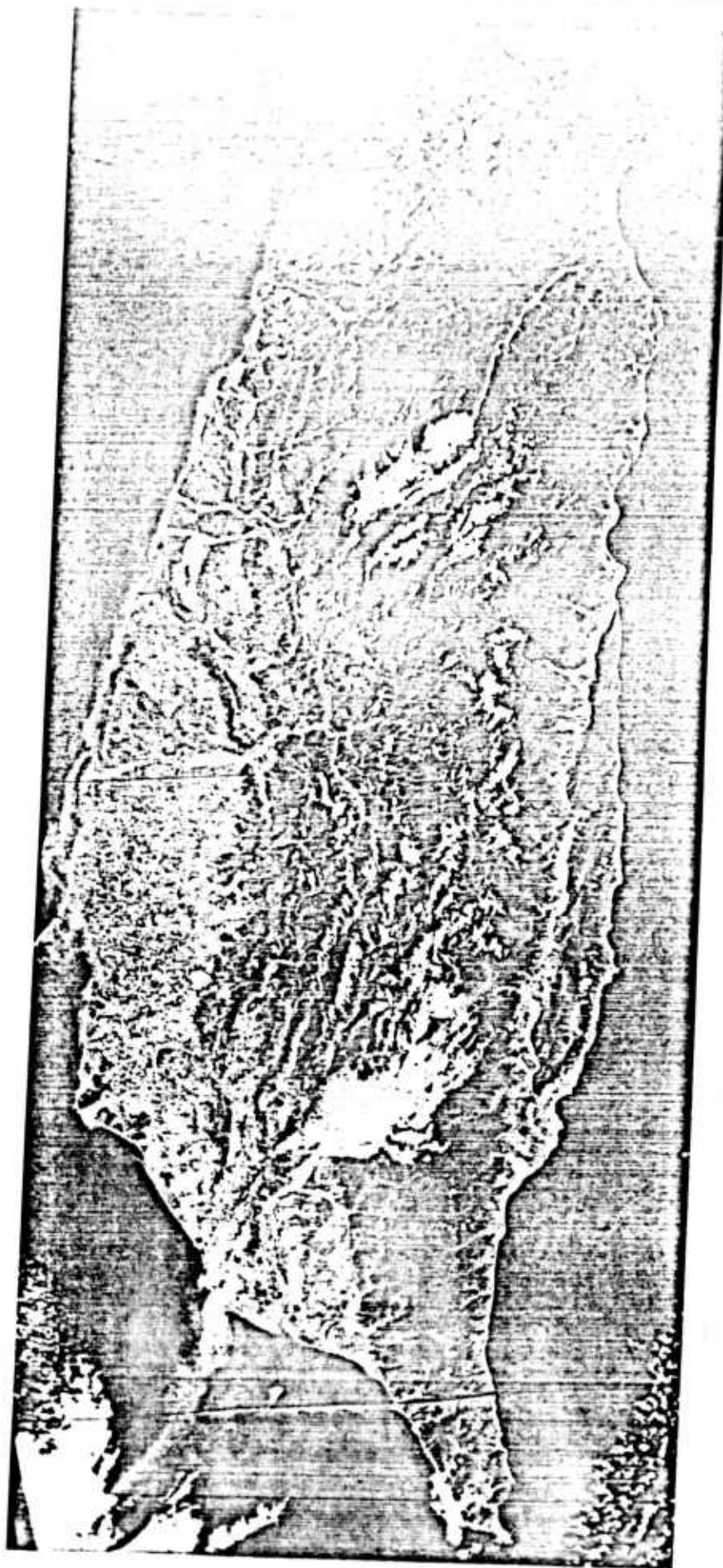


Fig
3

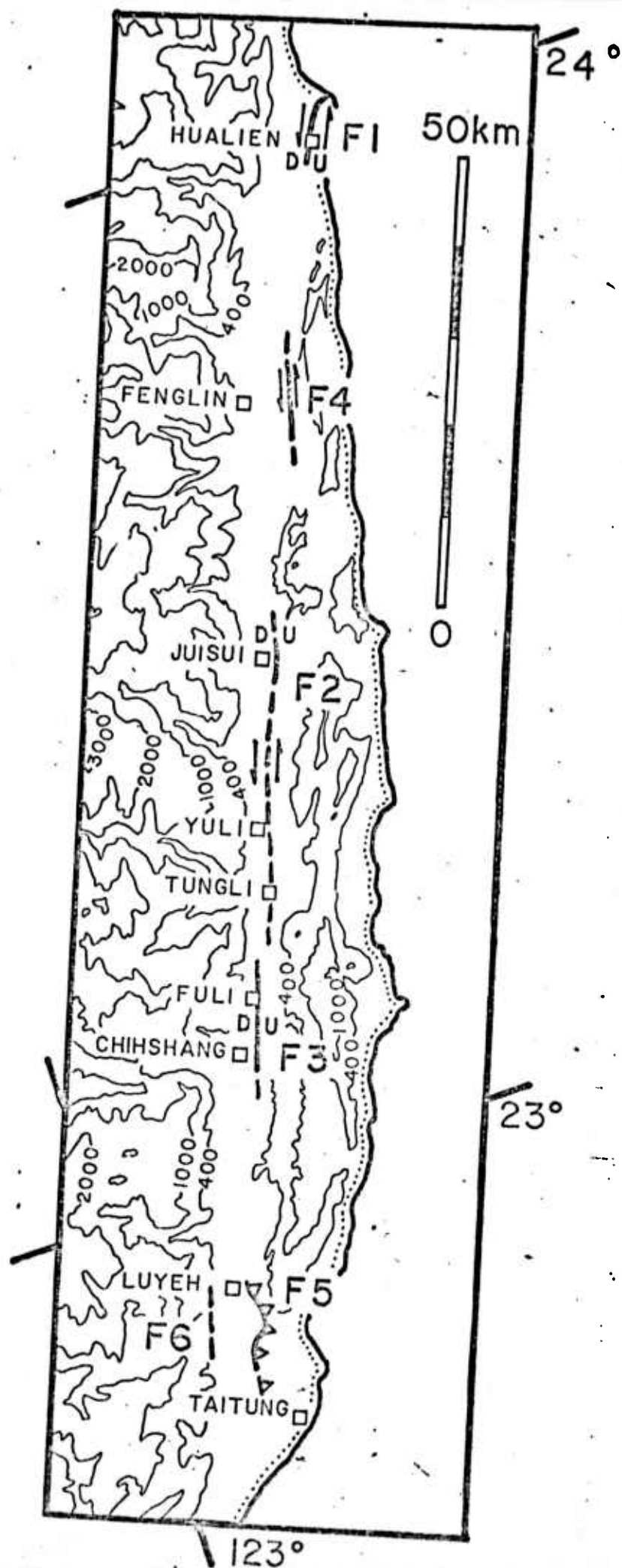


Fig. 4

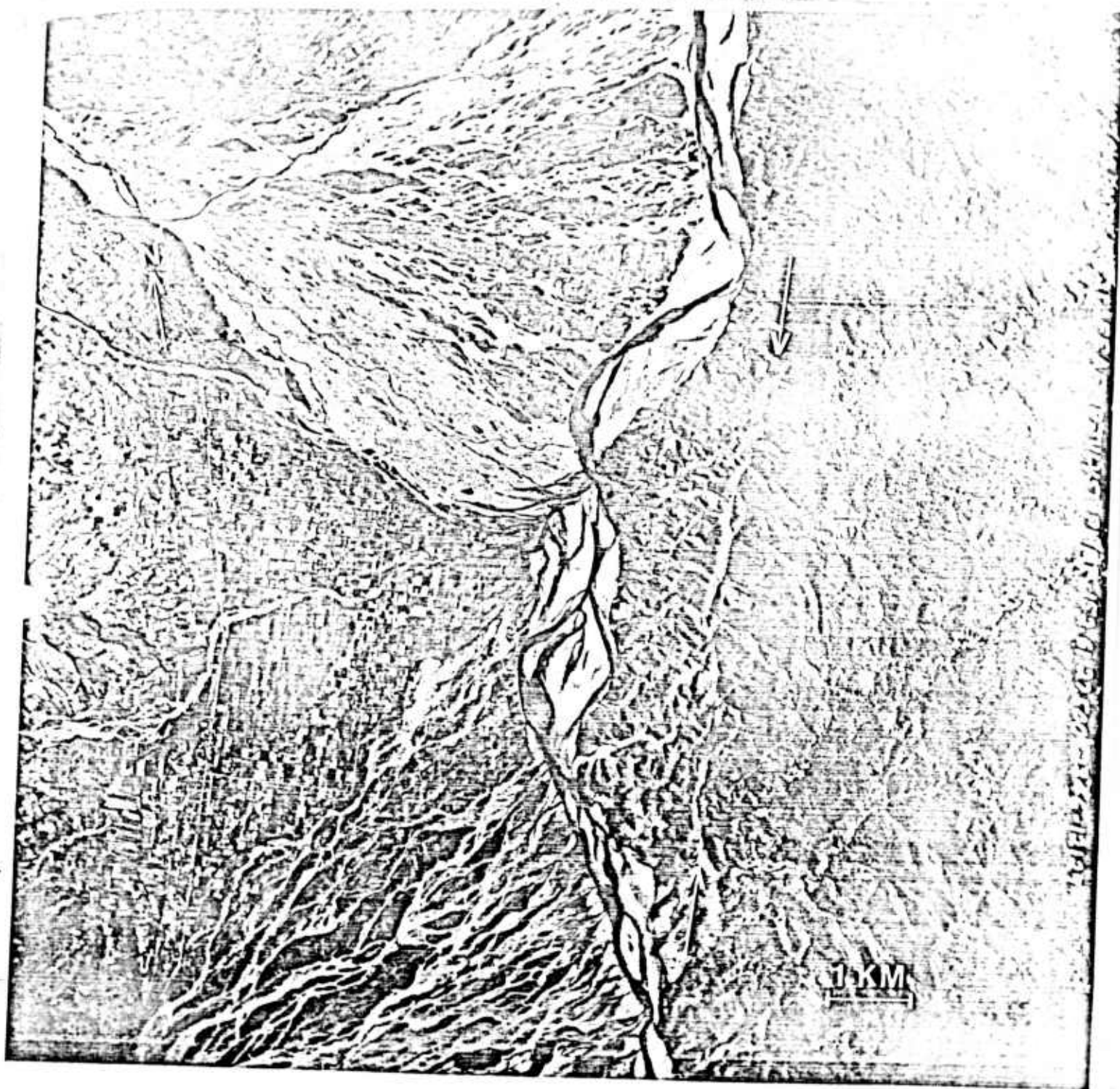
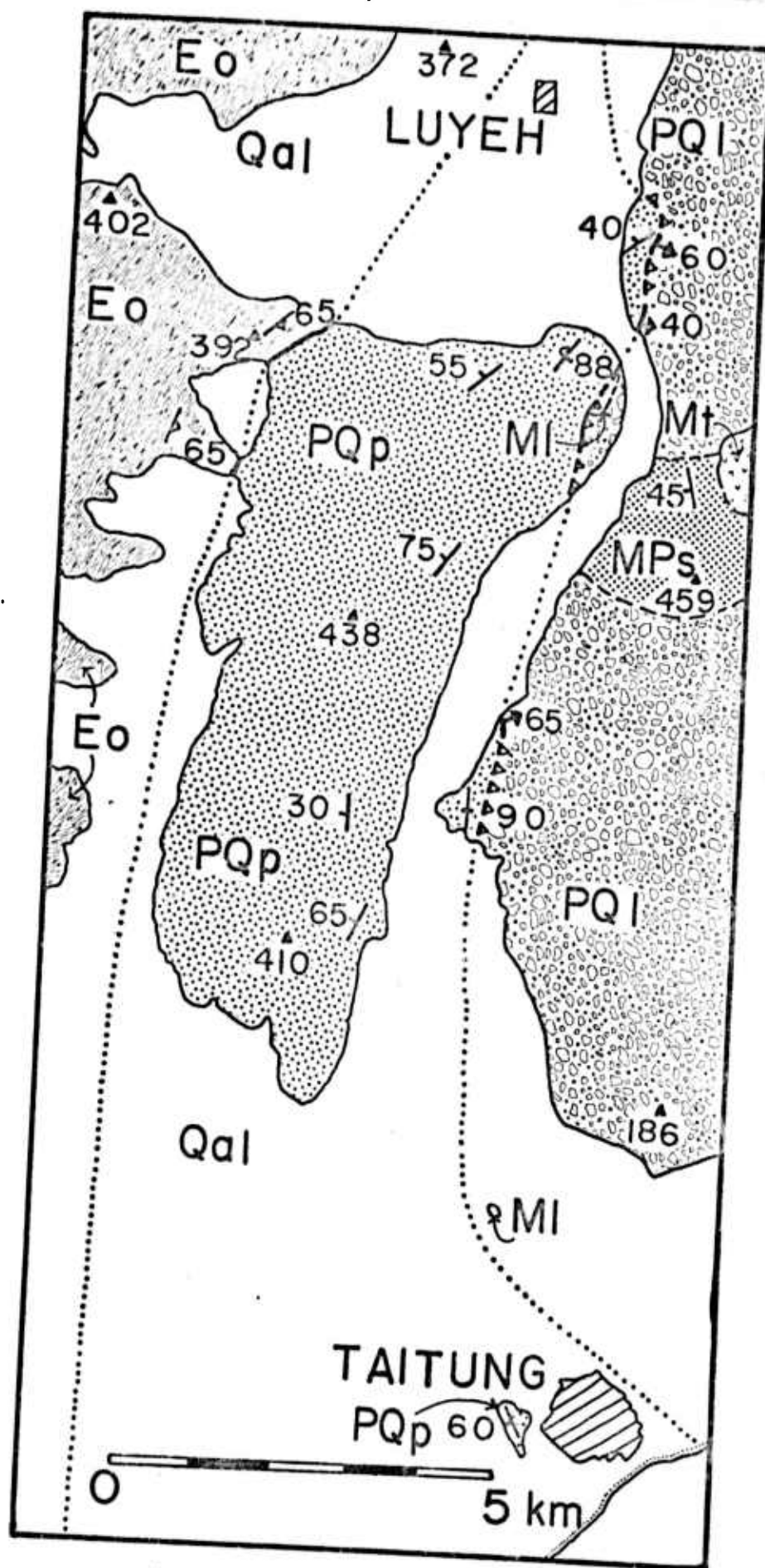


Fig. 5.

Fig
6

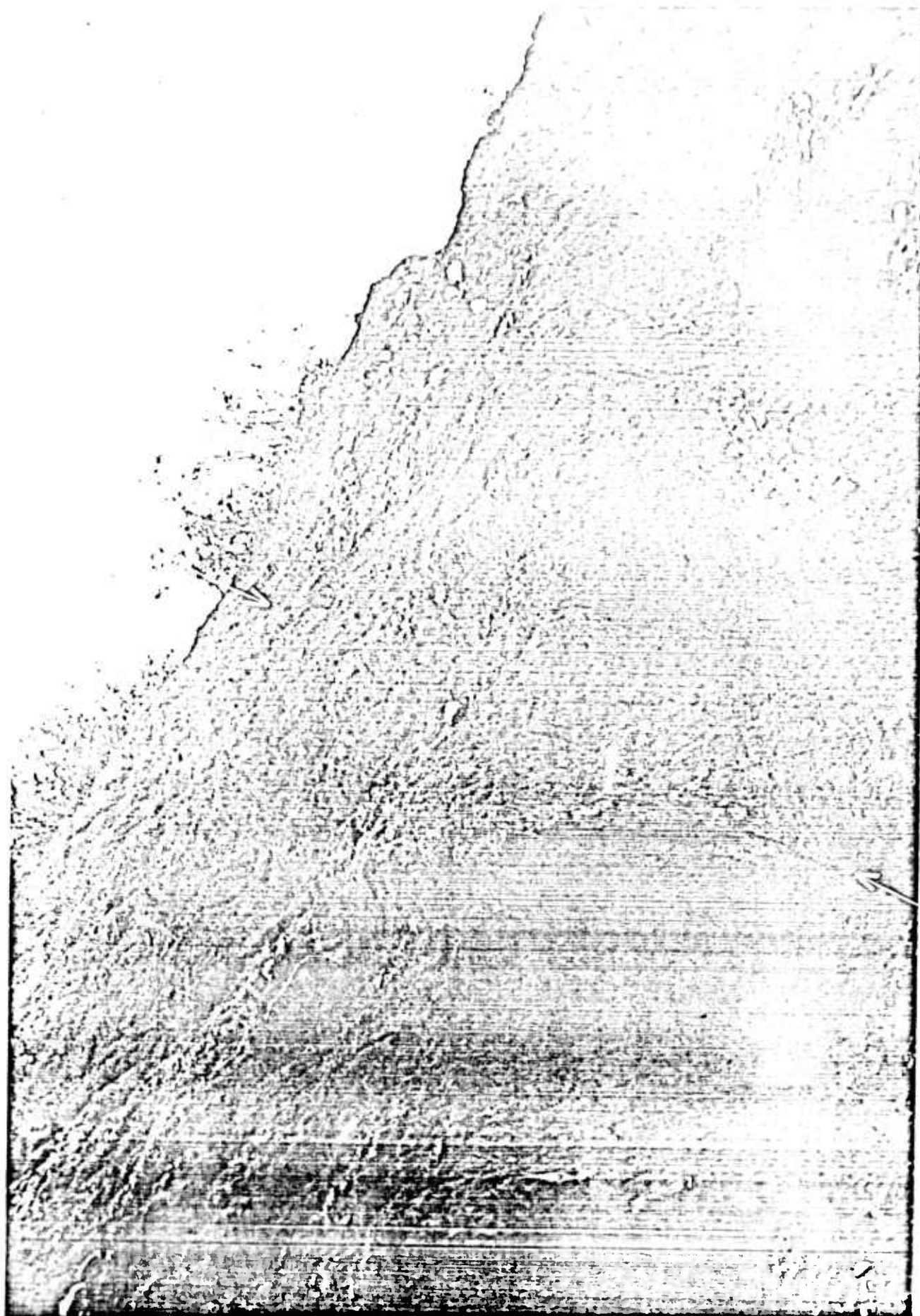


Fig. 7

RECENT VERTICAL CRUSTAL MOVEMENTS

by Larry Brown

Comparison of leveling and tide gauge results

Elevation change data derived from the results of sequential precise levelings and sea level changes measured at tide gauge stations are the principle sources of information about recent vertical crustal movements in use today. The two methods are independent and should yield compatible results assuming proper corrections for extraneous effects and errors have been applied. Unfortunately, the determination of the proper corrections is very difficult. Tide gauges measure the height of local sea level relative to some fixed point on land. The local height of sea level is affected by numerous factors such as secular tectonic movements, eustatic changes in sea level, temperature, atmospheric pressure, salinity, river runoff, and secular variations in tidal parameters. To distinguish the tectonic movement term from the other factors is an extremely difficult task. Analysis of leveling results must also take into account possible sources of error, such as tidal, lighting, refraction, and ocean loading effects as well as possible ground water variations and bench mark instabilities.

In order to estimate the reliability of the two methods, a comparison of precise leveling results and tide gauge measurements was made for a profile along the eastern seaboard, from Calais, Maine to Key West, Florida. The results of that comparison are shown in Figures 1-3. The leveling data is primarily first-order with time separations between leveling and releveing averaging about 30 years. The profile was constructed using the same criteria as in previous studies (Brown and

Oliver, 1976). The tide gauge measurements were taken from Hicks (1974), and represent the slopes of least squares regression lines to the time series of annual mean sea level values. Figure 1 is an index map of the Atlantic coast showing the route of leveling and the location of tide gauge stations used in this study. In Figure 2 is the velocity profile calculated from leveling data (adjusted to be compatible with the tide gauge at Portland, Maine) as well as the tide gauge measurements calculated as rate of land movement with respect to sea level. The squares represent tide gauges located farther than 5 km from the leveling line whereas the triangles represent those stations closer than 5 km. The vertical dimension of these symbols represents two standard deviations for the slope of the regression line for the sea level data. One standard deviation for the leveling measurement of the velocity at Key West, Florida relative to Calais, Maine is less than 4 mm/yr. The abbreviations at the inside top of Figures 2 and 3 represent cities along the leveling profile and those on the outside top are for tide gauge locations.

From Figure 2, it is clear that there is a serious disagreement between the two types of data. Leveling indicates that Key West, Florida is rising relative to Portland, Maine at a rate of about 16 mm/yr whereas tide gauges at these two locations show a difference of only 0.2 mm/yr, a discrepancy of two orders of magnitude, four times the standard deviation of the leveling measurement. It is not clear a priori which set should be given the most credence. The most likely candidates for errors affecting leveling are tidal and lighting effects, both of which have a tendency to accumulate on north-south lines (Bomford, 1971). However, for such errors to be significant they must be exceedingly large in magnitude and must appear predominantly and consistently in either the initial survey or the repeat survey (depending on the sign of the

accumulation), so that they are not cancelled when velocities are computed. Barring unknown sources of systematic error, therefore, it is very difficult to attribute the discrepancy to leveling errors alone.

Tide gauges, mentioned previously, also may be subject to extraneous influences. For example, atmospheric pressure, wind, salinity, precipitation, currents, tides, and river runoff might have secular components which could affect the sea level measurements. As yet, the effect of such influence has not been clearly established, although the work of Meade and Emery (1971) virtually eliminates river runoff as a significant factor in this problem. Until these factors are fully investigated, it is impossible to evaluate their effect on crustal movement studies.

At this point, therefore, four hypotheses are suggested. Either A) the sea level measurements are essentially correct and leveling results are dominated by some type of systematic error, B) the leveling results are correct whereas the sea level measurements are contaminated by some dominant non-tectonic secular variation, C) both methods are registering significant and unrelated non-tectonic effects, or D) both results are essentially correct. Alternative D is possible if one postulates that sea level is systematically moving as a non-geoidal surface, an assumption difficult to justify on physical grounds.

Since resolution of this disagreement would appear to hinge on geodetic and oceanographic studies not yet carried out, one must accept the data at face value and use the results of both methods as best possible while bearing in mind the consequences of the above hypotheses. In order to proceed, therefore, a number of crustal movement profiles have been constructed combining the two sets of data according to various hypotheses, including those above. Figure 3 shows the results of one simple adjustment in which the leveling data have been linearly corrected

to match the tide gauge measurements at Portland, Maine and Key West, Florida.

Comparison of Figures 2 and 3 points up a number of differences. The ubiquitous northward tilt of the coastal plain is present in 2 but absent in 3. The New England segment in 2 tilts down to the north but tilts to the south in 3. Agreement between tide gauges and leveling is considerably better in 3 than 2, even though only one additional tide gauge is used as a constraint. On the other hand, a number of smaller scale features appear in both versions, for example, the minima at 1650, 2400, and 3350 km and the maxima at 1200-1500, 1900, and 2800 km. Although the differences might become even more pronounced in other adjustments, it is not clear at this point that they are justified. Therefore, interpretations of the data represented by Figures 2 and 3 have been made which, although preliminary, appear justified at this stage.

The first 1000 km of the profile seems to be the least certain, yet one of the most important sections, as it lies within the previously glaciated northeastern United States. In Figure 2 this section shows a consistent tilting down to the north whereas in Figure 3 it is tilting down to the south. Figure 2 shows agreement between tide gauges at Portland, Maine and Eastport, Maine, whereas Figure 3 gives better agreement with tide gauges from Portland, Maine south to New York, New York. Since this segment lies within an area which might be expected to be undergoing glacial rebound, it would seem that the alternative most in keeping with the glacial rebound model might be preferred. However, inspection of the post-glacial deformation pattern revealed by geomorphic studies (Flint, 1971, p. 360) shows that the profile runs more or less parallel to the isobases of glacial deformation; therefore, within the error

limits of the deformation pattern, either interpretation may be permissible. On the other hand, the movements in this region may reflect a process totally unrelated to glacial rebound, in which case rebound models using such data may be in error (Chappell, 1974). At present it is not possible to resolve this uncertainty.

Between about 1000 km and 1100 km both profiles show a rapid tilting down to the north. This segment traverses from New Haven, Connecticut to Yonkers, New York and corresponds to a marked change in the tectonics of the area (King, 1969), but there is as yet no satisfactory explanation for this correlation.

The next prominent feature is the minimum in the profile at about 1700 km corresponding to the traverse across the Chesapeake-Delaware embayment. This minimum is prominent not only in the leveling data but is also discernable in the tide gauge data alone. The leveling and tide gauge data in this area have been extensively studied by others (Holdahl and Morrison, 1973; Vanicek and Christodulidis, 1974) so they will not be discussed further here except to say that the profiles in this report are in good agreement with these other studies. One somewhat anomalous feature in this area, though, is the very sharp peak in the data at 1850 km, corresponding to the traverse of the profile down the southern end of the Chesapeake peninsula. There is no good explanation for this feature, although the geometry of the traverse suggests that some type of ocean loading mechanism might be affecting the leveling.

South of the Chesapeake Bay region, neither version of the leveling profile shows good agreement with tide gauge data. Leveling indicates a strong northward tilt reaching as far south as Wilmington, North Carolina, which lies near the axis of the Cape Fear arch, a positive structural element of the basement. This correlation seems too remarkable

to be coincidental. In addition, the minimum in the curve at 2200 km, when tied to the changes in direction of the corresponding leveling route, indicates possible doming of the seaward part of the Cape Fear region relative to the inland area. Further south, another positive feature (maximum) in the curve is evident in the Savannah, Georgia area. The bench marks showing the large downward offsets, it should be noted, are due to water withdrawal and subsequent aquifer compaction (Poland and Davis, 1969). Since both the Cape Fear and Savannah regions are anomalously seismic, a possible correlation might be inferred between such movements and seismicity. However, Charleston, South Carolina is located between these two areas and shows no such behavior even though it is the most seismic portion of the Atlantic coastal plain. Thus no clear connection between these phenomena is apparent.

The next feature common to both versions of this profile is the minimum near 3300 km at Melbourne, Florida. This feature also seems to correspond to a basement ridge which trends northwest and passes through Melbourne and out to sea. Interestingly, this ridge seems to merge with the main line of the Bahamas Islands (King, 1969). Again, as coincidence is unlikely, this correlation seems to be very significant and is being more closely investigated. The last feature in this profile seems to be the subsidence of Key West relative to the tip of continental Florida.

Although detailed investigation of these correlations has not been completed, preliminary results indicate that they represent real and significant crustal movements. This one profile contains a great deal of information concerning both the reliability of leveling and tide gauge data as well as the contemporary tectonics of the eastern seaboard.

Short period variations in crustal movements

Inherent in most approaches to the study of leveling and/or tide gauge data is the assumption that the tectonic movements which are to be studied have constant rates, at least over the period of their measurement. This assumption is based on the observation that most geologic processes are slow and last over large time spans. Also, analogy is made to models of crustal rebound due to various loads which predict slow, linear movements on the time scale which is sampled by leveling and tide gauges. However, there are no direct observations to support such a universal assumption. Relatively short period variations of crustal movement are quite possible as long as their net long term effect matches that inferred from geologic and geomorphic data. If significant short period (i.e. about 100 years) fluctuations in the rates of crustal movement do exist, the implications for analysis of leveling and tide gauge results alone are very serious. For example, if the time difference between leveling and releveing coincides with the natural period of some oscillatory type of crustal movement, analysis of the leveling would reveal no movement, regardless of the actual amplitude.

A number of releveled profiles do indicate that short period changes in the rate of crustal movement are occurring. For example, in Figure 7 are plotted a number of crustal movement profiles (all relative to some arbitrary base) which traverse the Atlantic coastal plain in roughly a northwest to southeast direction. The first three curves, 27a, b, and c represent the results of comparing levelings in 1897 and 1935, 1897 and 1968, and 1935 and 1968, respectively. Whereas 27a indicates that this area was tilting down to the west between 1897 and 1935, 27c indicates that it was tilting up to the west between 1935 and 1968, and 27b shows that the net tilt from 1897 to 1968 was also up to

the west. Clearly there has been some change in the rate of movement indicated by the leveling between 1897 and 1960.

Unfortunately leveling, although spatially continuous, usually does not provide very much information on the changes in rate of movement with time. On the other hand, tide gauge data, which are spatially very discontinuous, do provide a continuous time history of secular movement. Therefore, one method to investigate both the time and space variations in crustal movement would be by properly combining leveling and tide gauge measurements. The difficulties in this approach lie in the uncertainties inherent in the data itself, as well as the scarcity of conveniently located leveling and tide gauges.

One area which meets most of the requirements is the segment of the profile in Figure 1 which lies between the Eastport, Maine and Portland, Maine tide gauges. In Figure 4 are plotted two versions of the segment of the Atlantic coast profile between Calais, Maine and Yonkers, New York. In version 1, the segment from Calais to Bangor is based on levelings in 1927 and 1966, whereas in version 2 it is based on levelings in 1942 and 1966. As can be seen from Figure 4, there is a great difference between the two versions. Version 1 shows a velocity difference of about 1 mm/yr going from Eastport ($x = 30$ km) to Portland ($x = 444$ km) yet version 2 gives a difference of 10.5 mm/yr. Since tide gauges exist in Eastport and Portland, a check can be made on this apparent velocity change. In Figure 5 is a plot of differences between yearly sea level means at various tide gauges and the corresponding means at Portland. The topmost curve, therefore, shows the difference in sea level as a function of time between Eastport and Portland. Since the difference in velocity of sea level rise between two gauges is equivalent to the velocity of the rise in the sea level differences, the net velocity of apparent crustal

movement can be computed for the time intervals of 1927 to 1966 and 1942 to 1966. Since sea level measurements only began in 1930, the interval 1930 to 1966 is used instead of 1927-1966. The results are, respectively, 1.52 mm/yr and 3.46 mm/yr, which agree in sign to the velocity change indicated by leveling but disagree quantitatively by a factor of four. Thus, in this instance tide gauges seem to support the occurrence of changes in the velocities of apparent crustal movements on the time scale of 50 to 100 years, although significant disagreement in the magnitudes of these changes remains.

To further investigate possible changes in the magnitude of crustal movement over short time intervals, the differencing technique mentioned above was applied to all tide gauges on the eastern coast of the United States. The eastern coast was divided into sections and a reference station was chosen for each section on the basis of record quality and length. Then annual mean sea level curves of the reference stations in each section were subtracted from the sea level curves of all the sections. Figures 5 and 6 show some of the results. In Figure 5, the sea level differences between the northernmost stations and the Portland, Maine gauge, located within the section, are shown. In Figure 6, the same set of stations have been differenced with the Charleston, South Carolina gauges, located in the southernmost section. Since the plots are to the same scale, it is immediately obvious that the curves in Figure 6 show more variation than those in Figure 5, i.e. the character of the sea level curve at Portland is more similar to the other curves in the northeast than is the Charleston station, as one would expect. In addition, the longer period components of the sea level differences show considerable variation in space and time for both sets of curves. Since all of the factors affecting sea level are also space and time

dependent, it is not immediately obvious that these spatial and temporal variations in trend can be attributed to short period tectonic movements. The important conclusion to be drawn from these results is that such rapid changes in tectonic movement are not ruled out by sea level measurements, and in fact sea level measurements can be used, as in the above example, as a check when successive relevelings seem to indicate such movements. Until proven otherwise, the possibility of short period variations must be kept in mind when comparing leveling data derived from incompatible time intervals.

Southeastward tilting of the Atlantic coastal plain

Brown and Oliver (1976) noted that the vast majority of the longer profiles of vertical crustal movement which traversed the Atlantic coastal plain in a roughly northwest to southeast direction indicated that the continental interior was rising with respect to the coast. To test the universality of this statement, a survey was made of all leveling profiles with a prominent northwest-southeast component to determine if they all showed a tilting down to the coast. In addition, for lines which were leveled more than twice, the average velocities were computed for each possible pair of levelings. 91 profiles were collected and plotted. A least squares regression line was fit to each profile in order to provide an objective measure of the direction of tilt, i.e. a negative slope corresponding to an oceanward tilt, a positive slope to an interior downward tilt. Figure 7 shows a sample plot of some of these profiles. Analysis of these results is as yet preliminary. However, the first analysis of the least squares results indicates that about 65% of the lines show a negative regression slope, i.e. tilt down to the coast, supporting the contention that this is the dominant mode of movement in the Atlantic coastal plain. With further analysis, i.e. the

elimination of poorest quality lines, this percentage will probably increase. It remains to be determined whether or not there is a spatial pattern to the distribution of lines of opposite slope and what the causes of such tilts, both toward and away from the continent, could be. Since all relevelings are being used, analysis of this data set is also providing information on temporal variations in the rates of movement, although there appear to be no tide gauges so situated as to provide some type of independent control.

Relationship of vertical crustal movements to seismicity

Results, such as those above, continue to indicate that the eastern "aseismic" United States is characterized by a very "active" crust, undergoing vertical movements with very large rates when compared with geologic averages. As yet there has been no evidence uncovered to clearly link these movements with seismic hazard, although some interesting correlations have been found between patterns of apparent crustal movement and seismicity. The time series of both seismic and leveling data is short and sparse, as is the spatial coverage of sea level measurements, so it is not surprising that the problem of determining their relationship is not a simple one.

References

- Bomford, G., Geodesy, 3rd ed., Claredon Press, Oxford, 732 pp., 1971.
- Brown, L.D. and J.E. Oliver, Vertical crustal movements from leveling data and their relation to geologic structure in the eastern United States, in press, Reviews of Geophysics and Space Physics, 1976.
- Chappell, J., Late Quaternary glacio- and hydro-isostasy, on a layered earth, Quaternary Res., 4, 405-428, 1974.
- Flint, R.F., Glacial and Quaternary Geology, Wiley and Sons, New York, 892 pp. 1971.
- Hicks, S.D., Trends and variability of yearly mean sea level, 1893-1971, NOAA Tech. Mem. NOS 12, 13 pp., 1973.
- Holdahl, S.R., and N.C. Morrison, Regional investigation of vertical crustal movements in the U.S. using precise relevelings and mareograph data, paper presented at the Symposium on Recent Crustal Movement and Associated Seismic and Volcanic Activity, 1973, 24 pp., 1973.
- King, P.B., Tectonic Map of North America (map), U.S. Geol. Surv., 1969.
- Meade, R.H. and K.O. Emery, Sea level as affected by river runoff, eastern United States, Science, 173, 425-428, 1971.
- Poland, J.F. and G.H. Davis, Land subsidence due to withdrawal of fluids, in: Reviews in Engineering Geology II, Geol. Soc. Amer., Boulder, Colorado, 187-269, 1969.
- Vanicek, P. and D. Christodulidis, A method for the evaluation of vertical crustal movement from scattered geodetic releveling, Can. J. Earth Sci., 11, 605-610, 1974.

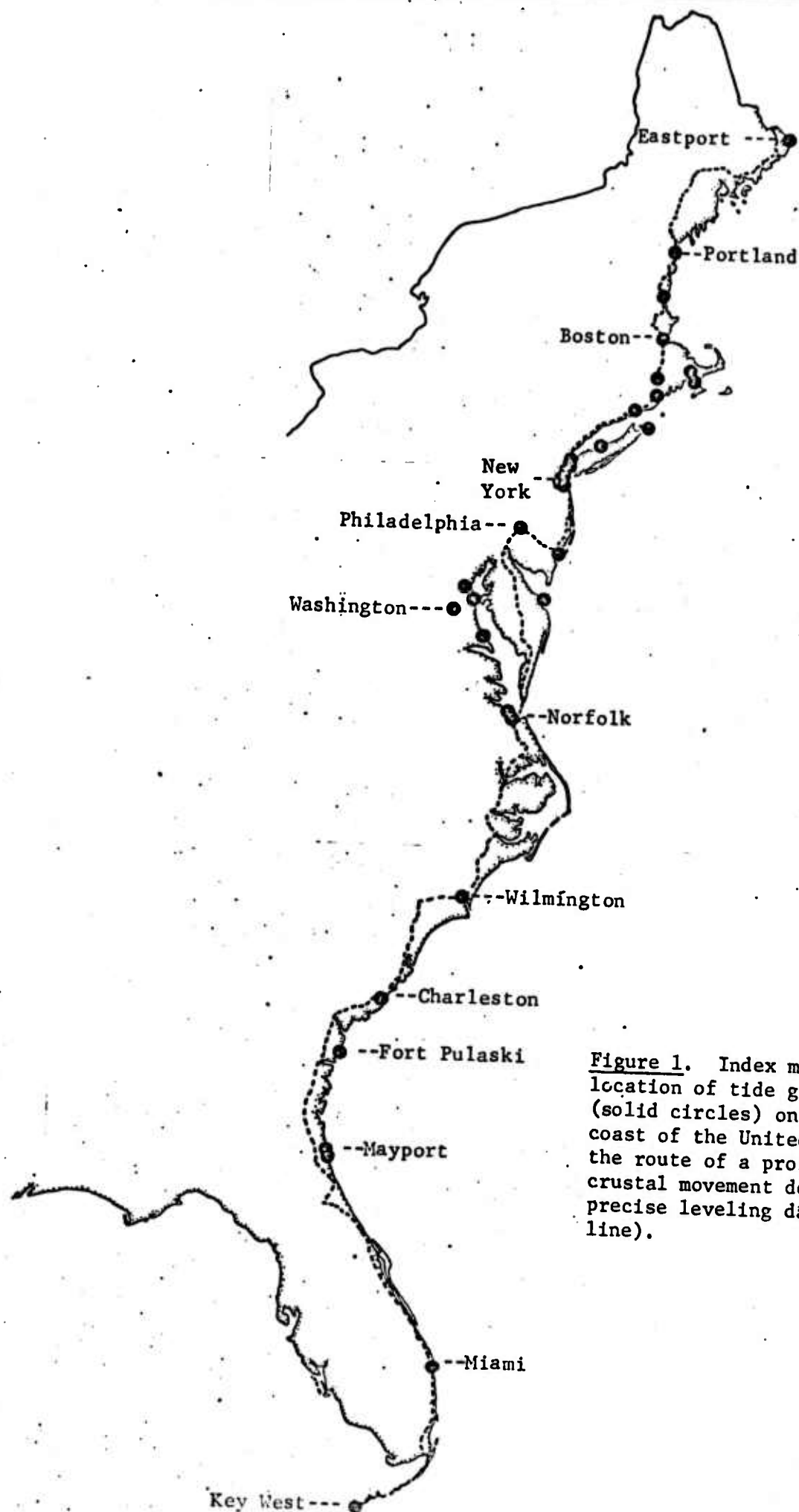


Figure 1. Index map showing the location of tide gauge stations (solid circles) on the eastern coast of the United States and the route of a profile of vertical crustal movement derived from precise leveling data (dashed line).

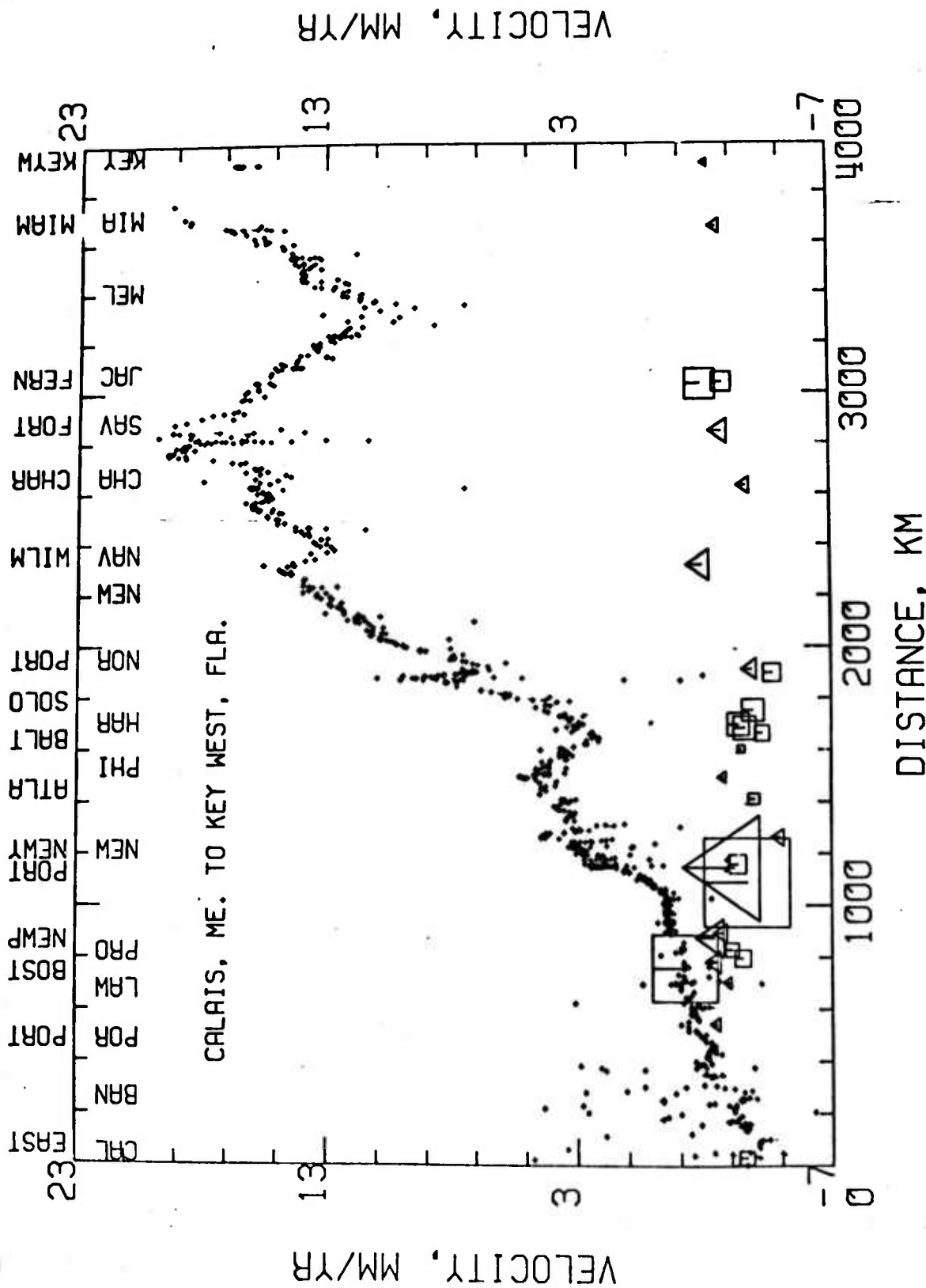


Figure 2. Vertical crustal movement profile from Calais, Maine to Key West, Florida. Dotted curve represents movements derived from leveling results. Triangles and squares represent sea level measurements of crustal movement, with triangles denoting tide gauge stations closer than 5 km to leveling profile route and squares denoting those further than 5 km from leveling route. The vertical dimension of the squares and circles represent two standard deviations for the measurement. Abbreviations at inside top represent selected cities along profile route, those at outside top represent selected tide gauge locations.

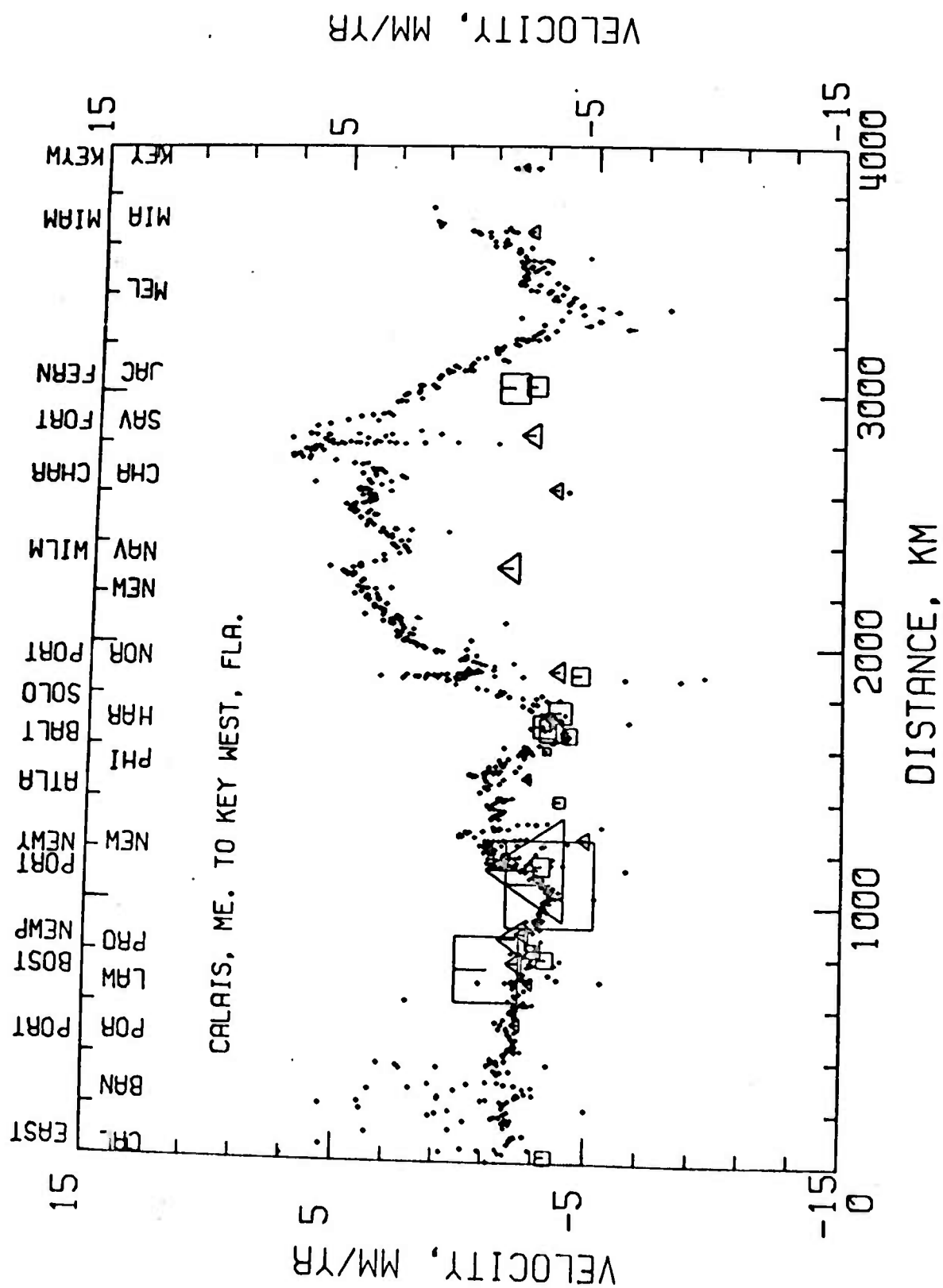


Figure 3. Adjusted vertical crustal movement profile from Calais, Maine to Key West, Florida. Leveling profile adjusted to be compatible to tide gauges at Portland, Maine and Key West, Florida. Same conventions as in Figure 2.

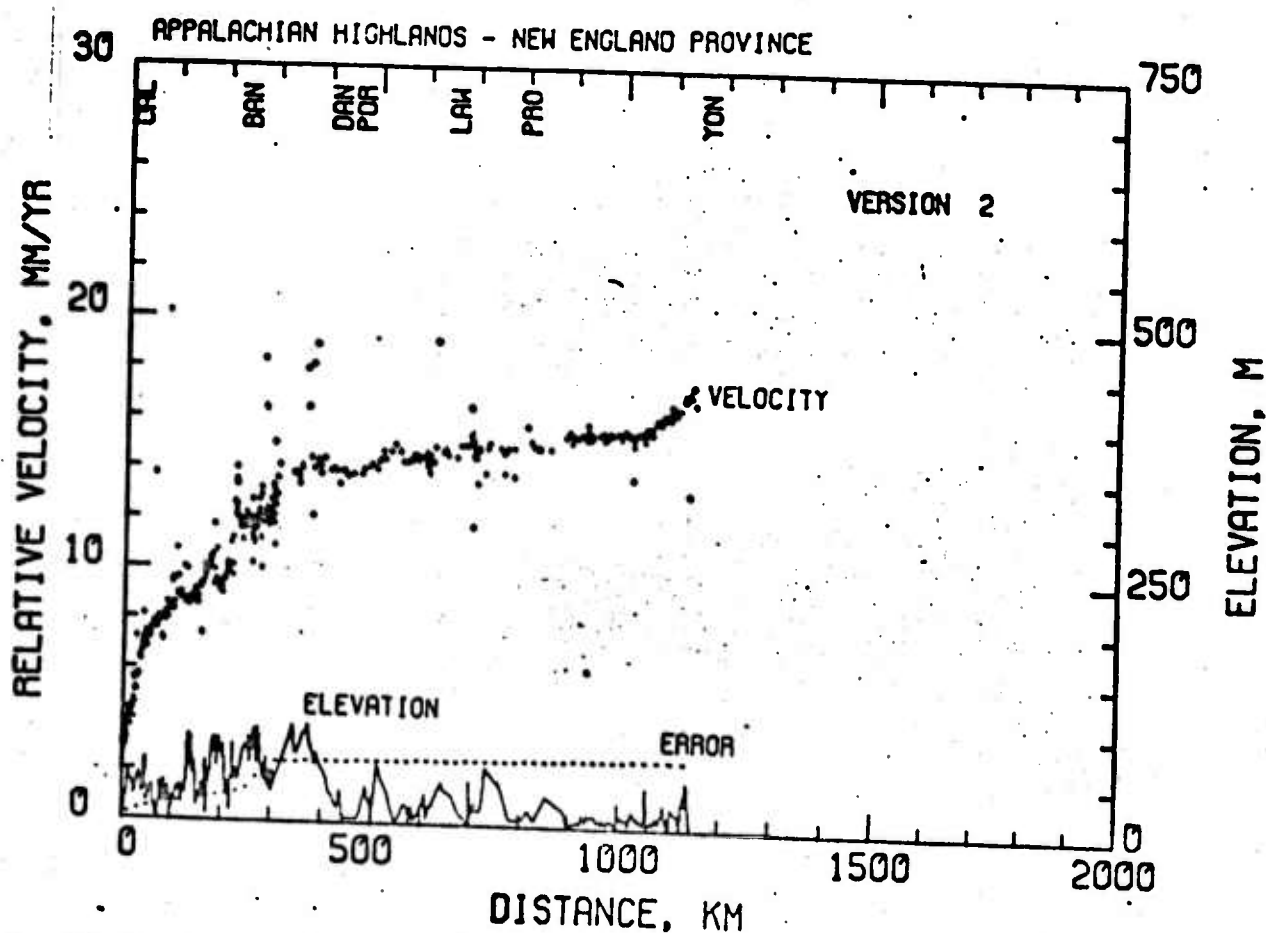
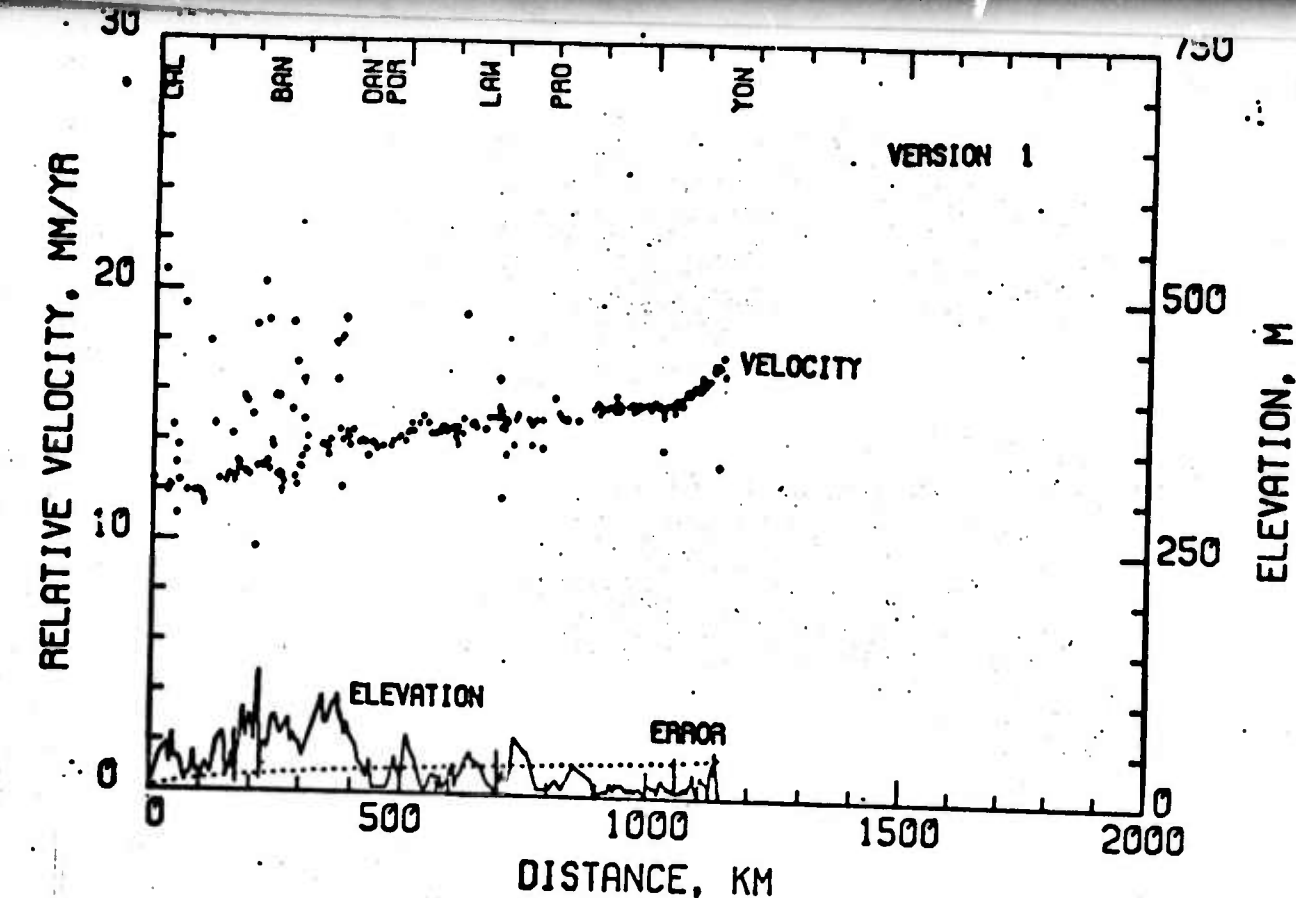


Figure 4. Vertical crustal profiles from Calais, Maine to Yonkers, New York. Discontinuous curves represent relative velocity of vertical crustal movement derived from leveling. Solid curve represents absolute elevation along the profile route. Dashed line represents the rate of random error propagation along the profile route. The abbreviations at the top represent cities along the profile route. The leveling data set used to derive the velocity curve segment from Calais, Maine (CAL) to Danville, Maine (DAN) differ in Versions 1 and 2. See text.

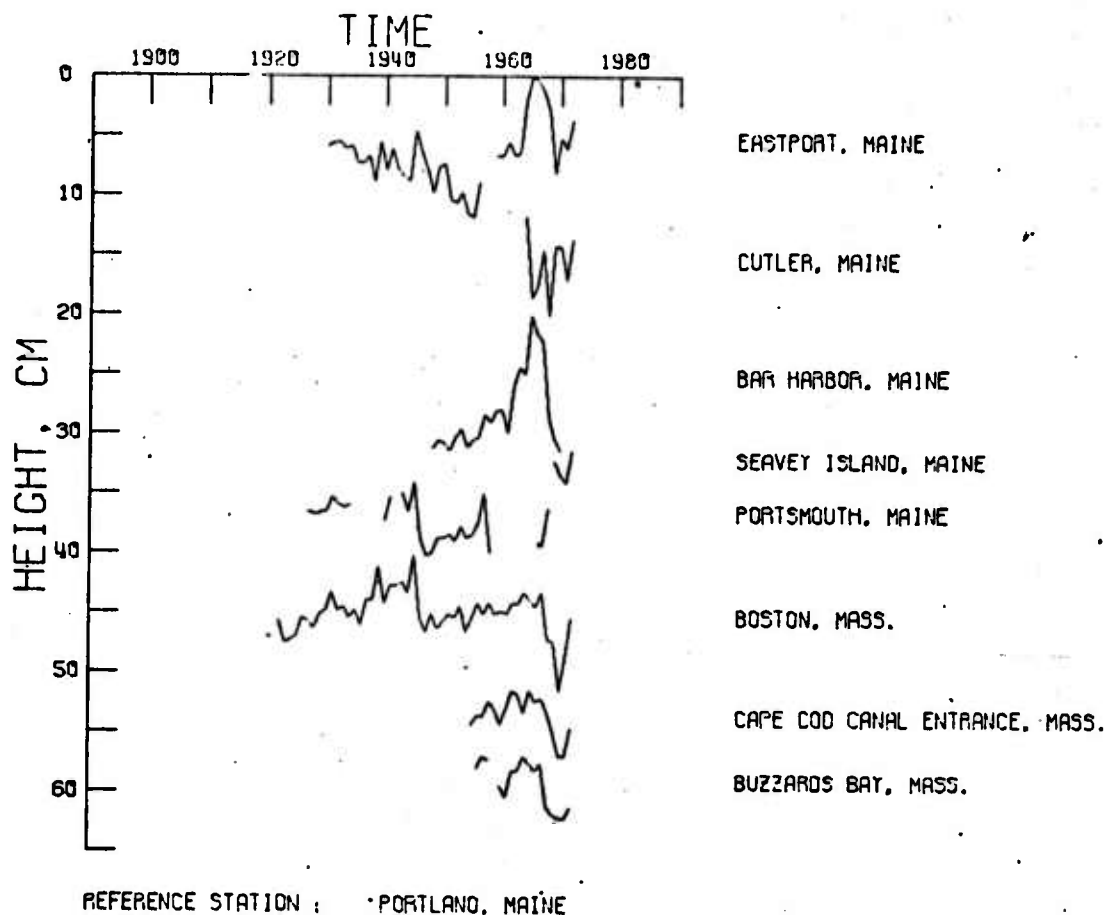


Figure 5. The difference in yearly mean sea level between selected tide gauges and the Portland, Maine gauge.

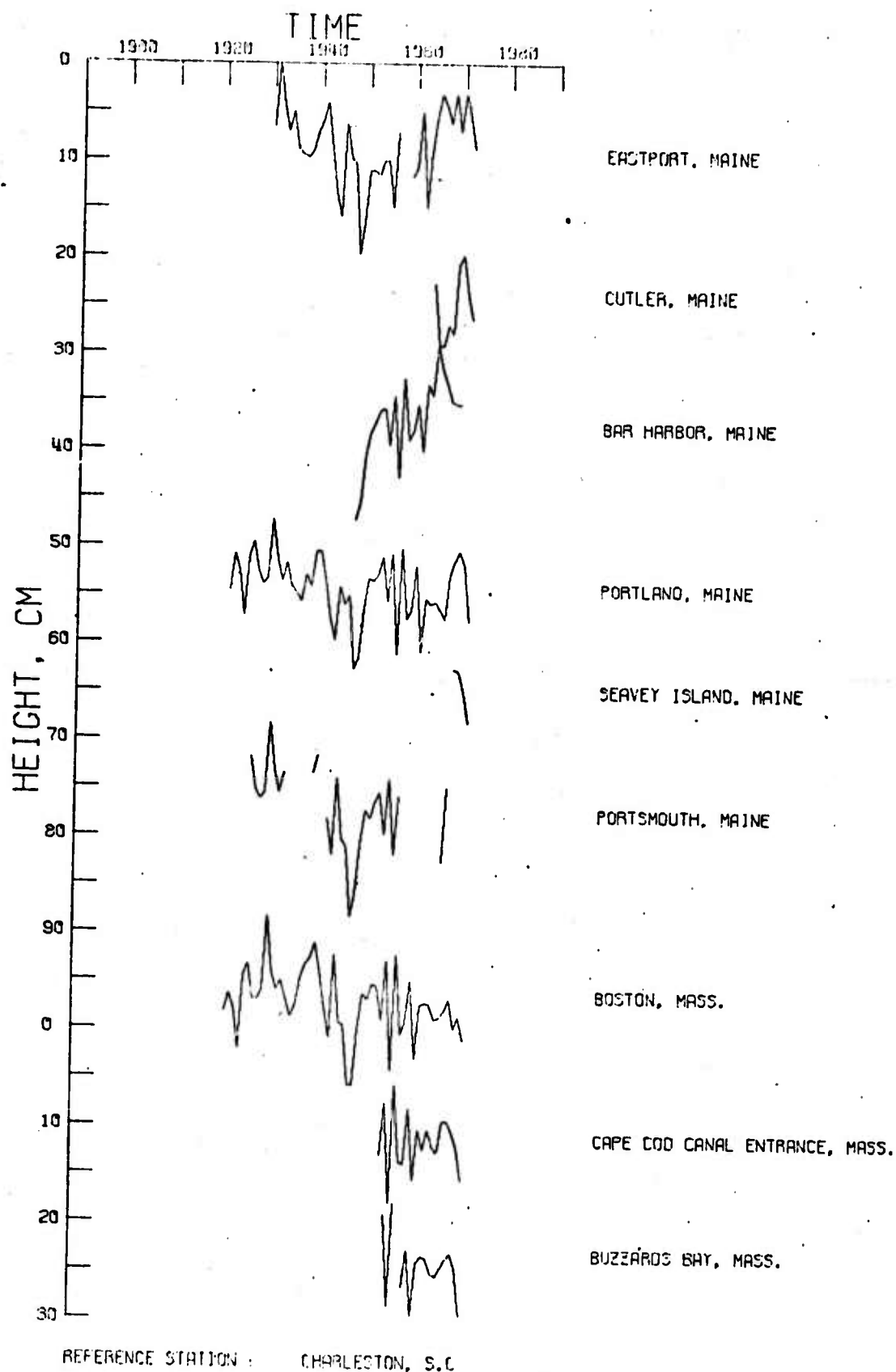


Figure 6. The difference in yearly mean sea level between those tide gauges in Figure 5 and the Charleston, South Carolina gauge.

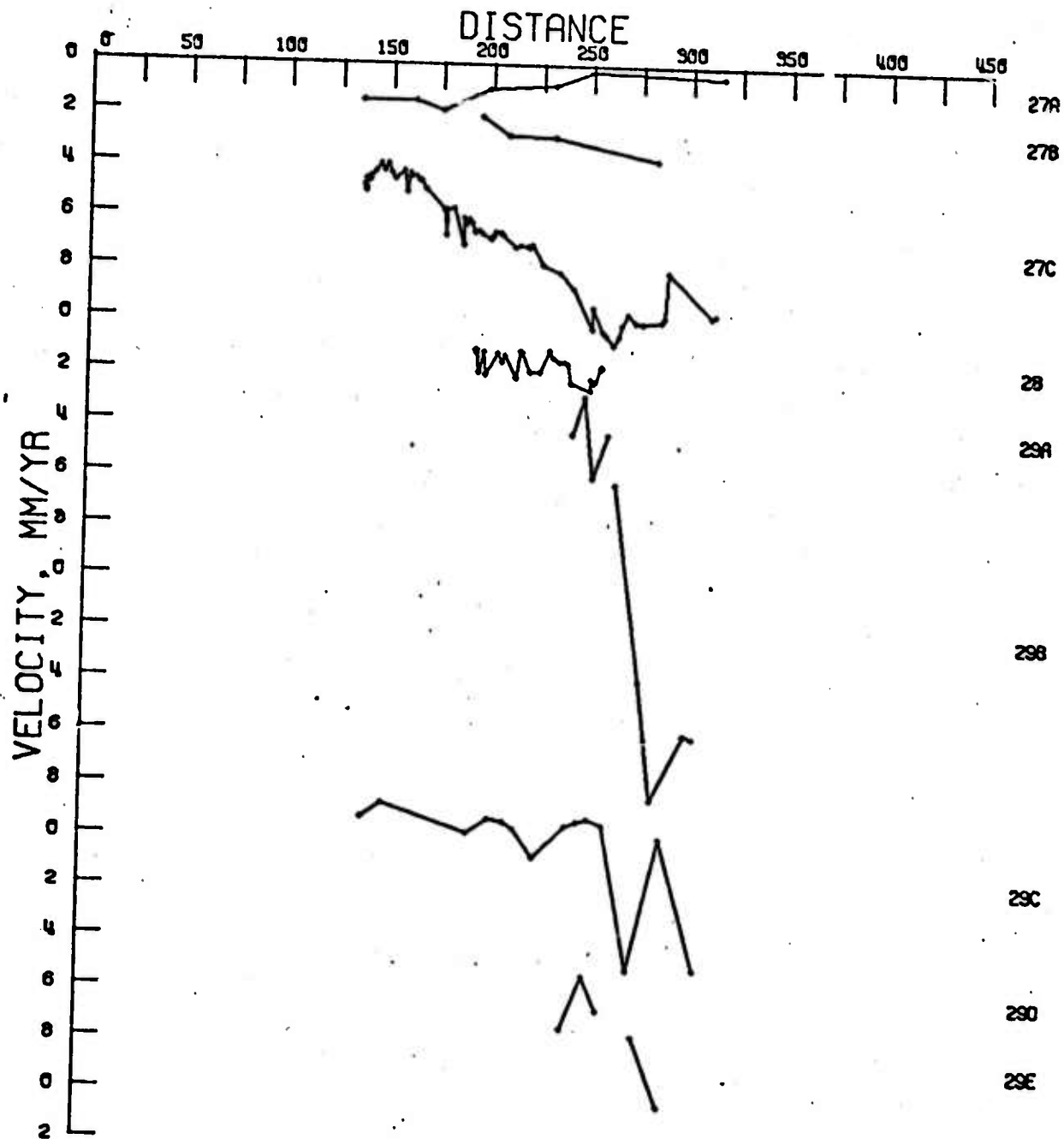


Figure 7. Selected northwest-southeast trending profiles of crustal movement derived from leveling data. Arbitrary datum.

APPENDIX D

SUBSURFACE FAULT MOVEMENT AND PRECISE RELEVELING:

A CASE STUDY IN WESTERN KENTUCKY

F. Steve Schilt

Department of Geological Sciences

Cornell University

Ithaca, New York 14853

ABSTRACT

Both geological and geophysical data are consistent with the existence of a concealed, high angle, dip-slip fault (possibly a normal fault) in extreme western Kentucky, located within the northern boundary of the Mississippi Embayment and the New Madrid seismic zone. Inferred faults have previously been proposed in this region (Stearns and Wilson, 1972), but recent analysis of first order leveling data lends strong support to the existence of a potentially active fault or fault zone which has experienced approximately 31 mm of relative displacement in a 21 year interval.

The location is defined to within 10 km by an abrupt steep gradient in the relative vertical movement profile, which is derived from leveling measurements by dividing the change in elevation by the time interval. A trend of NNE is obtained for the fault from other geological and geophysical evidence. A focal mechanism for a nearby earthquake which occurred between the times of leveling suggests a normal fault, although it is not certain this mechanism correlates with the alleged fault.

In Nevada, anomalies in elevation changes similar to that reported here have been correlated with known surface faults and

interpreted as post-earthquake slip (Savage and Church, 1974). Workers in Hungary and Japan have postulated faults at depth to explain relative vertical surface movements monitored by leveling and accompanying earthquake (Bendefy, 1966; Mizoue, 1969). The results presented here may constitute a similar phenomenon, as the region studied is a zone of known seismicity. They further demonstrate the utility of precise leveling as a tool to measure crustal movements and evaluate earthquake hazard. It is recommended that the appropriate bench marks be resurveyed in five to ten years to monitor any additional movements, and after any earthquakes that occur in the vicinity.

INTRODUCTION

The purpose of this study is to examine the possibility that apparent deformation of the surface, as measured by repeated precise leveling surveys, can indicate vertical displacements across a fault situated at some depth below the surface. If such a fault is not mappable at the surface, and insufficient drill holes exist to allow subsurface mapping, leveling measurements could conceivably be the most direct evidence for such fault movement.

Specifically, such faults may exist in the Mississippi Embayment at the New Madrid seismic zone. The area studied here is near Wickliffe and Paducah, Kentucky, and the leveling data suggest dip-slip displacement along an unmapped, concealed fault when supplemented with other geological and geophysical information.

In a recent paper by Brown and Oliver (1976), regional structural features of the eastern United States are compared with relative vertical crustal velocities (time-averaged) as determined from multiple first-order leveling surveys. They find a significant correlation between

the velocity patterns and large scale (hundreds of kilometers) geological structure. The same data they have used is here examined on a more local scale, with interest in shorter wavelength behavior.

Regional Structure and Geology

The dominant structural feature in this region (see Figure 1) is the Mississippi Embayment, which began to form in Late Cretaceous when the Pascola Arch (then connecting the Ozark and Nashville domes) was downwarped. The cause of this subsidence is not well understood, but it has been viewed as an isostatic adjustment subsequent to Precambrian rifting, which extended into the continent as the so-called failed arm of a triple-junction (Burke and Dewey, 1973; McGinnis and Ervin, 1975). Depression continued as a linear trough until late Eocene, accumulating about 3000 feet of sediment in the central portion of the embayment. A cover of alluvial deposits is Late Tertiary in age, and is locally overlain by Pleistocene loess.

Nearly all of the observed surface faults lie in the Paleozoic rocks surrounding the Cretaceous and younger fill of the Mississippi Embayment. The major displacements on these Paleozoic faults probably occurred in Pennsylvanian and Mississippian time (King, 1969). Far fewer faults are mapped within the Cretaceous and younger rocks of the embayment, yet the major pattern of historical seismicity is a northeast linear trend approximately coincident with the embayment axis (Figure 2a). This may be largely due to a masking effect of the unconsolidated alluvial cover, and Fisk (1944) inferred an orthogonal fault pattern within the embayment from a detailed study of lineations. More recently, Stearns (1975, manuscript in preparation) has made a similar study, and his inferred faults based on well data and lineations show some correlation to seismic focal plane solutions. York (1976, in press) has collected

from the literature and sought in the field the few known examples of Cretaceous and Cenozoic faults (considering only those for which there is direct evidence) for this region, and suggests that pre-Cretaceous faults are being reactivated with some consequent faulting in the younger embayment sediments.

Local Structure

The locality of this study is the northern tip of the Mississippi Embayment, where southern Illinois meets western Kentucky. Here the dense Paleozoic faulting of the western Kentucky faulted area disappears at the northeastern edge of the embayment. The western Kentucky faulted area has been mapped in detail and shown to be a northeast trending horst and graben fault complex with vertical displacements commonly 500-1500 ft, associated with a northwest-southeast lateral extension of approximately 1 mile (Hook, 1974). Normal faulting (with dips averaging 70° - 75°) is predominant, although minor strike-slip motion is evident. This fault zone is apparently now quiescent, as almost no seismic activity is situated there.

Considerable evidence, however, suggests the continuation of basement faulting beneath and/or into the embayment. In southernmost Illinois, subsurface mapping has revealed a complex of buried grabens and faults just within the northern boundary of the embayment. At least a part of these displacements occurred after the formation of the sub-Cretaceous erosional surface, with episodic activity dating Late Cretaceous, post-Eocene, Pliocene, and Pleistocene (Ross, 1963a, b).

Seismotectonics

The pattern of historical seismicity since 1928, mostly instrumentally determined, is shown in Figure 2 (Hadley and Devine, 1974). The major

characteristics are the moderately well-defined northeast trend within the embayment and a more diffuse pattern outside it. The existence of smaller scale northeast trending lineaments in the seismic pattern has recently been confirmed by results from a microearthquake study (Stauder, 1975). The inset rectangle seen in Figures 1 and 2 indicates the locality for which leveling data will be presented, and Figure 3 shows this locality at large scale. The center of Figure 3 is approximately 75 km northeast of New Madrid, Missouri, the site of the very large earthquakes of 1811-12.

Figure 3 shows the seismicity near the leveling route for two different time intervals. Solid circles represent events between 1947.5 and 1968.7 (listed in Table 1), the times of first-order leveling surveys. Open circles represent events for all other time since 1928 (listed in Table 2). If all historical seismicity were shown in Figure 3, the greatest activity would appear at Cairo, Illinois. Since 1855, 29 events have been located at Cairo, including one damaging event (intensity VI-VIII) in 1883. The sharp clustering at Cairo, however, may reflect to some extent population bias, in absence of instrumental locations before 1928.

The published depths of hypocenters for earthquakes of the New Madrid seismic zone range from 5 to 38 km. Only five published depth determinations exist for the area shown in Figure 3, as noted in Table 2. The precision of these depths is limited by inadequate station distribution, but better depth information should be forthcoming from the recently installed microearthquake network.

Although all three types of mechanisms are evident in Figure 3, three important points should be noted:

- (1) Six of the eight nodal planes of the four mechanisms in

Figure 3 strike north-northeast between 356° and 031° , a span of 35° .

(2) A large majority of nearby focal mechanisms (within about 1° of Figure 3) are thrust mechanisms, as noted by Street et al. (1974).

(3) If the strike-slip event in southern Illinois can be associated with movement along the trend of the New Madrid fault zone, the sense of diaplacement is consistent with east-west compression.

If pre-Cretaceous faults are being reactivated, it is interesting to note that reactivation is apparently largely ESE-WNW compression, in contrast to the Paleozoic southeast-northwest extension seen in the adjacent western Kentucky faulted area.

Leveling Data

The bold line in Figure 3 is a path twice surveyed by first order leveling, once in 1947 and again in 1968. By arbitrarily choosing one bench mark as a fixed reference point (in this case the bench mark at Wickliffe, Kentucky), one can measure the change in elevation of all other bench marks relative to the reference. The relative displacements describe the deformation of the surface, to the extent that the bench marks are stable, i.e. do not move with respect to the surface. If these displacements are divided by the time interval, an average relative velocity of the surface at discrete points is obtained. (The main purpose of this division operation would often be to normalize profiles with different time intervals -- a problem which does not concern us here.)

Topography along the route is shown by the curve labelled "elevation". The "error" curve shows the accumulation of random error relative to the reference bench mark, and grows as the square root of the distance multiplied by a precision factor (Bomford, 1962; Brown and Oliver, 1976). With regard to random error, the local slope of the velocity profile may

be significant if it exceeds the local slope of the error curve. Both surveys were first-order, and therefore double-run, with differences between forward and backward measurements not allowed to exceed $4L^{\frac{1}{2}}$ mm, where L is the distance surveyed in kilometers. In practice, this difference is usually closer to $2L^{\frac{1}{2}}$ mm.

Figure 4 shows the relative vertical velocity profile along the bold line path in Figure 3. A striking anomaly in the velocity gradient (or equivalently, the displacement gradient) is apparent between bench marks A and B, which represents a tilt rate of

$$\frac{1.5 \text{ mm/yr}}{9.0 \text{ km}} = 1.6 \times 10^{-7} \text{ rad/yr}$$

It should be noted that this is a minimal tilt rate, since there is a hiatus of 5 km from B to the first bench mark towards A. A reasonable upper limit to the tilt is obtained by using bench mark A and the first bench mark towards B, given by

$$\frac{.76 \text{ mm/yr}}{2.3 \text{ km}} = 3.3 \times 10^{-7} \text{ rad/yr}$$

which suggests that the tilt rate is in the range of $1.0\text{--}4.0 \times 10^{-7}$ rad/yr.

Figure 5 (from Brown and Oliver, 1976) shows the regional velocity profile from Wickliffe, Kentucky to New Bern, North Carolina, with the data of Figure 4 visible in the first 60 kilometers. In Figure 5, the steep tilt of segment AB can be seen superimposed on an opposite regional tilt of 1.0×10^{-8} rad/yr. The tilt rate of segment AB is about an order of magnitude larger than most regional tilts in the eastern United States, and is definitely larger than random error could account for. In general, larger tilts are seen only in areas of intense fluid withdrawal such as near Galveston, Texas. Although there are some

apparently similar irregularities along other parts of Figure 5, most have lesser tilt rates than segment AB. More importantly, the slope discontinuity AB is more distinct and isolated, and lies amid noticeably less bench mark scatter than much of the long profile in Figure 5.

DISCUSSION AND INTERPRETATION

The location of segment AB lies between and along the trends of the Big Creek fault zone (as defined by Fisk in 1944) and the western Kentucky faulted area (Hook, 1974), as shown in Figure 1. It seems possible and not unreasonable, in light of the evidence previously presented, that the movement indicated by Figure 4 is fault related. Before immediately invoking a fault, however, possible errors and various alternative explanation of the leveling data should be considered.

Neglecting blunders (which the double-run procedure renders highly improbable), leveling errors may be classified as random or systematic. Random error has already been examined and shown to be of insufficient magnitude to explain the apparent movements.

The known sources of systematic error include:

- (1) rod miscalibration or other instrumental misalignment
- (2) refraction of the line-of-sight due to temperature gradients (typically 5 mm/100 m rise)
- (3) tidal forces (important only on north-south lines)
- (4) gravity anomalies due to mass redistribution (which may distort the equipotential reference)
- (5) atmospheric pressure changes

Except for gravity anomalies, these kinds of systematic error are most important for long wavelength features, and less so for the short wavelength phenomenon reported here. The reader is referred to Brown

and Oliver (1976) for a more detailed discussion of leveling errors, which concludes that observed regional tilts (generally of magnitude 10^{-8} rad/yr) cannot be completely accounted for by known systematic errors.

If, as the author believes, the tilting of segment AB is not entirely due to systematic error, there remain many non-tectonic geologic explanations. Fluid withdrawal with consequent sediment compaction is a known cause of vertical movement (subsidence). However, there are no oil or gas wells in this part of Kentucky, nor are there any large municipalities that consume sufficient amounts of water to depress the water table. In fact, the State of Kentucky regards the largely untapped ground water of this area as a natural resource for stimulating economic development. Although karstlands occur in west-central Kentucky, the region studied here is not karstland (National Atlas of the United States, 1970).

Local bench mark instability due to frost heaving, soil/sediment compaction, mineral dissolution, or slumping can show large movements, but the resulting movements are too localized and irregular to explain the pattern here extending over several kilometers. Such local perturbations could be expected to contribute to scatter over wavelengths like the bench mark spacing, but would be unlikely to account for the systematic variation observed. Furthermore, there is little correlation between relative movements and type of monumentation along this line. Table 3 lists bench mark monumentation, with bench marks divided about equally into two major categories, bench mark post and concrete construction (a distinction defined in Table 3). If these two groups of bench marks are viewed independently, the curves of Figure 4b are obtained. If each curve in Figure 4b were smoothed to suppress apparent noise of wavelength ≤ 5 km, the resulting smoothed curves would

coincide quite closely. This implies that the tendency for a bench mark to rise or sink unstably is the same for both types of monumentation. In general, one would expect different responses to instability processes from different types of monumentation. It is therefore suggested that both types of bench marks are approximately stable in an absolute sense.

Crustal loading (e.g. reservoirs) has been shown to cause appreciable downwarps, but the author discovered no such large artificial loads near segment AB. McGinnis (1963) found evidence that water loading due to fluctuation of the water level of the Mississippi River is correlated with seismicity, and may act as a trigger for earthquakes. He subsequently reasoned that the crust must be regionally subsiding, which is logically unclear.

Whether or not river level is related to crustal movements, the evidence supports the hypothesis that the anomalous tilt in Figure 4 is in fact due to fault movement. The four open circles in Figure 3 from 88.9° to 89.0°W are a series of four events that occurred in 1930-31 and may have been associated with the same fault zone postulated on the basis of the leveling data. The sense of surface deformation (downward to the west) would be consistent with a westward dipping normal fault or an eastward dipping thrust fault, assuming the motion is predominantly dip-slip (a reasonable assumption on the basis of regional focal plane solutions, very few of which are strike-slip). The closest focal mechanism is a thrust type (about 10 km southwest), which occurred four years after the second leveling survey. A mechanism farther to the south (about 20 km away) and within the time interval between surveys is a normal type, which makes it difficult to associate the inferred fault with one or the other type.

Various ways to reconcile the existence of both kinds of mechanisms

so near each other are illustrated by Figure 6. In all these cases, a regional compressional stress system in the basement is postulated. This compressive stress results in tensional stresses in a less competent, less consolidated upper strata, which are represented by the Cretaceous coastal plain sediments that overly Paleozoic basement. Any of these models could explain the rather singular normal fault mechanism in the midst of mostly reverse ones, and it would be reasonable to ascribe the measured movements to the normal event since it occurred within the specified time interval. However, the movement need not be associated directly with earthquakes at all, since it could alternatively be aseismic creep.

After the suspicion of a hidden fault in this region, a search for lineations was undertaken. Although aerial photography (scale 1:13,000) gave no definite indication of lineaments near the segment AB, the local stream pattern (Figure 7, taken from U.S.G.S. topographic quadrangle maps) does exhibit a noticeable lineation pattern trending approximately 11° - 14° north-northeast. This trend closely parallels the trends of the nodal planes of the normal event, the trend of the structural trough formed by the top of the Paleozoic, and the trend of the Mississippi River as it bounds western Kentucky. While the presumed faulting probably does not break the surface here, it may have influenced the drainage pattern.

Previous Fault-Movement Interpretations Based on Precise Leveling

One of the first (and few) studies of deformation of the earth's surface as measured by precise leveling in connection with earthquakes was that of Bendefy (1966) in Hungary. The leveling surveys were done in 1955-56, before and after the 12 January 1956 earthquake at Dunahavaszti, near Budapest, Hungary. Although I.S.C. lists no magnitude or depth for

this event, it was reported by over 90 stations as far as 144° away, and the village of Dunaharaszti was completely destroyed. Thus a magnitude of 6.0 or greater is likely.

Bendefy reported dynamic undulations of the crust within 100 km of the epicenter, clearly associated with the stress accumulation and release of the earthquake. Permanent relative displacement was a maximum of 40 mm near the epicenter (Dunaharaszti) and was observed between bench marks separated by 1.5 km, although no surface faults or fractures were reported. The relative velocity profile (in units of 10^{-3} mm/day) for a time interval containing the earthquake is shown in Figure 8a as the curve labelled G_2 . The steepest gradients occur directly over the epicenter, and indicate an uplift of the region west of the epicenter with respect to the east, suggesting a fault at some depth with a component of dip-slip motion.

In an attempt to determine the degree of dip-slip motion associated with this 1956 earthquake, a preliminary focal mechanism was constructed by the author from 16 first motion data presented in I.S.S. (January, 1956). These data (plotted in Figure 9) are consistent with a thrust mechanism with some strike-slip component, although some of the data is not internally consistent and the mechanism is not strongly constrained. However, the better defined nodal plane dips northwest and trends northeast and, as the fault plane, would be consistent with the sense of displacement (uplift to the west) seen in the east-west leveling line crossing the epicenter. From an examination of other leveling lines as well, Bendefy postulated a regional northwest-southeast compressional strain pattern.

The Japanese have studied surface deformations associated with several earthquakes by repeated precise leveling surveys (Mizoue, 1969). Perhaps the best example of apparent fault movement reflected in surface

leveling measurements was noted after the 19 October 1955 Futatsui earthquake ($M = 5.7$). An antisymmetric relative displacement pattern (Figure 8b) shows a maximum offset of 140 mm between adjacent bench marks approximately 2 km apart. Mizoue suggested the existence of a "hidden seismic fault" at a depth of a few kilometers in absence of surface faulting.

More confidence can be placed in these fault-at-depth interpretations by examining leveling displacement patterns near recently active fault breaks. Such a case exists in the study of Savage and Church (1974), who looked at first order surveys of 1955 and 1967 which passed over numerous fault scarps (Slemmons, 1957) mapped after a sequence of earthquakes (magnitudes 6.6-7.1) in 1954. They found a clear correlation between several distinct waveforms (amplitudes of 10^1 - 10^2 mm) in the relative displacement profile and the fault scarps, and therefore concluded that post-earthquake slip was occurring along normal faults to a depth of several kilometers.

Leveling Data and Regional Vertical Crustal Movements

Figure 10 shows a free air gravity profile from northern to southern Illinois, with a large positive gradient as southern Illinois reaches the Mississippi Embayment (from McGinnis, 1974). McGinnis (1970, 1974) considers the high positive anomalies near southernmost Illinois to be a reflection of rift-intrusive igneous bodies which are uncompensated and thus causing isostatic subsidence. If the intrusive activity stopped in the Cretaceous (the youngest dated igneous rocks), the crust should have been mechanically compensated by now, with only small thermal/erosional effects remaining. From a study of the geology of the area, Stearns and Wilson (1972) state: "since Eocene time the region (Mississippi Embayment)

appears to have been relatively stable but perhaps subjected to regional uplift." There were probably adjustments following the deposition of extensive Plio-Pleistocene gravels also.

The lack of compensation seen in the free air anomaly, however, may not be due solely to mass-excessive intrusives. If regional uplift is occurring as the leveling data imply, the anomaly may be a reflection of non-isostatic movements. The evidence for relative uplift is seen in two leveling profiles previously examined by Brown and Oliver (1976). Figure 5 shows the eastward tilting of western Kentucky, at the rate of 1.0×10^{-8} rad/yr from 0-100 km on the abscissa, and decreasing to 1.0×10^{-9} rad/yr from 100-300 km. Figure 11 shows a northward tilting of 1.1×10^{-8} rad/yr which appears to begin approximately where the large positive gravity gradient of Figure 10 becomes prominent. Taken together, these two lines suggest a possible doming centered near the border of Illinois and Kentucky. That uplift should be occurring there subsequent to Eocene subsidence is not completely unreasonable, as the geologic record shows that northwestern Louisiana was domically uplifted to form the Sabine Uplift in Miocene time, which had been part of a basin through the Jurassic (King, 1969). Other similar uplifts are known in Louisiana.

If the crust near the head of the embayment were being uplifted, it would provide a qualitative explanation for the regional compressional stress pattern apparent there. The Paleozoic basement structure there is a regional downwarp, and if a downwarp is uplifted near its center, the crust would be subjected to crustal shortening.

CONCLUSION

Evidence presented here suggests that precise leveling can indicate subsurface fault movement not apparent from other observations. In particular, a leveling profile of relative movement in western Kentucky resembles previous leveling measurements which have been interpreted as subsurface faulting. Furthermore, a fault interpretation is consistent with other geophysical and geological evidence, and seems more plausible than other alternative explanations. Additional leveling in this region would certainly seem warranted after an appropriate time interval has elapsed, or after any earthquakes occur.

In view of the above, precise leveling should be considered a valuable tool (especially in the long term) in site decision for large construction projects whose vulnerability to damage by earth movements must be minimized.

Although inconclusive, leveling data is not consistent with regional subsidence of the northern tip of the Mississippi Embayment, as has been previously suggested. Whether or not subsidence is occurring (with some unknown long-range systematic error in the leveling) or the area is indeed uplifting should be a subject for further study.

References

- Bendefy, I., Elastic, plastic, and permanent deformations of the earth's crust in connection with earthquakes, Proc. 2nd Intern. Symp. on Recent Crustal Movements, Helsinki, 57-65, 1966.
- Bomford, G., Geodesy, Clarendon Press, Oxford, 1962.
- Brown, L.D., and J.E. Oliver, Vertical crustal movements from leveling data and their relation to geologic structure in the eastern United States, submitted to Reviews of Geophysics and Space Physics, 1976.
- Burke, K., and J.F. Dewey, Plume-generated triple junctions: key indicators in applying plate tectonics to old rocks, J. Geol., 81, 406-433, 1973.
- Docekal, J., Earthquakes of the stable interior, with emphasis on the mid-continent, Ph.D. dissertation, Univ. of Nebraska, 1970.
- Ervin, C.P., and McGinnis, L.D., Reelfoot Rift: reactivated precursor to the Mississippi Embayment, Bull. Geol. Soc. Amer., 86, 1287-1295, 1975.
- Fisk, H.N., Geological investigation of the alluvial valley of the lower Mississippi River, U.S. Army Corps of Engineers, Mississippi River Commission, Vicksburg, Mississippi, 1944.
- Gerlach, A.C., ed., The National Atlas of the United States of America, U.S. Department of Interior, Geological Survey, p. 77, 1970.
- Hadly, J.B., and J.F. Devine, Seismotectonic Map of the Eastern United States, U.S. Geol. Surv., 1974.
- Heyl, A.V., and others, Regional structure of the southeast Missouri and Illinois-Kentucky mineral districts, U.S. Geol. Surv. Bull. 1202-B, 1965.
- Hook, J.W., Structure of the fault systems in the Illinois-Kentucky fluorspar district, Kentucky Geol. Surv. Spec. Publ. 22, Series X, 1974.
- International Seismological Summary, January 1956, p. 32.

- King, P.B., The Tectonics of Middle North America: Middle North America East of the Cordilleran System, Hafner Publishing Co., New York, 203 pp., 1969.
- Lammler, D.R., Spar, M.L., and J. Dorman, A microearthquake reconnaissance of southeastern Missouri and western Tennessee, Bull. Seism. Soc. Amer., 61, 1705-1716, 1971.
- McGinnis, L.D., Earthquakes and crustal movement as related to water load in the Mississippi Valley region, Illinois Geol. Surv. Circ. 344, 1963.
- McGinnis, L.D., Tectonics and the gravity field in the continental interior, J. Geophys. Res., 75, 317-331, 1970.
- McGinnis, L.D., and C.P. Ervin, Earthquakes and block tectonics in the Illinois basin, Geology, 2, 517-519,
- Mizoue, M., Types of crustal movements accompanied with earthquakes in inner northeastern Japan, Problems of Recent Crustal Movements: Third Intern. Symp., 357-370, 1968.
- Nuttli, O.W., Magnitude recurrence relation for central Mississippi Valley earthquakes, Bull. Seism. Soc. Amer., 64, 1189-1207, 1974.
- Ross, C.A., Structural framework of southernmost Illinois, Illinois Geol. Surv. Circ. 351, 1963a.
- Ross, C.A., Faulting in southernmost Illinois, Geol. Soc. Amer. Spec. Publ. 73, 229, 1963b.
- Ross, C.A., Geology of the Paducah and Smithland quadrangles in Illinois, Illinois Geol. Surv. Circ. 360, 1964.
- Savage, J.C., and J.P. Church, Evidence for post-earthquake slip in the Fairview Peak, Dixie Valley, and Rainbow Mountain fault areas of Nevada, Bull. Seism. Soc. Amer., 64, 687-698, 1974.
- Slemmons, D.B., Geological effects of the Dixie Valley-Fairview Peak, Nevada, earthquakes of December 16, 1954, Bull. Seism. Soc. Amer., 47, 353-375, 1957.

- Stauder, W., and others, Relation of microearthquakes in southeastern Missouri to structural features, Trans. Amer. Geophys. Union, 56, no. 6, 398, 1975.
- Stearns, R.G., and C.W. Wilson, Jr., Relationships of earthquakes and geology in west Tennessee and adjacent areas, Report for TVA, Nashville, Tenn., Vanderbilt Univ., 344 pp., 1972.
- Stearns, R.G., and A. Zurawski, Post-Cretaceous faulting in the head of the Mississippi Embayment, manuscript in preparation, 1975.
- Street, R.L., R.B. Hermann, and O.W. Nuttli, Earthquake mechanics in the central United States, Science, 184, 1285-1287, 1974.
- U.S. Dept. of Commerce Coast and Geodetic Survey, Bench Mark Descriptions, Wickliffe to Paducah, Kentucky, 1972.
- York, J.E., and J.E. Oliver, Cretaceous and Cenozoic faulting in eastern North America, submitted to Bull. Geol. Soc. Amer., 1976.

Table I
Earthquakes near Cairo, Illinois from 1947 to 1968.7

Date (yr.mo.day)	Lat (N)	Lon. (W)	Depth (km)	Intensity	Magnitude	Ref used
1947.1.16	36°59'	89°11'	---	II-III	(3.2)*	a, b
1953.5.06	36°59'	89°11'	---	III	(3.4)	a, b
1953.5.15	36°59'	89°11'	---	III	(3.4)	a, b.
1957.3.26	37°05'	88°36'	---	IV	(3.8)	a, b
1958.1.27	37°03'	89°12'	---	V	(4.2)	a, b
1962.2.16	37.0°	87.7°	25	III-IV	(3.6)	b, d
1963.3.31 <u>M</u>	36.9°	89.0°	---	---	3.0	b, c
1963.5.02	36.7°	89.4°	---	---	3.1	a, b
1963.8.02 <u>M</u>	37.0°	88.7°	18	V	4.0	b, c, d
1965.8.13	37°19'	89°28'	33	IV	3.2	a, b, d
1965.8.14 <u>M</u>	37°2°	89.3	38	VII	3.8	b, c, d
1965.8.15	37°22'	89°28'	16	V	3.5	a, b, d
1965.8.15	37°24'	89°28'	---	V	3.4	a, b

a, Docekal (1970)

b, Nuttli (1974)

c, Street et al. (1974)

d, Stearns and Wilson (1972)

* () indicates estimation of Nuttli (1974)

M indicates focal mechanism of Street (1974)

Table 2
Earthquakes near Cairo, Illinois from 1928-1947 and 1968.7-1972

Date (yr.mo.day)	Lat (N)	Lon (W)	Intensity	Mag.	Ref. Used
1928.4.15	37° 17'	89° 32'	IV	(3.8)	a, b
1930.8.29	37.9°	89.0°	V	---	d
1930.9.03	36° 58'	88° 54'	III	(3.4)	a, b
1930.9.03	36° 58'	88° 54'	III	(3.4)	a, b
1931.4.06	36° 51'	89° 01'	IV	(3.8)	a, b
1933.10.24	37° 17'	89° 32'	III	(3.4)	a, b
1934.8.19	36° 56'	89° 12'	VI	(4.7)	a, b
1934.8.19	36° 59'	89° 09'	II-III	(3.2)	a, b
1936.8.02	36.7	89.0	III	(4.1)	a, b
1936.12.20	37° 17'	89° 32'	II	(3.0)	a, b
1939.4.15	36° 48'	89° 24'	III	(3.4)	a, b
1940.2.04	37° 13'	89° 29'	III	(3.4)	a, b
1940.5.31	37° 05'	88° 36'	V	(4.2)	a, b
1940.10.10	36.8°	89.2°	II-III	(3.2)	a, b
1941.10.21	36° 58'	89° 08'	IV	(3.8)	a, b
1941.11.22	37° 17'	89° 32'	II-III	(3.2)	a, b
1942.8.31	36° 59'	89° 11'	IV	(3.8)	a, b.
1942.11.13	36° 59'	89° 11'	IV	(3.8)	a, b
1970.12.24	36.7°	89.5°	IV	3.6	b
1972.6.18 <u>M</u>	37.0	89.1	III	3.2	c

Table 3
Bench Mark Tabulation

No.	Name	BM Design ¹	Monumentation ²	Distance (km)	Relative Movement (mm)
1	Wickliffe RM No. 1	RMD	P	0.00	0.0
2	Wickliffe RM No. 2	RMD	P	0.14	-0.4
3	M128	D	P	2.18	-1.0
4	Z130	D	(B)	3.92	-2.7
5	Y130	D	P	5.56	-5.8
6	X130	D	P	7.01	-2.5
7	W130	D	(B)	8.49	-5.4
8	Barlow RM No. 2	RMD	P	9.98	-11.5
9	Barlow \equiv "A"	TSD	P	10.01	-6.0
10	U130	D	P	12.29	9.6
11	T130	D	(C)	13.86	4.5
12	R130 \equiv "B"	D	(B)	19.08	24.9
13	Q130	D	P	21.15	27.8
14	P130	D	P	22.77	30.0
15	N130	D	(C)	24.51	30.5
16	M130	D	(C)	25.91	24.2
17	Kevil RM No. 2	RMD	P	27.37	24.8
18	Kevil	TSD	P	27.66	27.0
19	Kevil RM No. 1	RMD	P	27.69	-17.4
20	L130	D	(C)	29.14	27.3
21	G130	D	(B)	35.65	22.4
22	E130	D	(W)	36.21	7.1
23	F130	D	(W)	36.29	12.7
24	C130	D	(U)	38.50	20.3
25	64M	D (USGS)	P	40.44	19.2
26	B130	D	(U)	42.12	26.6
27	63M	D (USGS)	P	45.50	14.2

Table 3 (cont.)

No.	Name	BM Design ¹	Monumentation ²	Distance (km)	Relative Movement (mm)
28	L129	D	(F)	47.83	18.4
29	N129	D	P	50.87	16.7
30	P129	D	(B)	52.10	10.9
31 ³	R129	D	(FT)	55.01	11.3
32	G18	D	P	57.45	-4.2
33	F18	D	P	58.06	11.9
34	H129	D	P	59.02	6.9
35	E18	D	P	60.10	5.3

¹ RMD = a C & GS Reference Mark Disk
 D = a C & GS Bench Mark Disk
 TSD = a C & GS Triangulation Station Disk
 D (USGS) = a USGS Bench Mark Disk

² P = Concrete Bench Mark Post
 B = Highway Bridge
 C = Highway Calvert
 W = Concrete Wall
 U = Railroad Underpass
 FT = Concrete Footing

() designates a concrete construction type of monumentation,
 i.e. a pre-existing construction which accomodated a bench
 mark without requiring new installation of a standard bench
 mark support (usually a concrete post).

³ Paducah is between 31 and 32.

Figure Captions

Figure 1: Central United States portion of Hadley and Devine's tectonic map of the eastern United States (1974), with the addition of the Big Creek fault zone defined by Fisk (1944). The bold rectangle shows the locality of the leveling data analyzed, and is the area covered in Figure 3.

Figure 2a: Central United States portion of Hadley and Devine's epicenter map of the eastern United States (1974). The rectangular inset is the same as in Figure 1.

Figure 2b: Explanation for Figure 2a.

Figure 3: Seismotectonic map of the rectangular inset seen in Figures 1 and 2, showing the path of two leveling surveys (1947 and 1968.7). See text for further explanation. The basemap with faulting is adapted from Stearns and Wilson (1972).

Figure 4a: Plot of the relative vertical bench mark velocity (as described in text) versus distance from Wickliffe (WIC) to Paducah, Kentucky (PAD). Also shown are curves representing elevation and random error. Two bench marks have been labelled "A" and "B" for purposes of discussion.

Figure 4b: Same data as in Figure 4a divided according to type of bench mark monumentation. The solid line connects bench marks that are in concrete posts specially designed as stable supports for bench marks, and the dotted line connects bench marks that are in other concrete constructions, as listed and defined in Table 3.

Figure 5: Relative velocity curve from Wickliffe, Kentucky to New Bern, North Carolina (from Brown and Oliver, 1976). The small rectangle shows the fault-like offset seen in Figure 4.

Figure 6: Possible crustal models for which shallow normal faulting could accompany deeper, regional thrusting. Both 6a and 6b are schematics of gravitationally induced normal-faulting in relatively incompetent sediments over thrust-faulting in stronger basement rocks.

- (6a) Differential elevation of upper strata caused by thrusting acts to induce shearing in upper incompetent sediments.
- (6b) Curvature of steeply thrusting acts to produce normal bending stresses in upper strata with continued movement.

Figure 7: Stream-defined, north-northeast trending lineaments based on USGS 7½' topographic quadrangle maps. Bench marks A and B are shown by squares, and others by "x".

Figure 8: Examples from the literature of anomalously steep relative velocity (or displacement) gradients as measured by precise leveling, near earthquake epicenters (8a and 8b) and near surface faulting (8c).

- (8a) 40 mm relative displacement associated with the 12 January 1956 earthquake near Dunaharaszti, Hungary (Bendefy, 1966).
- (8b) 140 mm relative displacement associated with the 19 October 1955 earthquake near Futatsui, Japan (Mizoue, 1969).
- (8c) 20-70 mm relative displacement associated with surface faults in Nevada (Savage and Church, 1974).

Figure 9: Tentative focal plane solution for the 12 January 1956 earthquake (Dunaharaszti, Hungary) from 16 first motion data given in I.S.S.

Figure 10: Mean free air anomaly along latitude 89°W . Computation technique described by McGinnis (1970). Figure from McGinnis, (1974).

Figure 11: Regional relative velocity profile determined by precise leveling, from Davis Junction, Illinois, to Cairo, Illinois, to Meridian, Mississippi (figure from Brown and Oliver, 1976). The time spans over which particular segments were leveled is given in the lower portion of the figure.

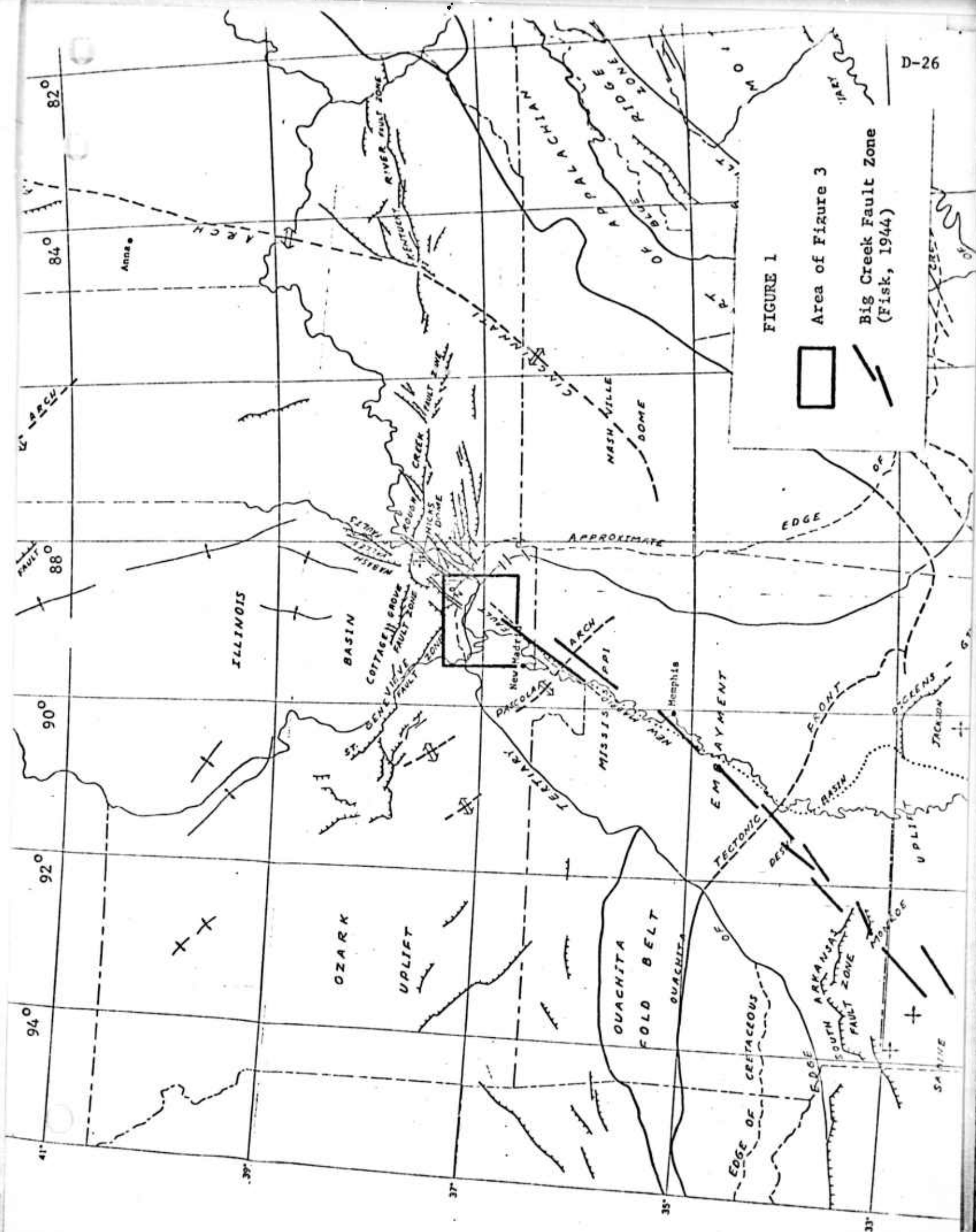
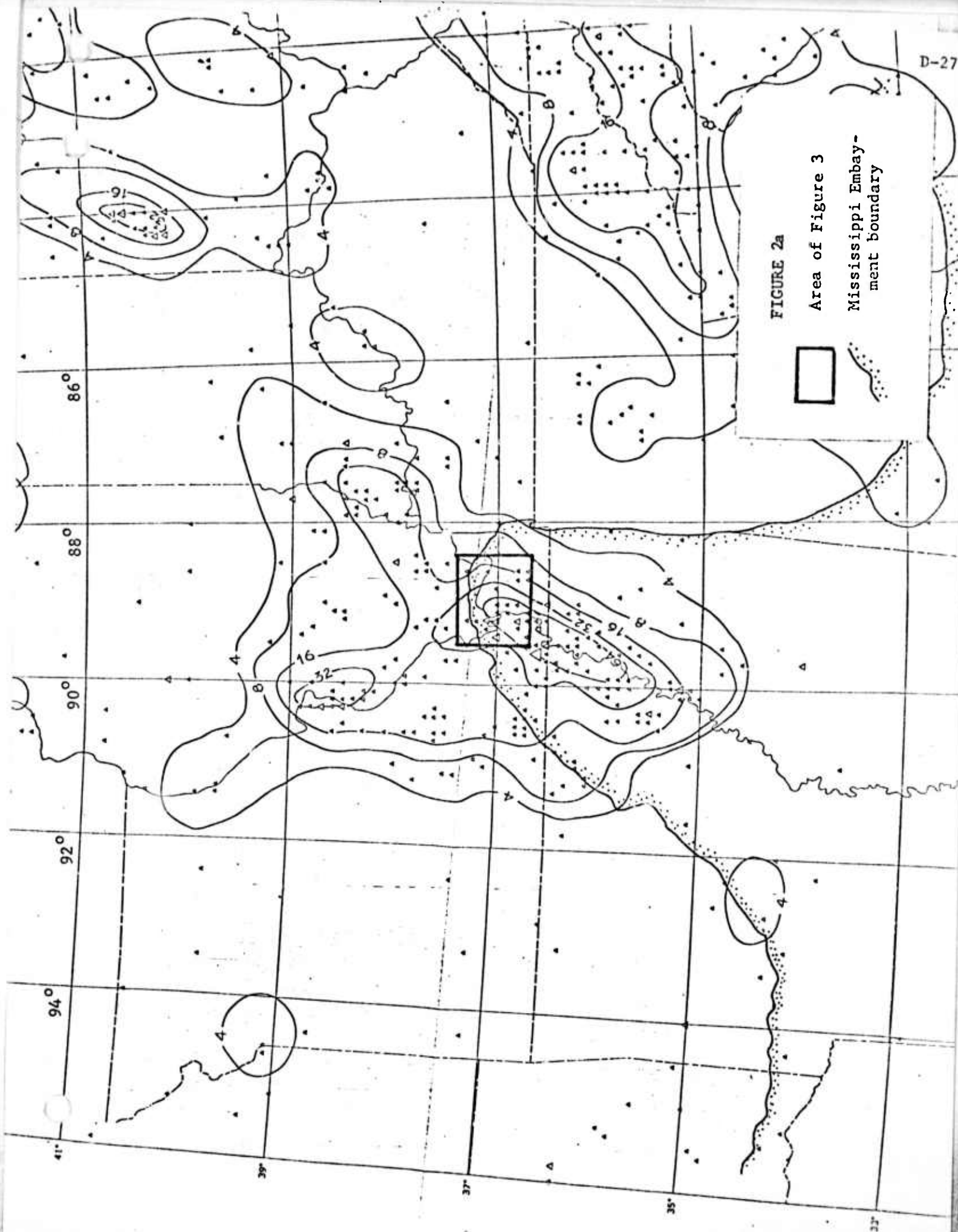


FIGURE 2a
Area of Figure 3
Mississippi Embay-
ment boundary



EXPLANATION

Modified Mercalli Intensity

- ▲
 III to VI
 △
 VII
 △
 VIII
 △
 IX-X
 △
 XII

A single epicenter of intensity XII is shown near New Madrid, Missouri

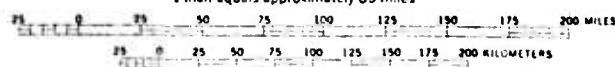
The center of each triangular symbol indicates the epicentral location of one or more seismic events, plotted to the nearest 0.1 degree of latitude and longitude. The intensity shown is maximum Modified Mercalli (MM) intensity in the epicentral area of the largest event at the plotted location. Most locations are based on observations of intensity rather than on instrumental records

Seismic frequency contour represents the areal distribution of earthquake epicenters with epicentral intensity of MM III and greater, as indicated by the total number per 10^4 km^2 during the period 1800-1972. Contour intervals are 0-4, more than 4 but less than 8, more than 8 but less than 16, more than 16 but less than 32, more than 32 but less than 64, and more than 64. The contours are considerably generalized and are shown only as a guide for estimating regional seismicity. They have no value for precise location of seismic boundaries

NOTE: This map was compiled in 1973 from earthquake data of the Environmental Data Service of the National Oceanic and Atmospheric Administration and from data of the Dominion Observatory, Ottawa, Canada

SCALE 1:5,000,000

1 inch equals approximately 80 miles



1972

UNITED STATES

FIGURE 2b

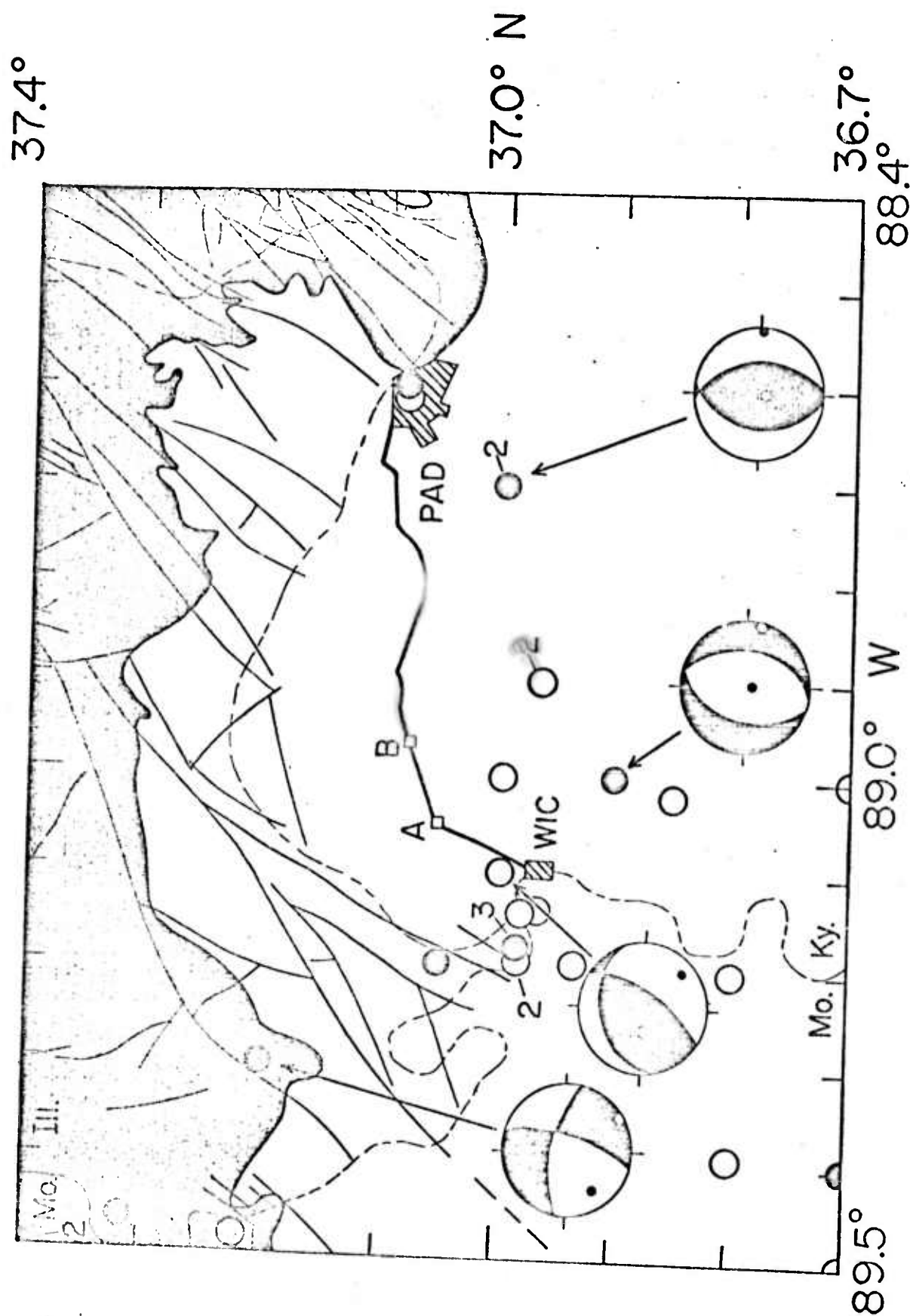


FIGURE 3

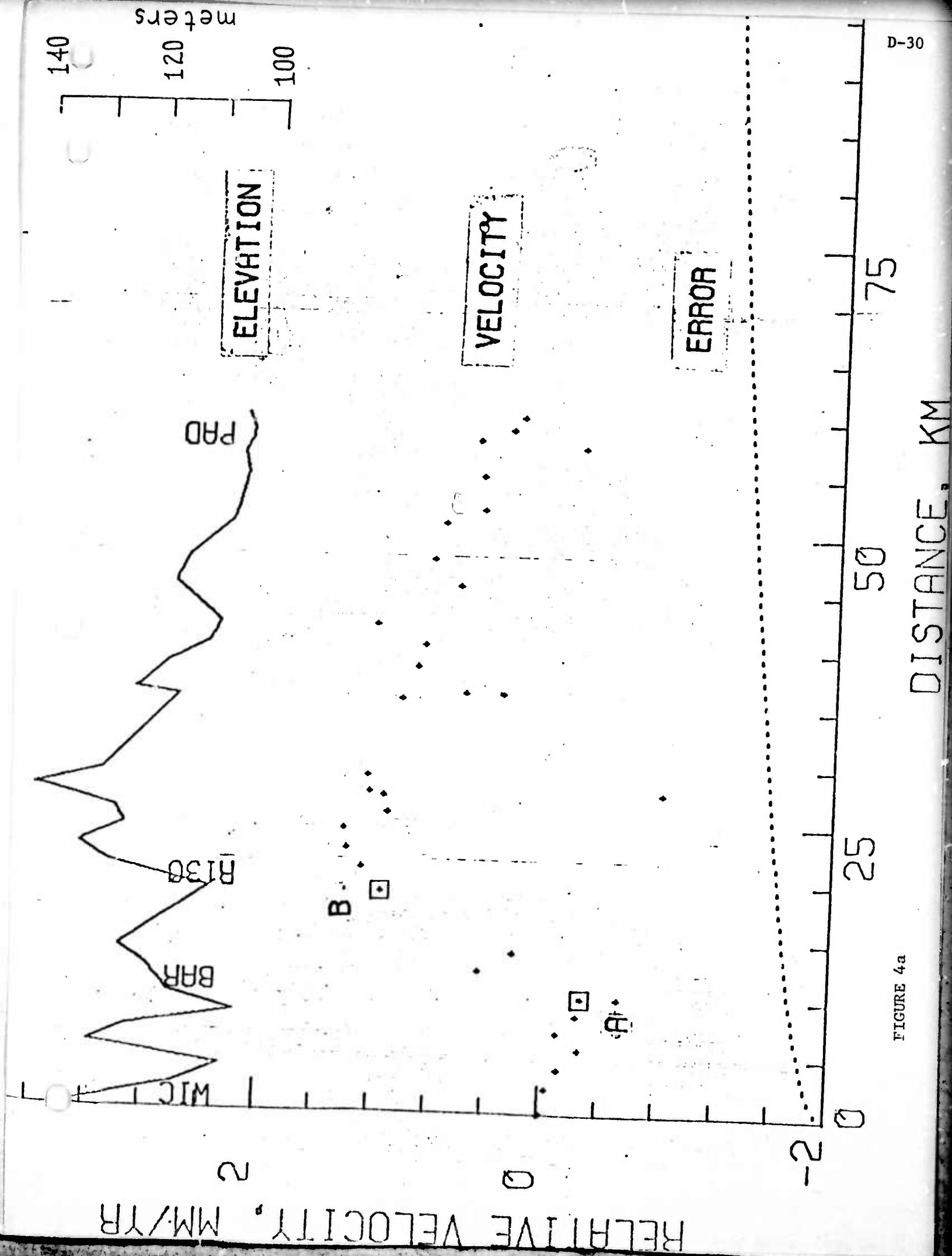


FIGURE 4a

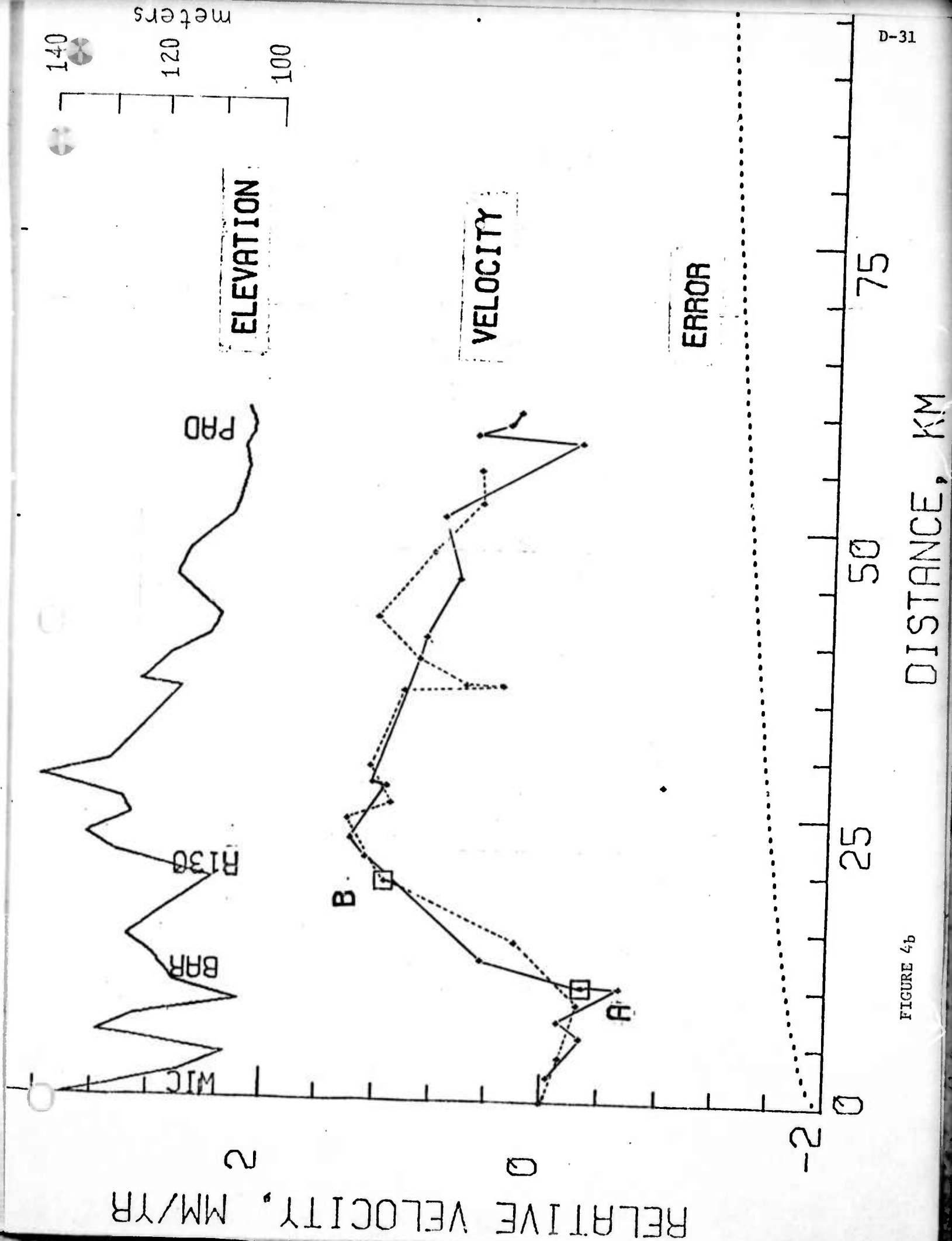


FIGURE 4b

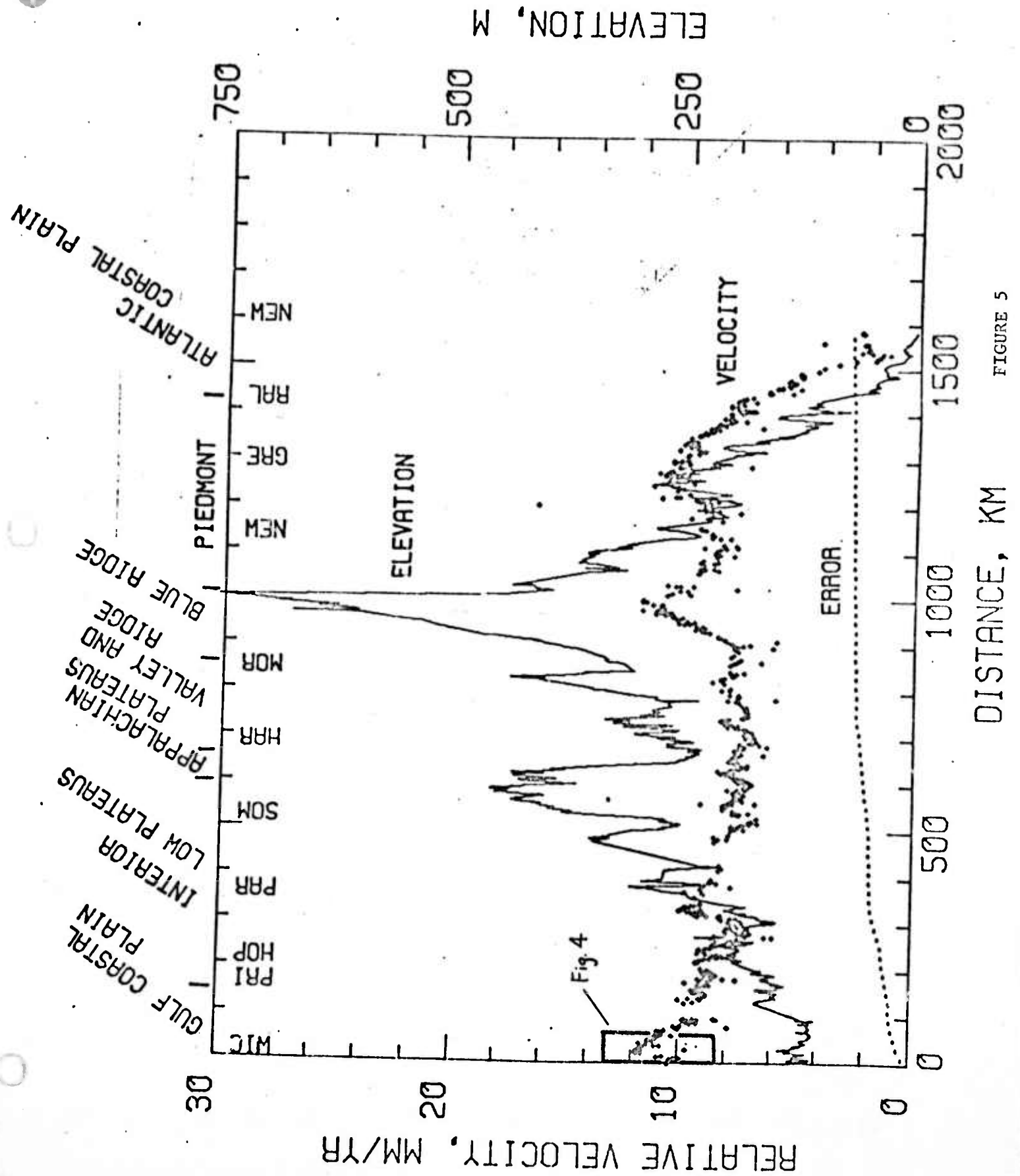
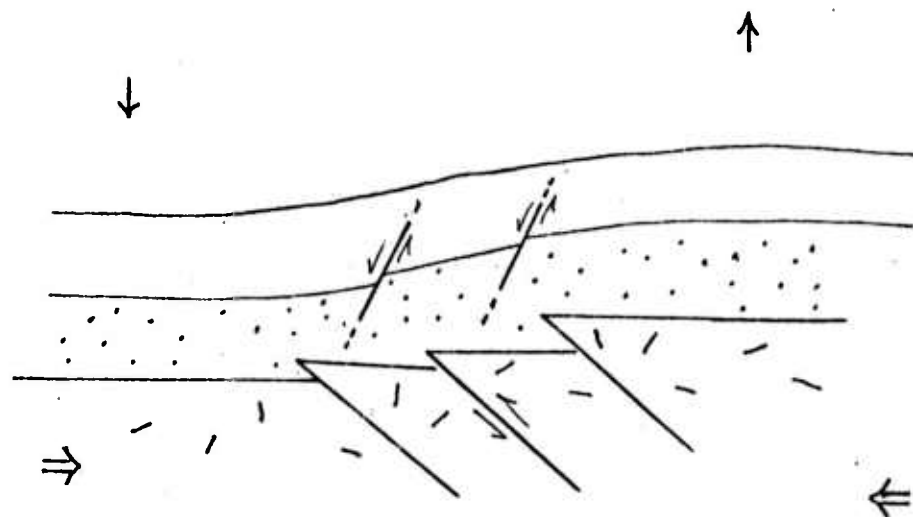
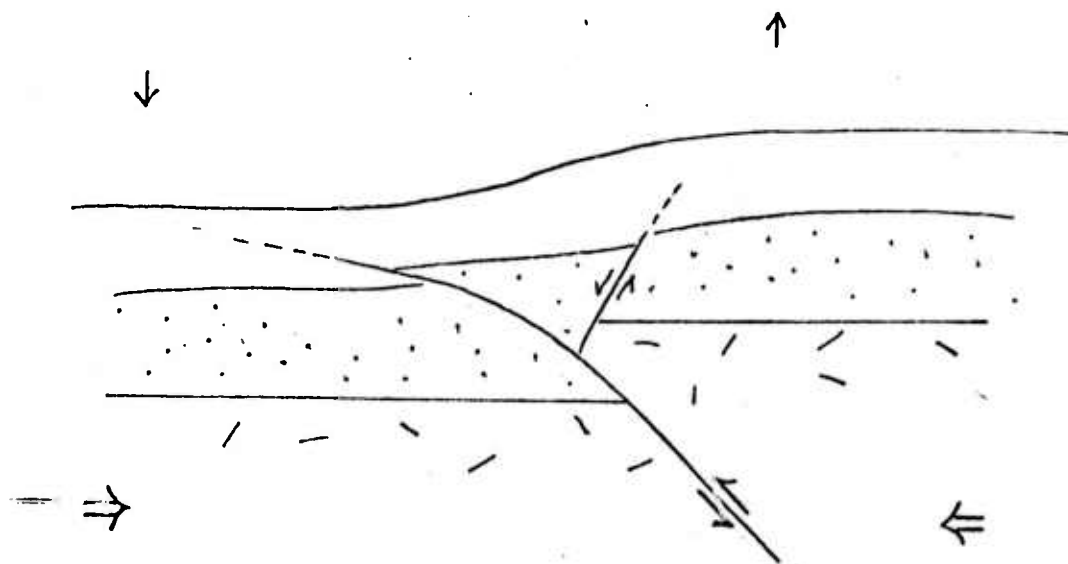


FIGURE 5



6a



6b

FIGURE 6

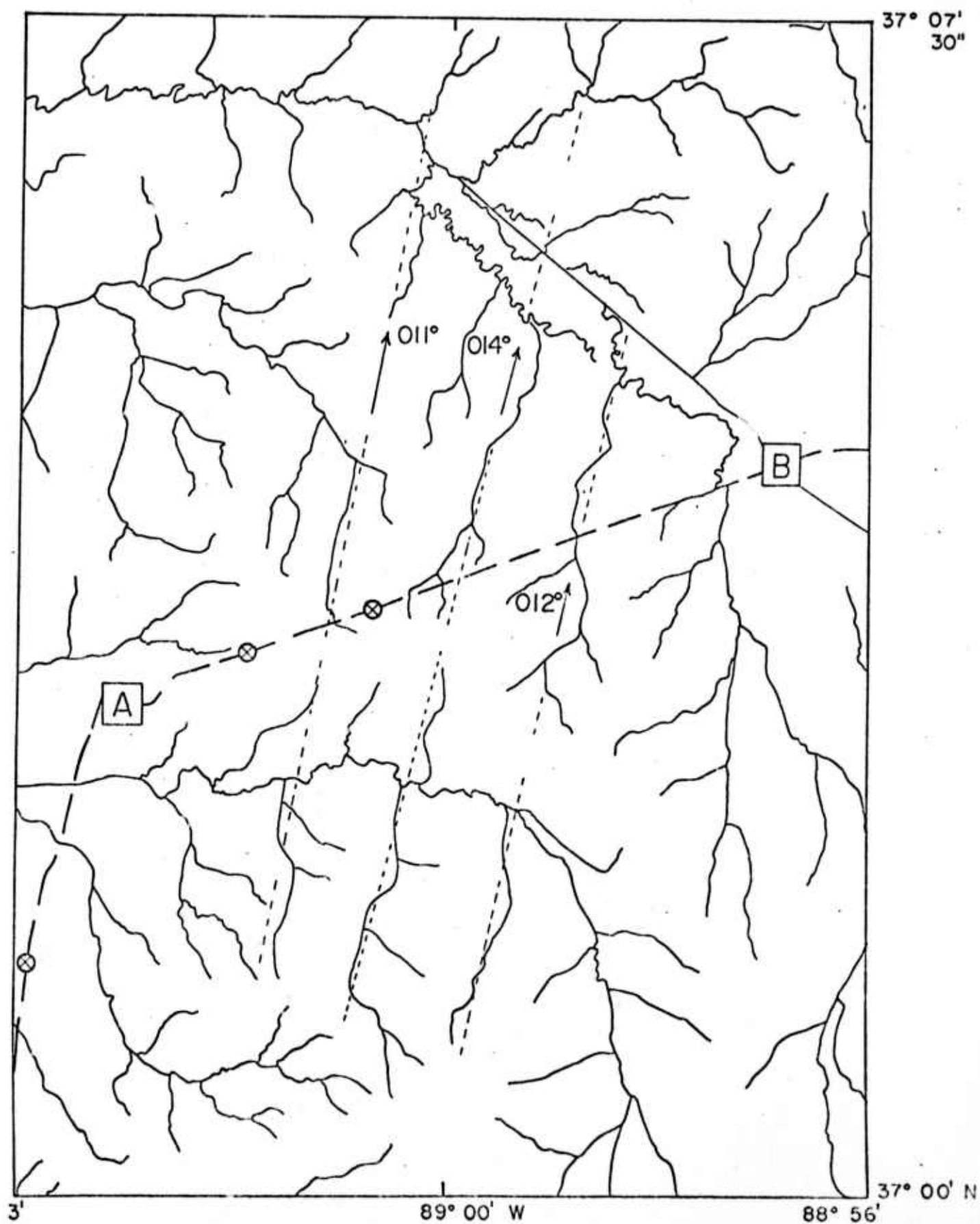


FIGURE 7

FIGURE 8a

B. BENDER, Elastic, plastic and permanent deformations

01

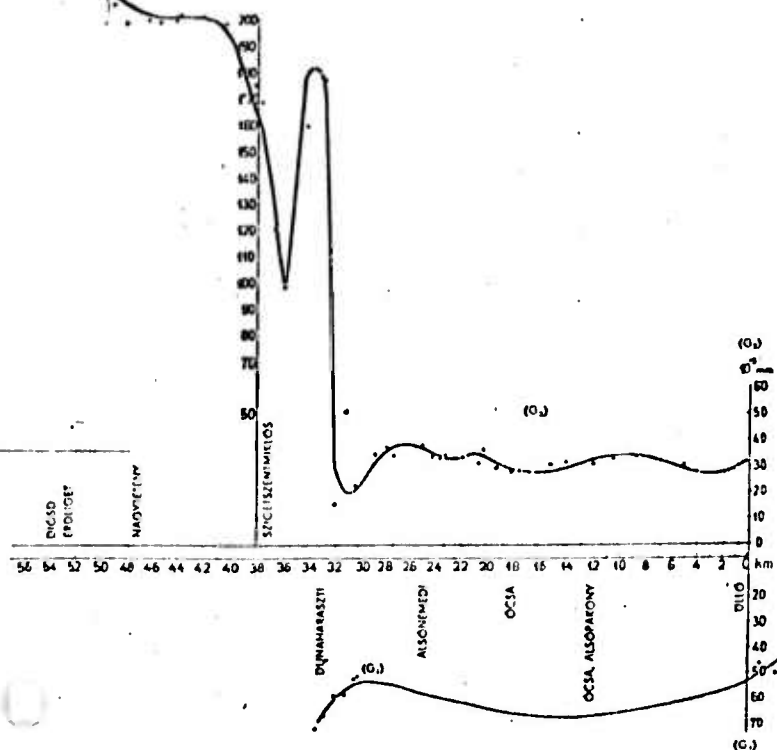
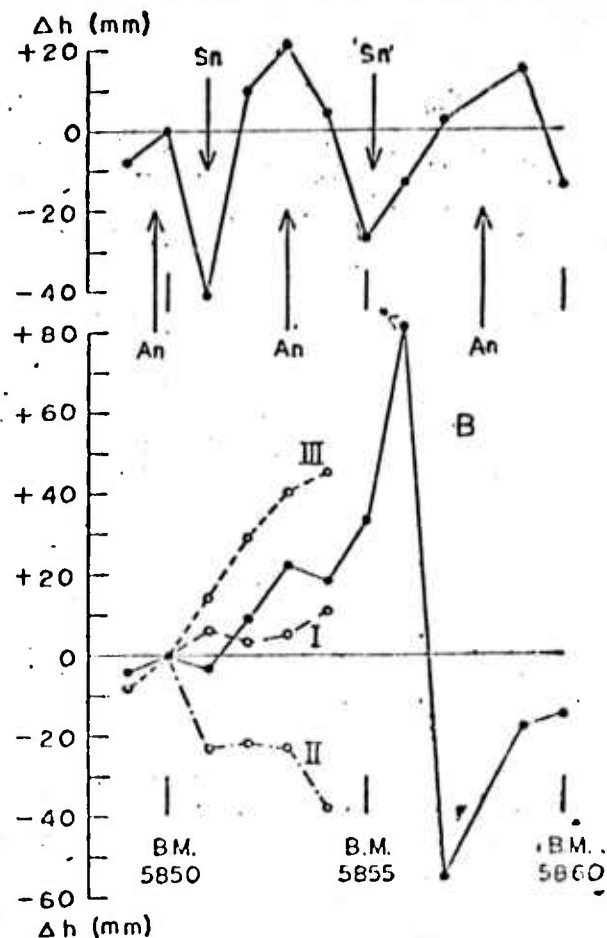
Fig. 4. Crustal deformations near the epicenter. Unit = 10^{-3} mm/day.

FIGURE 8b

D-35



A; 1938-1902 . B; 1955-1938

I 1942-1938 . II 1949-1942 . III 1955-1949

Fig. 3-a. Vertical crustal movements accompanied with the Fulsui Earthquake of 1955. An: Anticline, Sn: Syncline. (after S. Miyamura, and A. Okada, 1956).

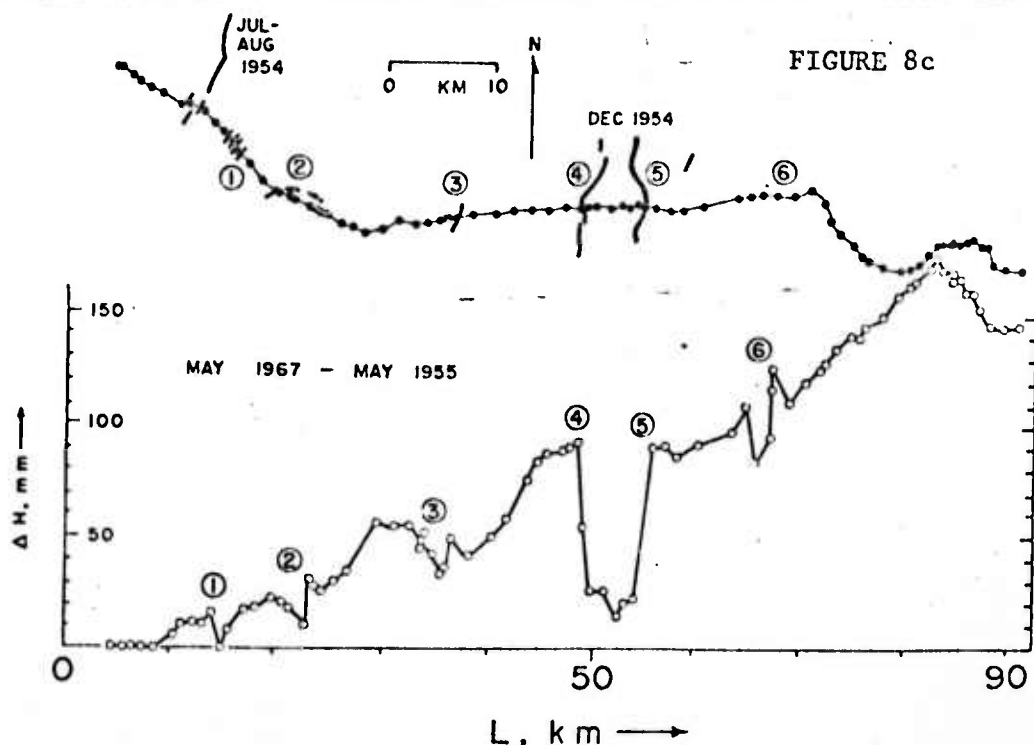


FIG. 2. Elevation changes indicated by the differences between adjusted elevations determined in the 1955 and 1967 surveys (lower line) as a function of distance measured west to east across the fault zone. The upper line is a plan view of the location of bench marks from BM R383 to Carroll Summit. The earthquake ground breakage along Highway 50 is also shown. Local anomalies in the lower curve are identified by numbers.

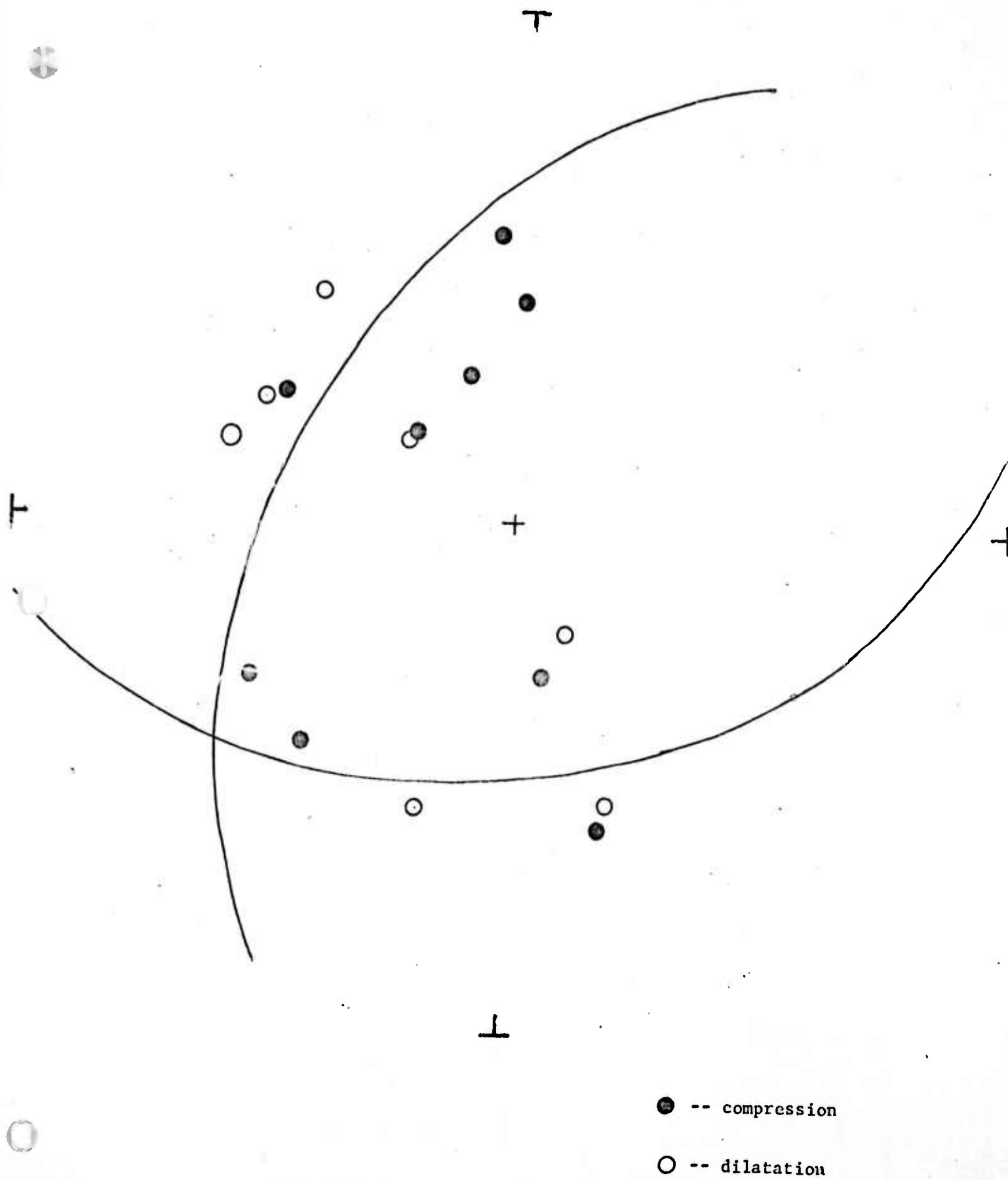


FIGURE 9

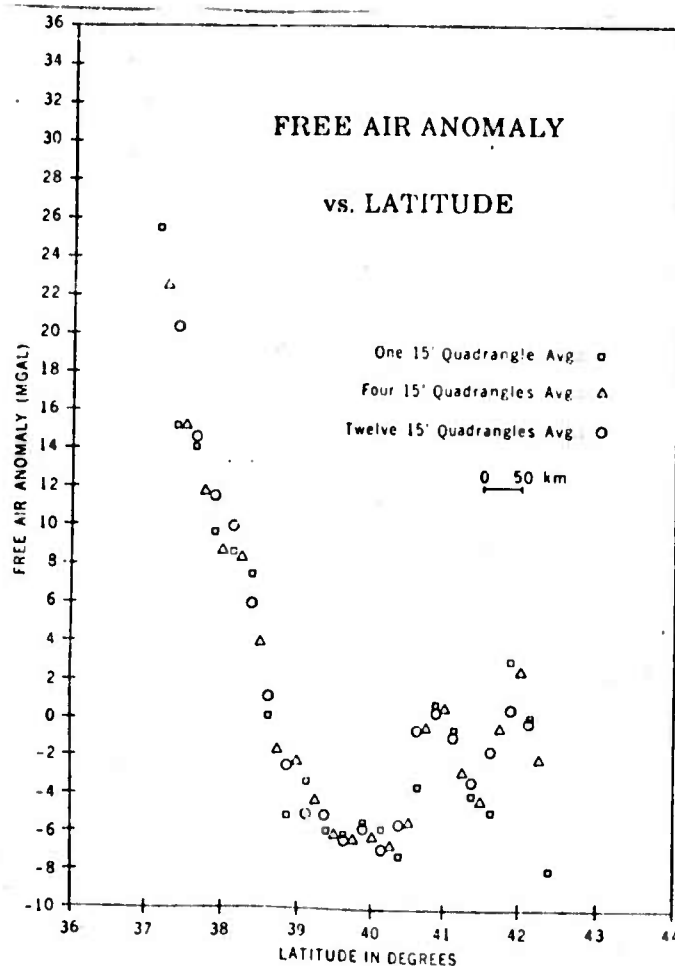


Figure 2. Mean free-air anomaly profile along long 89° W. Computation technique described by McGinnis (1970).

GEOLOGY

PRINT

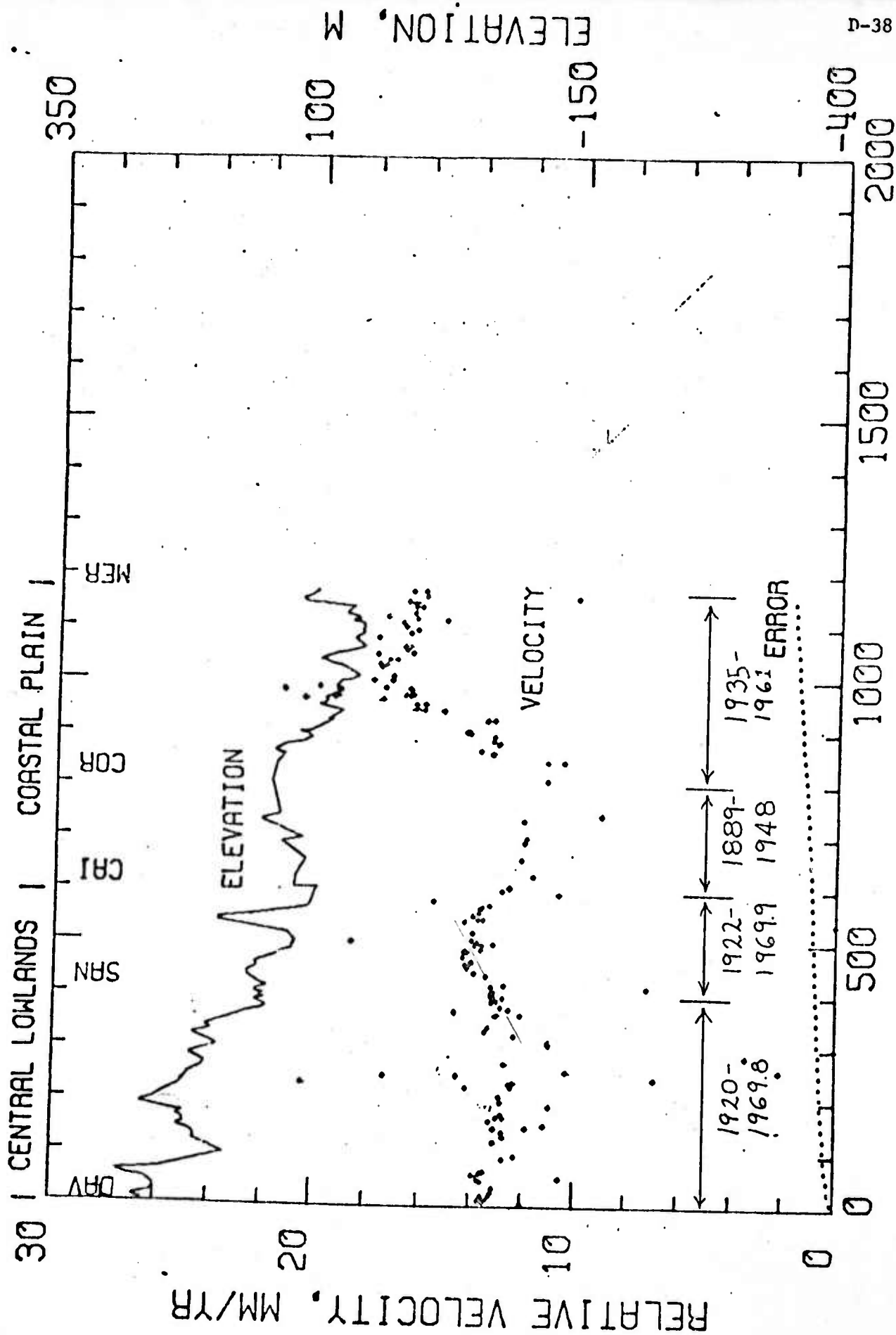


FIGURE 11

REFRACTION ERROR IN LEVELING

James E. York
Department of Geological Sciences
Cornell University
Ithaca, New York 14853

ABSTRACT

Previous estimates of the refraction error in leveling reached up to several tens of mm per 100 m change in elevation. Errors are found in these estimates. For a linear temperature gradient, the error is usually less than 1 mm per 100 m change in elevation. The refraction error is probably less than the standard deviation in leveling for a linear temperature gradient. However, non-linear temperature gradients may be important.

INTRODUCTION

Systematic errors in precise leveling which accumulate with elevation are difficult to detect. Two sources of such errors are incorrect calibration of the leveling rods and bending of light rays caused by changes in the index of refraction of light. In leveling a closed loop, these errors may give systematically high or low elevations without contributing to the error in loop closure. In addition, if two levelings of the same route are compared, and if the magnitude of the systematic error was different in the two surveys, then measurements of apparent, but unreal, vertical crustal movements would result.

If the apparent vertical movements were to correlate (either negatively or positively) with elevation, then such systematic errors might be suspected. In their studies of vertical movements from releveling data in the United States, Brown and Oliver (1975) have observed such correlations

(Figure 5). Therefore an investigation of the magnitude of possible refraction errors was made.

Changes in the index of refraction are caused by variations in temperature, pressure, and composition of the atmosphere. Kukkamäki (1938) has shown that the most important variations are those of temperature. Hence only temperature variations will be considered here.

A typical set-up used in leveling measurements, along with conventions and symbols for this paper, is shown in Figure 1. Mathematical symbols to be used in this paper are as follows:

- α acute angle between horizontal and ground surface
- a temperature at instrument ($^{\circ}\text{K}$)
- b temperature gradient ($^{\circ}\text{C}/\text{m}$)
- c a constant ($^{\circ}\text{K}$) relating n and T (equation 5)
- e net refraction error between foresight and backsight
($\text{mm}/100 \text{ m}$ change in elevation)
- h refraction error between instrument and rod (m)
- n index of refraction
- s horizontal sighting length (m)
- T temperature ($^{\circ}\text{K}$)
- x distance measured parallel to ground surface with origin
at instrument
- z distance measured perpendicular to ground surface with
origin at instrument
- subscripts: 0 values at instrument
 - 1 values where light ray intersects rod₁
 - 2 values where light ray intersects rod₂

PREVIOUS WORK

The calculation of the refraction correction is complicated by the uncertainty in the form of the temperature distribution. Even if a vertical temperature profile is known at one locality on a leveling route, the profile may change along the route and with time. A further complication is the difficulty in integrating many forms of the temperature distribution.

Based on some early temperature observations, Lallemand (1896) used

$$T = c_1 + c_2 \log (z+c_3) \quad (1)$$

where the c_i are constants. From more recent observations, Kukkamäki (1938) obtained the formula

$$T = c_4 + c_5 z^{c_6} \quad (2)$$

A third formula,

$$T = c_7 + c_8 z + c_9 z^2 \quad (3)$$

was used by Bomford (1928), because it simplified the mathematics.

All three of the above authors used Snell's law and a simple dependence of the index of refraction on temperature (see equation 5) to calculate the refraction error. The difficulty in integrating the resulting equations led each of these authors to make approximations. Because the refraction error is small, approximations must be made carefully or else they may greatly affect the obtained magnitude of the refraction error. Unfortunately, the approximations of these authors do have such effects. For example, they each give a net refraction error of zero for a linear temperature gradient (equation 4) with equal backsight

and foresight. As the present study shows, this net error is not zero. Therefore, further calculations were deemed necessary to determine possible magnitudes of the refraction error.

REFRACTION ERROR

Temperatures

A temperature distribution of the form

$$T = a + bz \quad (4)$$

will be assumed. This linear temperature gradient may be a fair approximation over vertical distances such as are encountered between instrument and rod (a few meters or less), but clearly this gradient cannot be extrapolated to much larger vertical distances. This advantage of this formula is its simplification of computations of the refraction error. Should a more complicated temperature distribution be found necessary, it could be approximated as a number of discrete linear sections and the formulas presented in this paper could still be used.

This simple formula also ignores any x-dependence of the temperature. Before refraction corrections based on equation 4 are made, temperature measurements should be made while leveling.

In the calculations that follow, the value of a used is 288°K . The sign of b is taken to be positive. If b is negative, only the sign, not the absolute value, of the net error is changed.

Index of Refraction

For a pure substance, the index of refraction for a given wavelength depends only on the density. Using an ideal gas law approximation

$$n = 1 + \frac{c}{T} \quad (5)$$

where c is a constant dependent on pressure, wavelength, and composition of the gas. Empirical evidence supports an equation of this form (Meggers and Peters, 1918). For the purposes of this paper, c is constant and equal to 0.0801°K .

Fermat's Principle

Fermat's principle is used to determine the path of the ray which travels between rod 1 and rod 2 and is tangent to the instrument. This principle states that the ray path is such that the value of the travel time is stationary. Thus the problem is one of the calculus of variations.

The integral

$$\int n \left[(dx)^2 + (dz)^2 \right]^{1/2} = \int n \left[1 + \left(\frac{dz}{dx} \right)^2 \right]^{1/2} dx \quad (6)$$

must be extremized. Because n is independent of x , the Euler-Lagrange equation becomes

$$\frac{dz}{dx} = \pm \sqrt{\left(\frac{n}{n_0} \right)^2 - 1} \quad (7)$$

where n_0 is a constant. Because the slope $\frac{dz}{dx}$ is $-\tan\alpha$ at the origin, equation 7 becomes

$$\frac{dz}{dx} = \pm \sqrt{\left(\frac{n}{n_0} \right)^2 (1 + \tan^2\alpha) - 1} \quad (8)$$

Calculation of Error

Using equations 4 and 5, the square root expression may be written in terms of z . Then equation 8 may be integrated from the origin to each rod. This procedure (see Appendix A) gives transcendental equations for the refraction errors h_1 and h_2 .

The transcendental equations can be solved iteratively by Newton's method (see Appendix B). In order to facilitate comparisons with apparent vertical movements indicated by leveling and releveing data, the net refraction error (in mm) per 100 m change in elevation is calculated for a given angle α , temperature gradient b , and sighting length s .

$$e = (h_2 - h_1) (1000) (\text{number of instrument set-ups necessary to change 100 m in elevation}) \quad (9)$$

Figures 2, 3, and 4 give e as a function of α , b , and s , respectively. The net refraction error is seen to vary as the square of both the temperature gradient and the sighting length. Therefore, temperature gradients must be well known before applying corrections. Also, the refraction error may be greatly reduced by shortening sighting lengths.

CONCLUSIONS

Because observed temperature gradients in the air are usually less than 1°C/m (see tables of Best in Kukkamäki, 1938), and because sighting lengths are usually less than 100 m in practice, the refraction error is usually less than 1 mm/100 m change in elevation for linear temperature gradients. This figure is approximately equal to the systematic error caused by inaccuracies in correcting for thermal changes affecting rod length (Thurm, 1971). It is also usually less than the estimated standard deviation in precise

leveling, which includes only random errors.

Some of the leveling profiles studied by Brown and Oliver (1975) show correlations of elevation with movement. If caused by systematic errors, these correlations would indicate errors ranging from 20 to 100 mm/100 m change in elevation (Figure 5). These hypothetical errors appear much too large to be explained by refraction caused by simple linear temperature gradients. Therefore, the apparent movements may reflect actual crustal movements, as Brown and Oliver (1975) suggest. Alternatively, non-linear temperature gradients may be important.

Thurm (1971) and Hytonen (1967) have made refraction corrections to leveling data based on Kukkamäki's (1938, 1939) formulas and tables. Because of errors in Kukkamäki's work, these corrections may not be valid. Before any refraction corrections are made, average temperature distributions must be known accurately. Because air movements cause rapid variations in temperature, only approximate, average corrections can be made. On long lines of near constant slope, where refraction errors could be larger than the standard deviation, using short sighting lengths will keep the error small.

ACKNOWLEDGMENTS

Beneficial discussions have been held with L. Brown, R. Reilinger, and S. Schilt. This research was supported by the Advanced Research Projects Agency of the Department of Defense and was monitored by the Air Force Office of Scientific Research under Contract Number AFOSR-73-2494. Cornell University Department of Geological Sciences Contribution Number: .

REFERENCES CITED

- Bomford, G., Three sources of error in precise leveling, Survey of India Professional Paper No. 22, 40 p., 1928.
- Brown, L.D. and Oliver, J.E., Vertical crustal movements from leveling data and their relation to geologic structure in the eastern United States, Rev. Geophys. Space Phys., 13, , 1975.
- Hytönen, E., Measuring of the refraction in the second leveling of Finland, Suomen Geodeettisen Laitoksen Julkaisuja Veröfentliehunger des Finnischen Geodätischen Institutes No. 63, 41 p., 1967.
- Kukkamäki, T.J., Über die nivellitische Refraktion, Suomen Geodeettisen Laitoksen Julkaisuja Veröfentliehunger des Finnischen Geodätischen Institutes No. 25, 48 p., 1938.
- Kukkamäki, T.J., Formeln und Tabellen zur Berechnung der nivellitischen Refraktion, Suomen Geodeettisen Laitoksen Julkaisuja Veröfentliehunger des Finnischen Geodätischen Institute No. 27, 18 p., 1939.
- Lallemand, C., L'erreur de réfraction dans le nivellement geometrique, Verhandlung Conferenz der Permanenten Commission der Internationalen Erdmessung, 24-27, 1897.
- Meggers, W.F., and Peters, C.G., Measurement of the index of refraction of air for wavelengths from 2218 A to 9000 A, National Bureau of Standards Bulletin, 14, 697-740, 1918.
- Thurm, H., Some systematic errors of precision leveling, Jena Review, 16, 172-176, 1971.

Appendix A

Derivation of Transcendental Equation for Refraction Error

Upon substitution of equations 4 and 5 into equation 8 and integration:

$$\begin{aligned}
 (A1) \quad \pm \int dx &= \int (a+c)(a+bz) \left[(a^2 \tan^2 \alpha - 2ac - c^2)(bz)^2 + \right. \\
 &\quad \left. (2a)(a+c)(a \tan^2 \alpha - c)(bz) + (a)^2(a+c)^2 \tan^2 \alpha \right]^{-\frac{1}{2}} dz \\
 &= F + \text{constant}
 \end{aligned}$$

From geometry of Figure 1:

$$(A2) \quad h_1 \cos \alpha = s \sin \alpha - z_1$$

$$(A3) \quad h_2 \cos \alpha = -s \sin \alpha - z_2$$

$$(A4) \quad h_1 \sin \alpha = -x_1 - s \cos \alpha$$

$$(A5) \quad h_2 \sin \alpha = -x_2 + s \cos \alpha$$

Integrating equation A1 from the origin to the rods:

$$(A6) \quad x_2 = -F(z_2) + F(0)$$

If the light ray is never tangent to a line parallel to the x -axis:

$$(A7a) \quad x_1 = -F(z_1) + F(0)$$

If the tangent to the light ray does become parallel to the x -axis:

$$(A7b) \quad x_1 = -F(z_p) + F(0) + F(z_1) - F(z_p)$$

where z_p is the value of z when the tangent is parallel to the x -axis. On either side of z_p the sign of the slope is different, and thus two integrations of equation A1 are necessary.

Substituting equations A2-A5 into equations A6 and A7:

$$(A8) \quad h_2 \sin \alpha = s \cos \alpha + F(-s \sin \alpha - h_2 \cos \alpha) - F(0)$$

If tangent to the light ray is never parallel to the x -axis:

$$(A9a) \quad h_1 \sin \alpha = -s \cos \alpha + F(s \sin \alpha - h_1 \cos \alpha) - F(0)$$

If tangent to the light ray does become parallel to the x-axis:

$$(A9b) \quad h_1 \sin \alpha = -s \cos \alpha - F(s \sin \alpha - h_1 \cos \alpha) - F(0) + 2F(z_p)$$

Equations A8 and A9 are the transcendental equations in h to be solved numerically.

The formulas for F are:

$$\text{if } a^2 \tan^2 \alpha - 2ac - c^2 > 0,$$

$$(A10a) \quad F(z) = (b)^{-1}(a+c)(a^2 \tan^2 \alpha - 2ac - c^2)^{-1} \left[(a^2 \tan^2 \alpha - 2ac - c^2)(bz)^2 + \right. \\ \left. (2a)(a+c)(a \tan^2 \alpha - c)(bz) + (a)^2(a+c)^2 \tan^2 \alpha \right]^{\frac{1}{2}} + \\ (a+c)(a^2 \tan^2 \alpha - 2ac - c^2)^{-\frac{1}{2}}(b)^{-1}(a) \left\{ 1 - [(a+c)(a \tan^2 \alpha - c) \right. \\ \left. (a^2 \tan^2 \alpha - 2ac - c^2)^{-1}] \right\} \ln \left\{ [(a^2 \tan^2 \alpha - 2ac - c^2)(bz)^2 + \right. \\ \left. (2a)(a+c)(a \tan^2 \alpha - c)(bz) + (a)^2(a+c)^2 \tan^2 \alpha]^{\frac{1}{2}} + \right. \\ \left. (a^2 \tan^2 \alpha - 2ac - c^2)^{\frac{1}{2}}(bz) + a(a+c)(a \tan^2 \alpha - c)(a^2 \tan^2 \alpha - \right. \\ \left. 2ac - c^2)^{-\frac{1}{2}} \right\}$$

$$\text{if } a^2 \tan^2 \alpha - 2ac - c^2 < 0,$$

$$\begin{aligned} (A10b) \quad F(z) = & (b)^{-1}(a+c)(a^2 \tan^2 \alpha - 2ac - c^2)^{-1} [(a^2 \tan^2 \alpha - 2ac - c^2)(bz)^2 + \\ & (2a)(a+c)(a \tan^2 \alpha - c)(bz) + (a)^2(a+c)^2 \tan^2 \alpha]^{\frac{1}{2}} + \\ & (a+c)(-a^2 \tan^2 \alpha + 2ac + c^2)^{-\frac{1}{2}}(b)^{-1}(a) \left\{ 1 - [(a+c)(a \tan^2 \alpha - c) \right. \\ & \left. (a^2 \tan^2 \alpha - 2ac - c^2)^{-1}] \right\} \text{Arcsin} \left\{ [(-2)(b)^2(a^2 \tan^2 \alpha - 2ac - c^2)(z) - \right. \\ & \left. (2ab)(a+c)(a \tan^2 \alpha - c)] [(2ab)^2(a+c)^2(a \tan^2 \alpha - c)^2 - \right. \\ & \left. 4(a)^2(b)^2(a+c)^2(a^2 \tan^2 \alpha - 2ac - c^2) \tan^2 \alpha]^{-\frac{1}{2}} \right\} \end{aligned}$$

The formula for z_p is:

$$\begin{aligned} (A11) \quad z_p = & \left\{ -(2ab)(a+c)(a \tan^2 \alpha - c) - [(2ab)^2(a+c)^2(a \tan^2 \alpha - c)^2 - \right. \\ & \left. 4(a)^2(b)^2(a+c)^2(a^2 \tan^2 \alpha - 2ac - c^2) \tan^2 \alpha]^{-\frac{1}{2}} \right\} \\ & [2(b)^2(a^2 \tan^2 \alpha - 2ac - c^2)]^{-1} \end{aligned}$$

Appendix B

Numerical Calculation of Refraction Error

Rewrite equations A8 and A9 in the form

$$(B1) \quad G(h) = 0$$

Then, if $G'(h)$ and $G''(h)$ do not change sign in the interval (h^1, h^2) and $G(h^1) \cdot G''(h^1) > 0$, $h^n \rightarrow h$ as $n \rightarrow \infty$, where

$$(B2) \quad h^{n+1} = h^n - \frac{G(h^n)}{G'(h^n)} \quad (\text{Newton's method})$$

and h^1, h^2, h^3, \dots represent successive approximations of h .

This method was found to compute h to sufficient accuracy after a few iterations.

To show that $G'(h)$ and $G''(h)$ do not change sign in the interval (h^1, h^2) , let equations A8 and A9 be rewritten as:

$$(B3) \quad \begin{aligned} A8 : G_2(h_2) &= 0 \\ A9a : G_{1a}(h_1) &= 0 \\ A9b : G_{1b}(h_1) &= 0 \end{aligned}$$

Then,

$$(B4) \quad G'_2(h_2) = -\cos \alpha [(a^2 \tan^2 \alpha - 2ac - c^2)(bz_2)^2 + (2a)(a+c)(a \tan^2 \alpha - c)(bz_2) + (a)^2(a+c)^2 \tan^2 \alpha]^{-\frac{1}{2}} - \sin \alpha \leq 0$$

By substituting z_1 for z_2 in the above formula, one obtains $G'_{1a}(h_1)$.
Thus

$$G'_{1a}(h_1) \leq 0$$

By also substituting $(+\sin \alpha)$ for $(-\sin \alpha)$ in B4, one obtains $-G'_{1b}(h_1)$.
Then

$$G'_{1b}(h_1) \geq 0 \text{ for reasonable values of } n \text{ and for } \alpha \text{ less than about } 30^\circ.$$

$$(B5) \quad G''_2(h_2) = a^2 bc (1 + \tan^2 \alpha) \cos^2 \alpha (a+c)(a+c+bz_2) [(a^2 \tan^2 \alpha - 2ac - c^2)(bz_2)^2 + (2a)(a+c)(a \tan^2 \alpha - c)(bz_2) + (a)^2(a+c)^2 \tan^2 \alpha]^{-\frac{3}{2}} \geq 0$$

By substituting z_1 for z_2 in equation B5 one obtains $G''_{1a}(h_1)$.

Thus

$$G''_{1a}(h_1) \geq 0$$

Finally,

$$G''_{1b}(h_1) = -G''_{1a}(h_1) \leq 0$$

Therefore $G'(h)$ and $G''(h)$ do not change sign in the interval (h', h^2) .

To insure that Newton's method will work, h' must be picked such that

$$G(h') \cdot G''(h') > 0.$$

For equations A8 and A9a, this condition is met if $h' = 0$.

For equation A9b, this condition is met if $h' \cos \alpha = s \sin \alpha - z_p$.

FIGURE CAPTIONS

Figure 1: Mathematical conventions and symbols used in this paper.

The net refraction error is $h_2 - h_1$.

Figure 2: Dependence of net refraction error e (mm/100 m change in elevation) on slope α , using sighting length s = minimum of 50 m or a sighting length such that the difference in elevation between the bases of the two rods is 4 m. $a = 288^\circ\text{K}$, $c = .0801^\circ\text{K}$.

Figure 3: Graph showing b^2 dependence of net refraction error e , where b is temperature gradient. $a = 288^\circ\text{K}$, $c = .0801^\circ\text{K}$.

Figure 4: Graph showing s^2 dependence of net refraction error e , where s is sighting length. $a = 288^\circ\text{K}$, $c = .0801^\circ\text{K}$.

Figure 5: Apparent vertical velocities between Morristown, Tennessee and New Bern, North Carolina, derived by comparing two levelings separated by 33 years. Each dot represents one bench mark. From Brown and Oliver (1975).

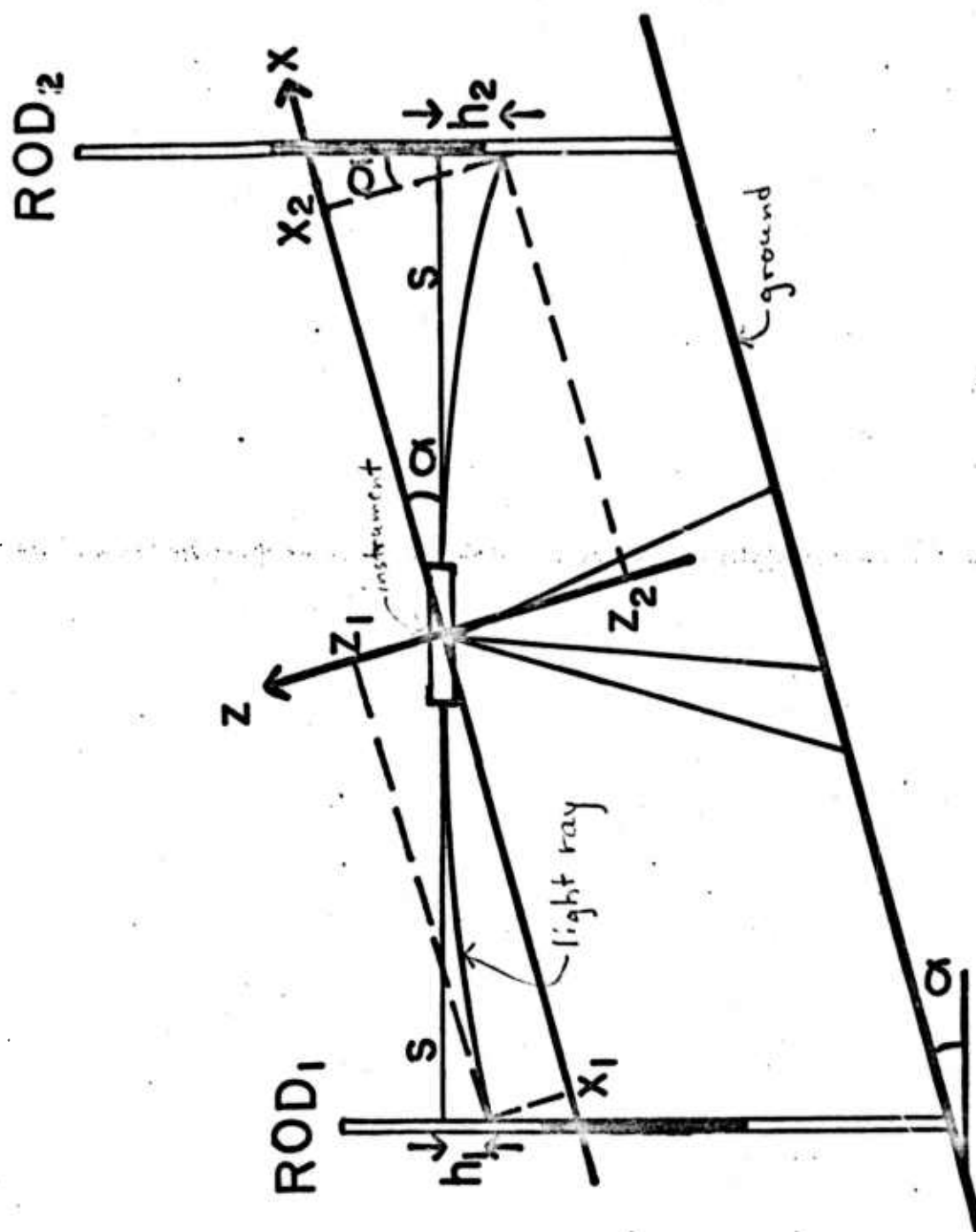


FIGURE 1.

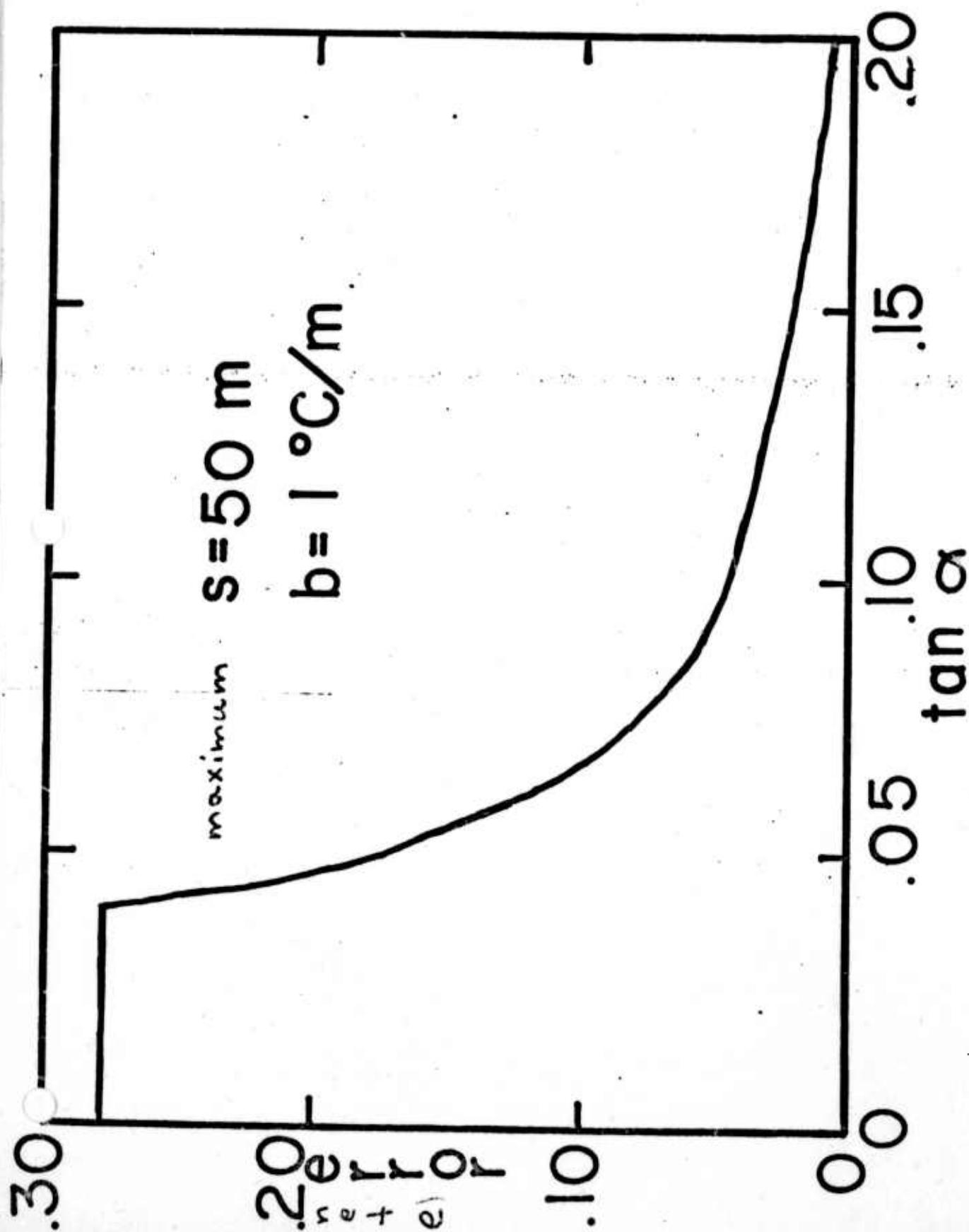


FIGURE 2.

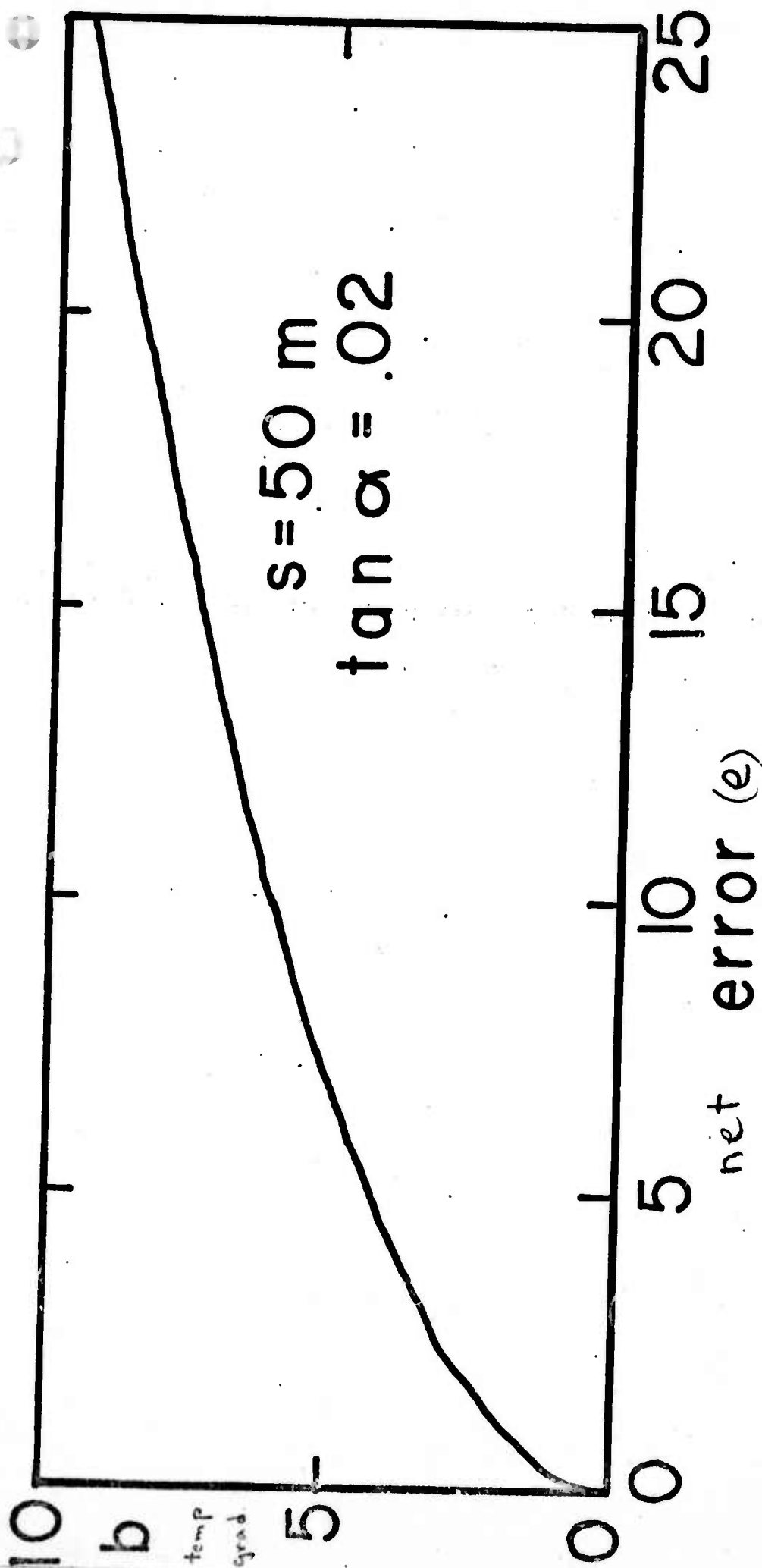


FIGURE 3.

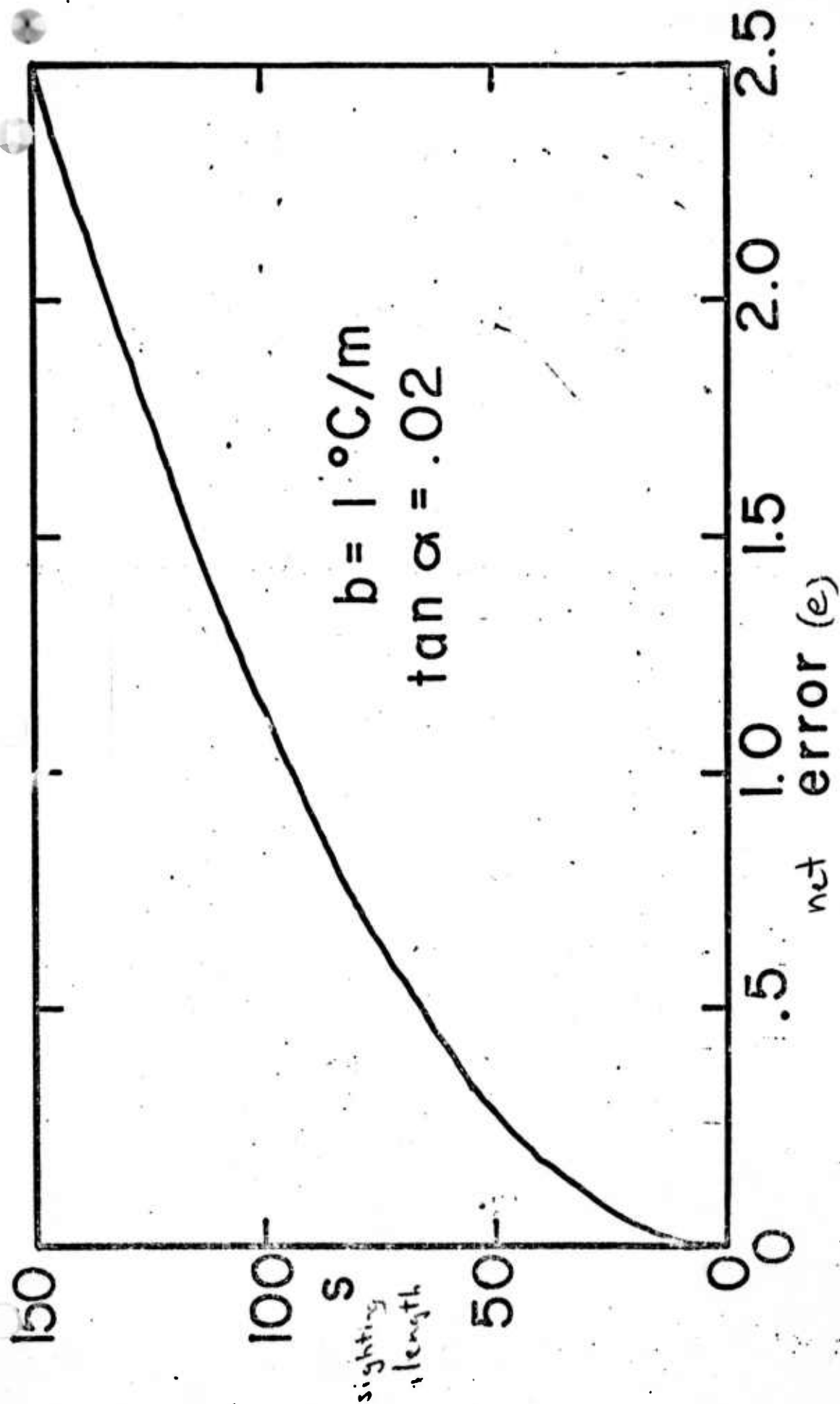


FIGURE 4.

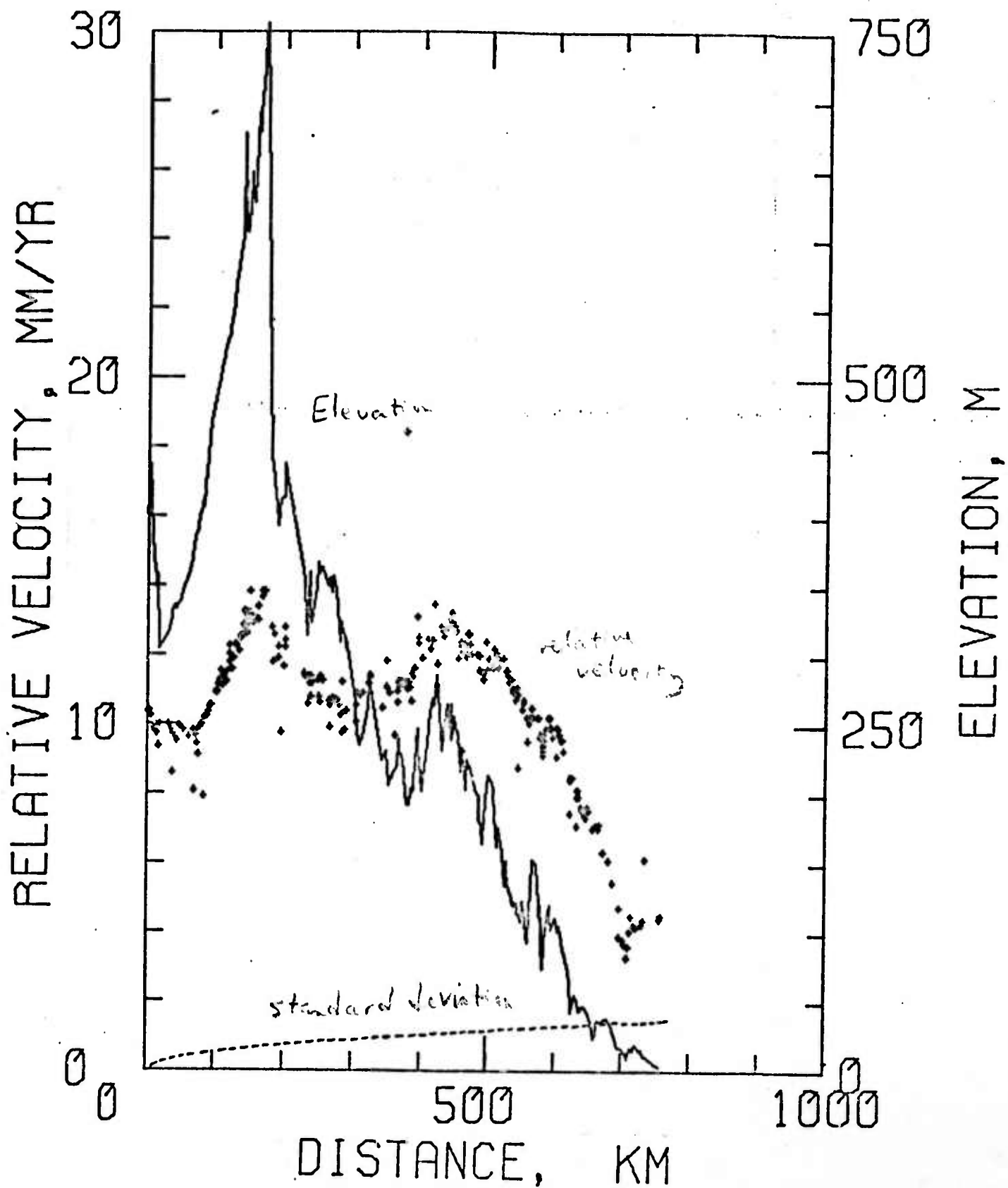


FIGURE 5.

Unclassified

SECURITY CLASSIFICATION OF THIS PAGE (When Data Entered)

REPORT DOCUMENTATION PAGE		READ INSTRUCTIONS BEFORE COMPLETING FORM
1. REPORT NUMBER	2. GOVT ACCESSION NO. AD-A108 351	3. RECIPIENT'S CATALOG NUMBER
4. TITLE (and Subtitle) INTEGRATED GEOPHYSICAL AND GEOLOGICAL STUDY OF EARTHQUAKES IN NORMALLY ASEISMIC AREAS		5. TYPE OF REPORT & PERIOD COVERED Semi-Annual Technical Report 1 April 1975 - 31 Sept 1975
7. AUTHOR(s) Steve Schilt, Larry Brown, James York Richard Cardwell		6. PERFORMING ORG. REPORT NUMBER
9. PERFORMING ORGANIZATION NAME AND ADDRESS Department of Geological Sciences, Cornell University, Ithaca, New York 14853		8. CONTRACT OR GRANT NUMBER(s) AFOSR 73-2494
11. CONTROLLING OFFICE NAME AND ADDRESS Air Force Office of Scientific Research, 1400 Wilson Blvd., Arlington, Virginia		10. PROGRAM ELEMENT, PROJECT, TASK AREA & WORK UNIT NUMBERS Program Element Code 62701E Project-Task A01827-5
14. MONITORING AGENCY NAME & ADDRESS (if different from Controlling Office) same		12. REPORT DATE
		13. NUMBER OF PAGES
		15. SECURITY CLASS. (of this report) Unclassified
		15a. DECLASSIFICATION/DOWNGRADING SC EOULE
16. DISTRIBUTION STATEMENT (of this Report) Approved for public release; distribution unlimited.		
17. DISTRIBUTION STATEMENT (of the abstract entered in Block 20, if different from Report)		
18. SUPPLEMENTARY NOTES None.		
19. KEY WORDS (Continue on reverse side if necessary and identify by block number) Intraplate Earthquakes, Releveling Measurements, Cenozoic Faulting, Unloading Stresses.		
20. ABSTRACT (Continue on reverse side if necessary and identify by block number) Recent crustal movements and earthquakes are being studied in several intraplate areas of the world, notably the United States and China, by analysis of seismicity, precise leveling, sea level variations, geomorphology, photo- geology, the sedimentary record, igneous activity, and faulting. Information from geodetic leveling and sea level monitoring indicates that the eastern United States is characterized by a complex pattern of vertical crustal movements which correlates strongly with topography and weakly with seismicity. Rates of		

DD FORM 1473
1 JAN 73

EDITION OF 1 NOV 65 IS OBSOLETE

Unclassified

SECURITY CLASSIFICATION OF THIS PAGE (When Data Entered)

Unclassified

SECURITY CLASSIFICATION OF THIS PAGE(When Data Entered)

vertical movement exceed the post-Jurassic average by 2-3 orders of magnitude. Occurrences of Cenozoic faulting in eastern North America indicate that tectonic activity in this region cannot be attributed to a simple stress pattern. Some of these faults appear to be reactivated Paleozoic faults. Seismicity maps have been prepared for the eastern United States and China. A bibliography of literature on the seismotectonics of China has been compiled. Investigation of the 1966 earthquake series in the North China Basin indicates that the basin is being strike-slipped southward relative to eastern China. Study of the Shansi graben area reveals a zone of tensional tectonics, with associated geologic and seismic features. The northwest orientation of the T axes of all fault plane solutions tends to support the idea that northeastern China is in tension.

Unclassified

SECURITY CLASSIFICATION OF THIS PAGE(When Data Entered)